The aftermath of multiyear droughts

A case study in Australia

Stijn van Terwisga

Technische Universiteit Delft

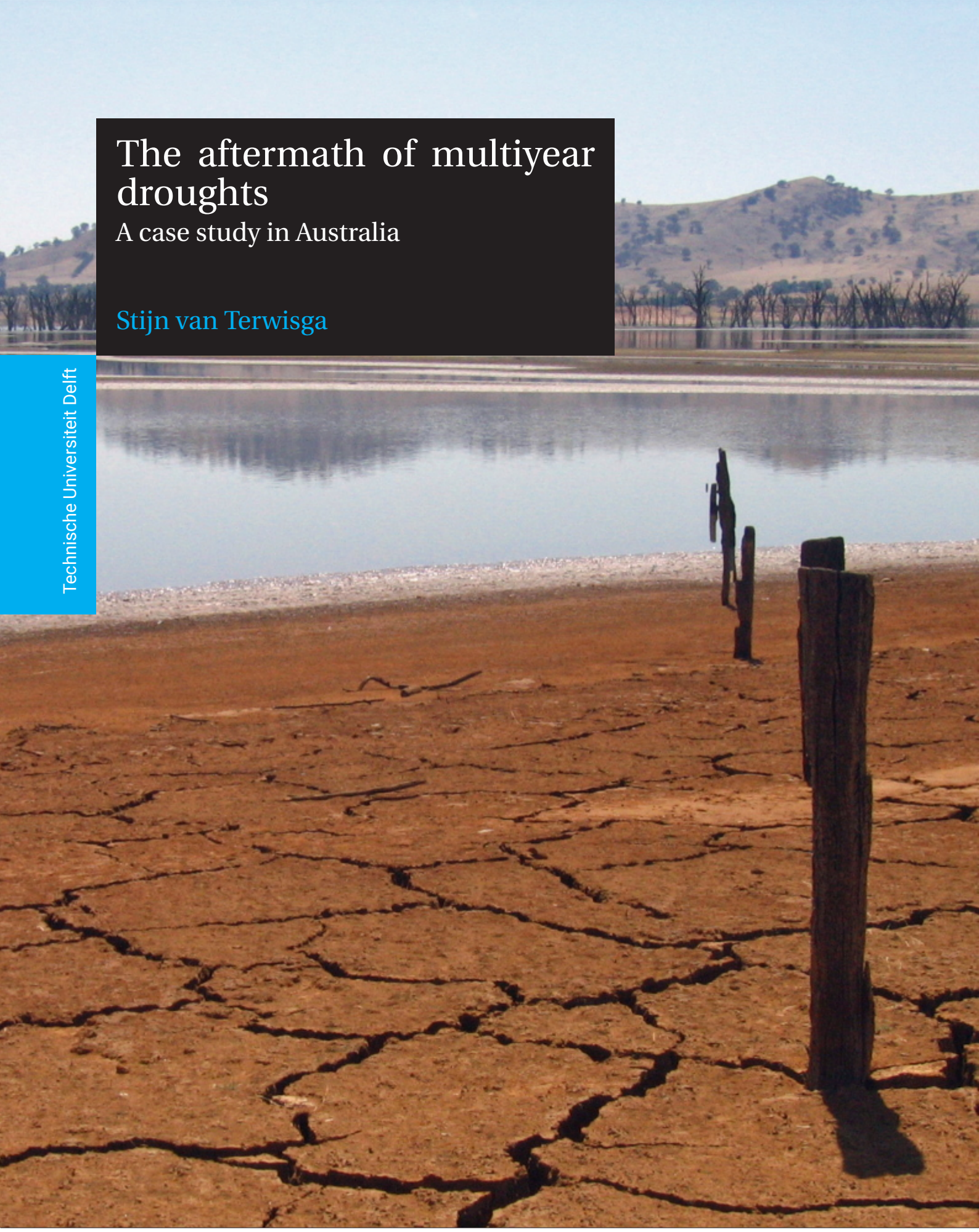

TU Delft Delft University of Technology

Challenge the future

The aftermath of multiyear droughts

A case study in Australia

by

Stijn van Terwisga

to obtain the degree of Master of Science in Civil Engineering
at the Delft University of Technology,
to be defended publicly on Monday August 31, 2020 at 14:00.

Student number:	4383680	
Project duration:	October 1, 2019 – August 31, 2020	
Thesis committee:	Dr. M. Hrachowitz,	TU Delft, supervisor
	Dr. Ir. M. Coenders,	TU Delft
	Dr. M. Vizcaino,	TU Delft

Front cover: Tim J. Keegan. Lake Hume at 4%. February 2007.
https://www.flickr.com/photos/suburbanbloke/381634787/.

TU Delft

Preface

In the past year I have worked on the research topic of droughts in Australia. During the work on my thesis, it has been interesting to see the relevance of my research topic, with the drought and forest fires in Australia and the ongoing drought in the Netherlands.

Firstly, I would like to thank my committee, Markus, Miriam and Miren, for their help and input during the process. Furthermore, I would like to thank all the other graduating students from Water Management for all the table tennis and (virtual) coffee breaks, my housemates for lunch breaks and drinks when working at the faculty was not possible anymore and all my other friends for being there, both in person and digitally. Lastly, thanks to my parents for their support during my complete studies and providing me with a place to work during the final months of my thesis.

Stijn van Terwisga
Delft, August 2020

Summary

In this report the hydrological response to multiyear droughts has been researched. Long-term droughts have resulted in an increase in tree die-off in affected areas. As the hydrological response is related to the vegetation in a catchment, it is of interest to find out whether catchment response regarding rainfall-runoff is different after a long-term drought relative to the situation before the drought. It is important to know this, because a good prediction of water availability is required for making decisions regarding water resources.

The research is conducted in Australia, where a long-term drought took place from 1997 up to 2008. The two research questions that have been investigated during this research are:

- Is there a change in runoff ratio (the fraction of precipitation that becomes runoff) in catchments after a long-term drought relative to the situation before the drought?
- Is there a change in the root-zone storage capacity (the amount of storage available in the root-zone of the soil) determined with the mass curve technique following a multiyear drought?

In this research, the runoff ratio observed after the drought has been compared to the runoff ratio before the drought. This is done to determine whether a change has taken place in the rainfall-runoff relationship of the catchment.

In the catchments where the rainfall-runoff relationship shows a change from the situation before the drought, a decrease in runoff ratio is mostly observed. In 54 out of the 196 analyzed catchments, the runoff ratio is lower than the 10 percentile of the runoff ratio before the drought. In 27 catchments, the runoff ratio after the drought is above the 90 percentile of the runoff ratio before drought. In most of the studied catchments no clear difference in the rainfall-runoff relationship can be found due to a long-term drought.

Factors that were found to play a role in the differences between the responses to a drought were the drought severity, which is a combination of the drought length and the intensity of the drought, and the seasonality of the precipitation. Catchments that had an increase in runoff ratio were more likely to have a longer drought period and a summer-based precipitation pattern.

For the second research question, the root-zone storage capacities have been determined using an earlier derived mass curve technique method, combined with a method that has been developed for recovering ecosystems. In order to compare root-zone storage capacities before and after a drought, a variable is introduced that describes the differences between the values for the root-zone storage capacities before and after the drought.

Catchments that showed an increase in the runoff ratio were also more likely to have a negative change in the root-zone storage capacity. This indicates that the root-zone storage capacity decreases in catchments that show an increase in the runoff ratio after drought.

Contents

List of Figures ix

List of Tables xi

List of Abbreviations and Symbols xiii

1 Introduction 1
1.1 Catchment response to drought. 1
1.2 Research goal and questions 3
1.3 Relevance 3

2 Theoretical background 5
2.1 Droughts 5
2.1.1 Drought indices. 5
2.1.2 Droughts in Australia. 5
2.2 Budyko framework 6
2.3 Change detection. 7
2.4 Root-zone storage capacity 8

3 Research area and data 9
3.1 Catchments. 9
3.2 Data 9
3.2.1 Climatic data 9
3.2.2 Testing climatic data validity. 10
3.2.3 Land use and land cover data 12
3.2.4 Climatic zones 12
3.2.5 Additional spatial datasets. 14

4 Methodology 15
4.1 Approach 15
4.2 Drought 15
4.2.1 Drought index. 15
4.2.2 Timeseries. 17
4.3 Methods for change detection in rainfall-runoff. 17
4.3.1 Basic idea 17
4.3.2 Expectations 18
4.3.3 Sampling 18
4.3.4 Determination of ω. 19
4.3.5 Empirical distribution of ω 20
4.3.6 Factors relating to change in rainfall-runoff 21
4.4 Methods for determining change in the root-zone storage capacity 22
4.4.1 Bucket model 23
4.4.2 Determination of fluxes 23
4.4.3 Interception capacity. 25
4.4.4 Yearly deficit 25

4.4.5 Long-term root-zone storage capacity 26
4.4.6 Recovery of root-zone storage capacity 26
4.4.7 Identification of change in root-zone storage capacity 27

5 Results 29
5.1 Drought identification 29
5.2 Results of detecting rainfall-runoff change 30
5.2.1 Distribution of change rainfall-runoff relationship 30
5.2.2 Changes in rainfall-runoff in Budyko framework 32
5.2.3 Investigation of factors affecting a change in rainfall-runoff 35
5.3 Results of detecting root-zone storage capacity change 41
5.3.1 Pre-drought root-zone storage capacity 41
5.3.2 Change in root-zone storage capacity. 41
5.4 Combined results. 44

6 Discussion 47
6.1 Drought detection 47
6.2 Rainfall-runoff relationship 47
6.2.1 Difference in response between short and long sample lengths 48
6.2.2 Reasons for changing rainfall-runoff relationship 48
6.2.3 Rainfall-runoff change methodology 49
6.2.4 Factors relating to change 50
6.3 Root-zone storage recovery 51

7 Conclusions 55

Bibliography 57

A Additional climatic condition plots 63

B Additional Land Use / Land Cover plots 65

C Comparison with Jaramillo 67

D Uncertainty of ω 69

E Python code 75

List of Figures

2.1 The Budyko framework, with the energy and water limit displayed 7

3.1 The location of all the different catchments of the Hydrologic Reference Stations. Data from Zhang et al. (2016) 10
3.2 All the HRS catchments displayed in the Budyko framework 11
3.3 Fraction of irrigated area for each catchment. Data: Australia Government Department of Agriculture (2016) 12
3.4 Fraction of forest covered area for each catchment. Data is from Australian Government Department of the Environment and Energy (2018) 13
3.5 Fraction of eucalypt covered area for each catchment. Data is from Australian Government Department of the Environment and Energy (2018) 13

4.1 SPEI comparison for an accumulation period of 12 and 36 months for station 405209. The dashed black line is the drought limit of -0.5. 16
4.2 The Budyko framework for different values of ω 18
4.3 The empirical cumulative distribution of ω values for catchment 405209. In this case the sample length is 5 years. 20
4.4 The Budyko framework for catchment 405209. In this case, the Fu equation is displayed for the median value of ω as well as for the 5 and 95 percentiles of ω 21
4.5 Basic display of the used model for the root-zone storage determination 23
4.6 The yearly deficit for a catchment 25
4.7 The monthly estimated transpiration after the drought for catchment 405209 using a water balance of (a) 2 years and (b) 3 years 28

5.1 The distribution of the longest determined drought durations for the 196 catchments used in the analysis. 29
5.2 Distribution of $F(\omega_{after})$ for different sample years 31
5.3 Correlation of $F(\omega_{after})$ for different sample lengths using the Pearson correlation coefficient. 32
5.4 Changes within the Budyko framework before and after the drought for catchments with a value of $F(\omega_{after}) < 0.1$. The arrow displays the change. The sample length is 5 years. 33
5.5 Changes within the Budyko framework before and after the drought for catchments with a value of $F(\omega_{after}) > 0.9$. The arrow displays the change. The sample length is 5 years. 33
5.6 $F(\omega_{after})$ versus the change in evaporative index in case of a sample length of 5 years. Each blue dot represents a catchment. A negative change in evaporative index indicates a decrease in evaporative index over the drought period, while a positive value indicates that the evaporative index has increased. 34
5.7 The drought severity for the different groups of $F(\omega_{after})$ 36
5.8 Mean SPEI after the drought 37
5.9 Aridity index before the drought 38
5.10 Boxplot climate zones 38

5.11 Violinplot Seasonality Timing . . . 39
5.12 Violinplot for forest cover . . . 40
5.13 Difference in NDVI . . . 41
5.14 Histogram for the determined values of the pre-drought S_R . . . 42
5.15 The spatial distribution of S_R . . . 42
5.16 Histogram for the determined values of $\Delta S_{R,1yr}$ . . . 43
5.17 The spatial distribution of $\Delta S_{R,1yr}$ . . . 43
5.18 Violinplot linking the found value of S_R with the changes found in the rainfall-runoff relationship . . . 44
5.19 Violinplot linking the changes found in the rainfall-runoff relationship to the change in root-zone storage capacity. . . . 45

6.1 $\Delta S_{R,1yr}$ compared to a relative change of NDVI. A negative value of $\Delta S_{R,1yr}$ indicates a decrease in the root-zone storage capacity over the drought period, while a positive value indicates an increase. . . . 52
6.2 Comparison for $S_{R,1yr}$ for differing values of I_{max} . . . 53

A.1 Violinplot comparing the drought intensity for the three different groups . . . 63
A.2 Violinplot comparing the drought length for the three different groups . . . 64
A.3 Violinplot comparing the seasonality index for the three different groups . . . 64

B.1 Violinplot comparing the fraction of the catchment covered by Eucalypt trees for the three different groups . . . 65
B.2 Violinplot comparing the max fraction of burned area in a month for the three different catchments . . . 66

C.1 Comparison between results of the method used in this research vs. method used by Jaramillo and Destouni . . . 67

List of Tables

2.1 Drought indices 6

3.1 Climatic zones present in Australia 14

5.1 The three groups that are used in the analysis, with the number of catchments that are in each group. The number of catchments is based on a sample length of 5 years. . . . 32
5.2 Change in evaporative index over the drought period 35
5.3 Statistics for the value of $\Delta_r NDVI$ for the different groups of $F(\omega_{after})$ 40
5.4 Statistics for the value of $\Delta S_{R,1yr}$ 44
5.5 Statistics for the value of $\Delta S_{R,1yr}$ for the different groups of $F(\omega_{after})$ 45

D.1 The values for ω at the 5 and 95 percentile and the difference between these two for a sample length of 1 year and 7 years. 69

List of Abbreviations and Symbols

D	Storage deficit	[L]
E_A	Actual evaporation	[LT^{-1}]
E_P	Potential evaporation	[LT^{-1}]
E_i	Interception evaporation	[LT^{-1}]
E_t	Transpiration	[LT^{-1}]
$F(\omega_{after})$	Variable that describes how the rainfall-runoff relationship after the drought is related to the rainfall-runoff relationship before the drought	[-]
I_{max}	Interception storage capacity	[L]
P	Precipitation	[LT^{-1}]
P_e	Effective precipitation	[LT^{-1}]
Q	Discharge	[LT^{-1}]
S_R	Root-zone storage capacity	[L]
S_i	Interception storage	[L]
$S_{R,1yr}$	1 year root-zone storage capacity	[L]
$\Delta(E/P)_r$	Residual change in evaporative index	[-]
ΔS	Change in storage	[L]
ω	Free parameter in equation of Fu	[-]
AI	Aridity Index	[-]
ECDF	Empirical Cumulative Distribution Function	
EI	Evaporative Index	[-]
HRS	Hydrologic Reference Stations	
KS	Kolmogorov-Smirnov	
NDVI	Normalized Difference Vegetation Index	[-]
SI	Seasonality Index	[-]
SPEI	Standard Precipitation Evapotranspiration Index	[-]

1 Introduction

Droughts are caused by temporary dry conditions in an area (Mishra and Singh, 2010). The effects of droughts are manyfold, differing from a reduction in the production of hydropower to conflicts between humans (Van Loon and Laaha, 2015). Droughts are characterized by a reduction in the availability of water, which can arise in different ways, like a lower amount of streamflow and a reduction in the precipitation (Dai, 2011).

The duration of droughts varies, from a few months to multiple years. Recent examples of multiyear droughts are the drought in California, which lasted from 2012 up until 2019 (National Integrated Drought Information System, nd) and the Millennium drought in Australia, lasting from 1997 up to 2008 (Potter and Chiew, 2011).

In Australia, the occurrence of droughts is related to the occurrence of El Niño (van Dijk et al., 2013). The presence of global warming will lead to more variable and extreme meteorological conditions, which is expected to make droughts more severe and their duration longer (Dai, 2011).

It is therefore of importance to know the effects droughts have on availability of water resources. Previous studies have already investigated the effects of drought on streamflow during the Millennium drought (Saft et al., 2015). However, the effect of droughts are not only limited to the period of the drought, but they can also have effects on the catchment after the drought. An important change that can occur during drought is a shift in vegetation (Mueller et al., 2005). These changes can have a long-term effect on the available water resources in a catchment. It is therefore of value to investigate the hydrological response of catchments after a long-term drought.

In this research a case study will be performed in Australia. Australia has been chosen because of its large data availability and the relatively long time that has passed since the end of the drought, compared to for example California.

1.1. Catchment response to drought

Hydrological response under drought conditions in Australia has been researched extensively (Potter and Chiew, 2011; Saft et al., 2015). Saft et al. (2015) found that during a long-term drought a significant change in the rainfall-runoff response could be found in 46% of the investigated catchments. Part of this change was thought to be related to groundwater declines and changes in deep soil moisture. Furthermore, it was found that a shift in rainfall-runoff was most often present in arid catchments. The effects of vegetation have been mentioned in this research, but have not yet been extensively analysed and was seen as an area for future research. Also, the research of Saft et al. (2015) only focussed on the response during the dry years and not on the response when the precipitation returned to pre-drought levels.

As hydrologic response to rainfall and vegetation characteristics are interrelated, it is important to not only consider the hydrological response, but also the response of the ecosystem during and after a long-term drought.

During droughts, the production of vegetation reduces due to water stress (Ciais et al., 2005; Zhao and Running, 2010). In certain cases, droughts can even lead to dying of trees and other vegetation (Allen et al., 2010; Anderegg et al., 2012; Goulden and Bales, 2019; Lewis et al., 2011; Mueller et al., 2005). As the vulnerability of a forest to mortality due to drought is independent of the mean annual precipitation of that catchment (Choat et al., 2012), it is an incident that can occur in very different climatic areas.

Droughts also increase the effects of wildfires (Anderegg et al., 2012). This happens in two ways. Firstly, the amount of organic material that is present for burning increases due to the increased tree mortality. The second effect on wildfires is due to the extreme temperature conditions during a drought.

A change in hydrological response also has an effect on hydrological models. Hydrological models are used in two main ways. First of all hydrological models are used in research, for testing hypotheses. A second way in which hydrological models are used is for the allocation of water resources (Savenije, 2009).

If models are used to allocate water resources, the model is used to predict water availability. Parameters in these hydrological models are often calibrated to existing data, with climatic data as input and runoff data as output. When the rainfall-runoff relationship changes, oftentimes the parameters that are calibrated to the pre-drought runoff are not valid anymore. This can lead to a bias in the model (Saft et al., 2016), with as a consequence a worse model performance and wrong water availability predictions.

One parameter that is often used in hydrological models is the storage capacity that is generated by the roots of trees. This parameter is often assumed to be static. However, recent research has shown that this is not the case (Gao et al., 2014; Nijzink et al., 2016; Vose et al., 2016).

One of the important components of the vegetation with regard to the hydrological response is the storage capacity that is created in the root-zone of the vegetation. As the vegetation after a drought can differ from before the drought, it is therefore of importance to look into the response of this parameter after a drought.

Currently, the main ways of determining the storage capacity (S_R) in the root-zone are based on catchment soil characteristics and root depths from literature. Another way in which the root-zone storage is determined is by calibrating the model on known runoff values (Nijzink et al., 2016). These methods are not perfect and have some disadvantages, being:

- The root depth approach is not very accurate, as these depths are dependent on climatic and soil characteristics. The measured root depth does not take the climatic conditions into account and oftentimes there are little measurements. Therefore, this method is only valid if the soil type and climate characteristics in the modeled site are equal to the site of the measurement.
- Calibration on runoff values does not give a lot of system knowledge. Furthermore, the root-zone storage capacity determined with this method is not transferrable to differing conditions.

An assumption in these methods is that the value of S_R is constant and does not change over time. The value of S_R is however not a static parameter, as it depends on climate and land cover conditions (Gao et al., 2014). To work with this, a mass curve technique can be applied to a catchment to estimate soil moisture capacity (de Boer-Euser et al., 2016; Gao et al., 2014; Nijzink et al., 2016; Wang-Erlandsson et al., 2016). The mass curve technique assumes that ecosystems evolve to overcome a

drought with a return period of 10-20 years (Gao et al., 2014). The climate-derived values for S_R have shown to be an improvement over soil-derived S_R values de Boer-Euser et al. (2016)

1.2. Research goal and questions

The goal of this research is to determine if there is a difference in catchment response to rainfall after a drought, relative to the situation before drought. If that is the case, the factors that play a role in these changes will be investigated.

To conduct this research, two research questions have been determined. The research questions that will be answered with this research are the following:

1. Is there a change in runoff ratio in catchments after a long-term drought relative to the situation before the drought?
2. Is there a change in the root-zone storage capacity determined with the mass curve technique following a multiyear drought?

The hypotheses belonging to these research questions are the following:

1. Long-term droughts lead to an increase in runoff ratio in a catchment.
2. The effect of a multiyear drought is a reduction in the root-zone storage capacity.

1.3. Relevance

Hydrological models are used in the prediction of water availability. The amount of water that is available is important in making decisions for water resources.

Research from Saft et al. (2016) has shown that models in catchments in which a shift occurs in the rainfall-runoff relationship perform significantly poorer than models in catchments where this shift does not occur. In most cases, the models overestimated the discharge. The shift in rainfall-runoff response is assumed to be an indicator of changes in the catchment characteristics.

It is therefore of importance to gain a better insight in the changes that occur in the catchments during a drought. This will help in improving the performance of models and get a more complete overview of what happens in a catchment during and after a drought.

If the water resources are limited, as is often the case in arid areas, decisions have to be made about the allocation of the available water. If the information on which these decisions are based are incorrect, conflicts can arise. Besides from conflicts, it can also lead to a reduction in water availability downstream.

In wetter areas, flood risk is an important factor to take into account. Incorrect predictions in the incoming discharge can have an effect on society. If the amount of incoming discharge is overestimated, measures will be taken to prevent floodings, like closing floodgates. These measures can be costly and can have other effects on society, like reduction of shipping. Reducing the number of times these measures are taken is therefore preferential.

On the other hand, in case of underestimation of runoff, it may be possible that there will not be any measures taken while they are necessary. In that case, floodings can occur, which can lead to loss of life and material damage.

2

Theoretical background

In this chapter the current state-of-the-art in the literature will be described. The information from this will be used in the methods section to set up an appropriate method and in the discussions to compare the findings to the current literature

2.1. Droughts

The precise definition of a drought does not exist (Mishra and Singh, 2010). As stated in Chapter 1, there are multiple classifications of drought. Often used classifications of drought are (Dai, 2011):

- Meteorological droughts, which are directly related to a decrease in precipitation and an increase in evaporation.
- Agricultural droughts, which are related to low soil moisture availability.
- Hydrological droughts, which are related to deficiencies in hydrological components, like reduced streamflow and lower reservoir levels.

This research will focus on the meteorological drought, which is often characterized by a lack of precipitation (Mishra and Singh, 2010). However, other factors are also important when considering a meteorological drought, like wind speed and temperature (Vicente-Serrano et al., 2009). As these influence the potential evaporation, they have an impact on the available water.

2.1.1. Drought indices

As there is not one method for specifying a drought, different methods have been developed for determining droughts. To identify meteorological droughts, drought indices are often used. Different drought indices calculate the level of dryness in varying manners (Svoboda et al., 2016). Furthermore, the data requirements for indices vary. In all cases, the precipitation is taken into account. However, other factors can also be included if the data is available, like potential evaporation or actual evaporation. In Table 2.1, several different indices are shown, together with the data requirements.

2.1.2. Droughts in Australia

Saft et al. (2015) conducted research into the effect of the Millennium drought on the rainfall-runoff response on a catchment scale. In 73 catchments out of the 158 investigated, a significant change in rainfall-runoff response was found during the drought. Out of those 73 catchments, 68 showed a downward relationship, meaning that the runoff has decreased. The shifts in rainfall-runoff that were found, were more often present in catchments that were less-forested, flatter and had a drier climate.

Table 2.1: Drought indices

Drought index	Abbreviation	Data required	Citation
Standard Precipitation Index	SPI	P	McKee et al. (1993)
Standard Precipitation Evapotranspiration Index	SPEI	P, E_P	Vicente-Serrano et al. (2009)
Drought Reconnaissance Index	DRI	P, E_P	Tsakiris and Vangelis (2005)
Deciles	-	P	

In Australia, dry conditions have led to a die-off of different type of trees (Allen et al., 2010). The occurrence of a large die-off can have diverse effects, like a change in the density of forests and a change in the tree species composition (Anderegg et al., 2012).

2.2. Budyko framework

The Budyko framework (Budyko, 1974), is a simple framework to describe the relation between the climatic forcing and the evaporation index. This is done by comparing the potential evaporation as a fraction of precipitation, the aridity index, to the actual evaporation as a fraction of precipitation, the evaporative index. In this way, the Budyko framework can be used to describe water availability. Because in this research, a change in water availability will be looked into, the Budyko framework can be used in assessing these changes.

Budyko (1974) introduced a curve that describes the way in which the climatic factors lead to discharge. In this simple equation, there are no free parameters. Therefore, in this equation the evaporation is only a factor of the potential evaporation and the precipitation. The Budyko curve is non-linear, meaning that there is a difference in how much the evaporative index changes in response to a change in the aridity index depending on the value of the aridity index. At low values of the aridity index, the changes in the evaporative index are bigger than at higher values of the aridity index.

In Figure 2.1, the Budyko framework is displayed visually. The Budyko framework has two bounds, the energy limit and the water limit. In case of the energy limit, the catchment is bounded by the amount of energy that is available for evaporation, as the potential evaporation is lower than the amount of precipitation. The actual evaporation is therefore bounded by the potential evaporation. If the potential evaporation is larger than the precipitation, which means that the aridity index is larger than 1, the actual evaporation is bounded by the amount of water that is available. In the long term, the total actual evaporation can never be larger than the total precipitation. The limit for the evaporative index is therefore equal to 1.

Additional research has been done on the Budyko framework and several additions have been made to the Budyko curve. Equations with one or more free parameters have been introduced (Fu, 1981; Zhang et al., 2015, 2001, 2004). One example is the equation of Fu (Fu, 1981; Zhang et al., 2004), displayed in Equation 2.1.

$$\frac{\overline{E_A}}{P} = 1 + \frac{\overline{E_P}}{P} - \left(1 + \frac{\overline{E_P}}{P}^{\omega}\right)^{\frac{1}{\omega}} \tag{2.1}$$

In case of the equation of Fu (1981), the free parameter is ω. This parameter does not have a given physical meaning. However, it is often seen as a parameter that is reflective of catchment properties, like soil and vegetative properties. Catchments with a smaller value of ω are often related to low plant available water storage capacity, high precipitation intensity and steep slopes (Zhang et al., 2004).

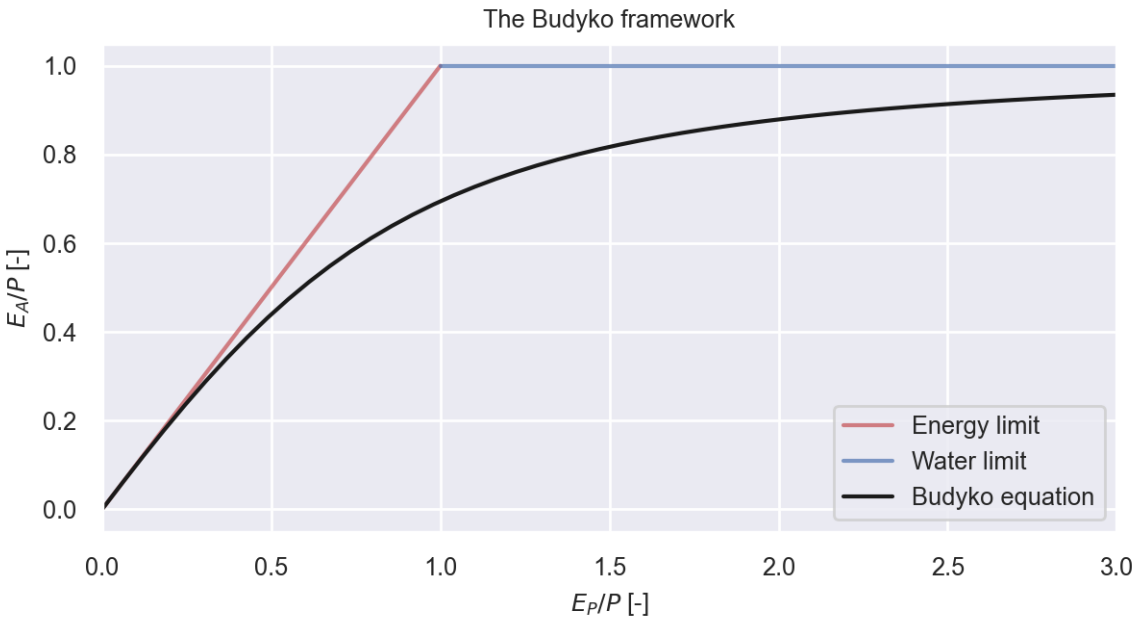

Figure 2.1: The Budyko framework, with the energy and water limit displayed

A new extension to the Budyko framework is the use of a probabilistic model (Greve et al., 2015; Guo et al., 2019). With the probabilistic Budyko model, the uncertainty within the Budyko framework is investigated. In the case of Guo et al. (2019), this is done by using bootstrapping to gather samples of the climatic conditions in the catchment. These climatic conditions are used together with the equation of Fu (Equation 2.1) to determine the ω value of the catchment. The samples are used to generate a confidence interval of the ω value for the catchment. This confidence interval gives an indication on how much water is available within a catchment, given a certain aridity index.

2.3. Change detection

Change detection is used to determine whether a change is present within a timeseries. As this study will go into change after a long-term drought, it is important to consider what change detection methods are used in current research.

In change detection, there is a distinction between two types of change, namely:

- Trend
- Step-change

The difference between these two types of change is that trend is a change that takes place gradually over a long period of time and a step-change is a change that occurs suddenly Rougé et al. (2013).

These changes are often detected by means of statistical testing. Tests that are often used in change detection are the Mann-Kendall test in case of a trend and the Pettitt's test for change in case of a step-change (Kundzewicz and Robson, 2004). However, a problem with these tests is that they do not always detect the expected type of change. Rougé et al. (2013) showed that often trend tests also detects step-change and vice versa.

Another way of detecting change in hydrological timeseries is to make use of the Budyko framework (Jaramillo et al., 2018; Jaramillo and Destouni, 2014; van der Velde et al., 2014). In this case, two separate periods are considered, which are analysed individually. The response in these two periods are thereafter compared. Contrary to the Pettitt's test, where the change point is identified by the test, the time of change has in this case been assumed before performing the test.

In case of Jaramillo et al. (2018), the change that is found within the Budyko framework is separated into change due to a change in climate and a change due to changing catchment characteristics. This is done based on the equation of Choudhoury, which is similar to Equation 2.1. The ω value is determined for the first period. Using the aridity index of the second period, the climatic evaporative index for the second period is determined using the found ω value. This value is compared to the evaporative index for the second period based on runoff measurements. The difference that is found between the climatic evaporative index and the observed evaporative index, gives information about changes in catchment characteristics.

2.4. Root-zone storage capacity

As stated in the introduction, using a mass curve technique to estimate root-zone storage capacities has shown to produce good results (de Boer-Euser et al., 2016; Gao et al., 2014; Wang-Erlandsson et al., 2016). Gao et al. (2014) found that root-zones evolve to overcome a deficit present once every 10 - 20 years.

To determine the value of S_R, yearly determined deficits are fitted to a Gumbel distribution. This Gumbel distribution is then used to determine the deficit value with a return period of 20 years. This is the value used for S_R. Wang-Erlandsson et al. (2016) showed that the performance of modeled evaporation using the mass curve technique had differing optimal return periods, depending on the land cover of an area. Crop and grassland performed better with short return periods, while forests in general performed better when longer return periods were used.

Nijzink et al. (2016) introduced a new variable, $S_{R,1yr}$. The idea behind this variable is that it can be used to determine the recovery of the root-zone storage capacity in a catchment after deforestation. Due to deforestation, the capacity for transpiration (E_t) is reduced. After deforestation, this is expected to increase gradually due to regrowth of forest.

Due to this variability in E_t, a long-term water balance can not be used. However, using a one-year water balance can lead to relatively large storage changes. As a middle ground, a water balance of 2 years is used to estimate the value for E_t. This estimation of E_t is used in the first of the two years to determine the yearly deficit. This yearly deficit is called $S_{R,1yr}$ and is assumed to be the root-zone storage capacity for that year.

3

Research area and data

In this chapter, the research area is presented. Furthermore, the different data sources that are used in the analysis are shown.

3.1. Catchments

As stated in previous chapter, the study area of this research is Australia. For this study the catchments defined by the Hydrologic Reference Stations (Zhang et al., 2016) are used. Data is available for 220 stations, that are spread across Australia. The locations of the different catchments can be found in Figure 3.1. From this Figure, it becomes clear that most of the catchments are located in the southeast of Australia. The larger catchments are located more in the north.

Stations that are used in this dataset are unregulated catchments with minimal land use change. Unregulated means that there are no weirs, dams or other structures present upstream from the discharge measurement. The areas of the catchments differ between 4.5 km^2 and 232,846.0 km^2. The median area is 328.65 km^2.

3.2. Data

For this research data has been collected from different sources. The data that has been used and the sources are described in this section. Furthermore, processing steps that have been taken to preprocess the data are described.

3.2.1. Climatic data

The climatic data that has been used consists of three elements:

- Runoff data
- Precipitation data
- Potential evaporation data

The runoff data comes from the same source as the catchment delineation, the HRS (Zhang et al., 2016). The runoff is given in aggregated daily volumes. Days where data is not available are gap-filled using a calibrated GR4J model (Perrin et al., 2003). The data comes with quality codes for each day, which can be used to assess the quality of the data. For each station, the time period for which data is available differs. The earliest available data is from January 1951 and the newest datasets end in December 2018. However, the exact data availability differs per catchment.

The runoff is given in 1000 m^3 per day. This has been converted to mm per day, to make the data compatible with other data sources. The area that has been used to convert this is the area that is given by the HRS.

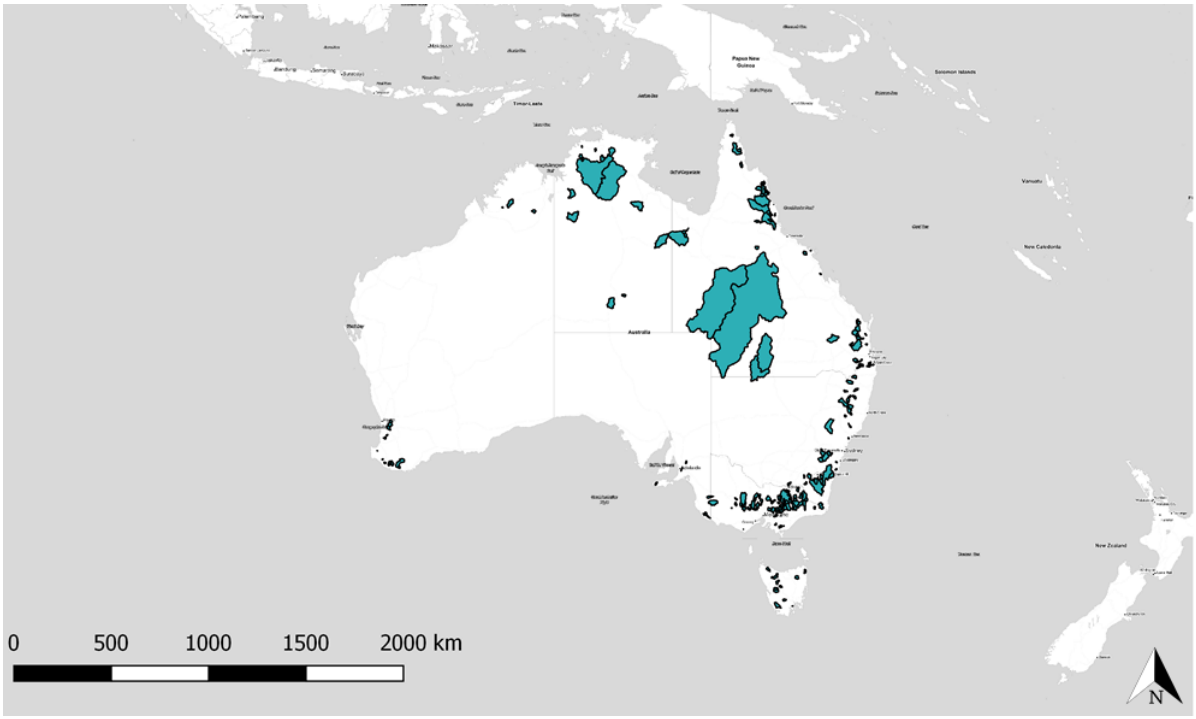

Figure 3.1: The location of all the different catchments of the Hydrologic Reference Stations. Data from Zhang et al. (2016)

The data that is used for precipitation and potential evaporation is from SILO (Jeffrey et al., 2001). The data is supplied as gridded daily precipitation and Morton's potential evaporation. The spatial resolution of the data is approximately 5 x 5 km. As the goal is to work with lumped catchment data, a geographical analysis has been performed to convert the gridded data to a daily value for each catchment. Each raster cell that touches the catchment shapefile, so is either fully or partly within the catchment, is taken into account. For each day the mean value of all these cells is taken to determine the daily precipitation and potential evaporation for the catchments.

The SILO data is available for a longer period than the data from HRS. Only the time period were runoff data is available from the Hydrologic Reference Stations are taken into account for the analysis. Therefore, the data that is used starts in 1951 and runs until 2018.

3.2.2. Testing climatic data validity

As the climatic data is the main input for this research, it is important to test the validity of the data. For testing the validity of the data two tests are performed, namely:

- A water balance test
- A test based on the Budyko framework

Firstly, the water balance is checked for each catchment. If the water balance does not close, it means that there is water that is unaccounted for. Especially since data comes from different sources, this is a real possibility. Possible reasons for inconsistencies could be data errors, interaction between catchments or irrigation.

The equation for the water balance is given in Equation 3.1. However, since the water balance is determined over a long period, the storage change is assumed to be small and is therefore neglected. The water balance without storage change is given in Equation 3.2. In this equation, the complete available timeseries is used.

$$\sum(P-(Q+E_A))+\Delta S=0 \tag{3.1}$$

$$\sum(P-(Q+E_A))=0 \tag{3.2}$$

As actual evaporation data is not available, the potential evaporation is used. Because potential evaporation is always larger or equal to the actual evaporation, the sum of the discharge and potential evaporation should be larger than the total amount of precipitation. The test that is used is displayed in Equation 3.3.

$$\sum(P-(Q+E_P))<0 \tag{3.3}$$

If this condition does not hold, there is a problem with the data. This would mean that this catchment is unsuited for the analysis. In this case all catchments meet the criteria and therefore no catchments are excluded based on this condition.

The second test is based on the Budyko framework. The evaporative index of the catchment, given in Equation 3.4, is required to be within the water and energy limit. As direct measurements for E_A are not available, the average actual evaporation for the timeseries is determined using precipitation and discharge measurements, given in Equation 3.5. Furthermore, the evaporative index should be larger or equal to 0. If this is not the case, the total runoff is higher than the total precipitation. These conditions are given in Equation 3.6.

$$\frac{E_A}{P}=1-\frac{Q}{P} \tag{3.4}$$

$$\overline{E_A}=\overline{P}-\overline{Q} \tag{3.5}$$

$$0\leq\frac{E_A}{P}\leq\begin{cases}\frac{E_P}{P} & if \quad \frac{E_P}{P}\leq 1\\ 1 & if \quad \frac{E_P}{P}>1\end{cases} \tag{3.6}$$

In Figure 3.2, the results of the Budyko test are displayed. All catchments are within the boundaries of Equation 3.6. Therefore, based on this test, all catchments are suited for the analysis.

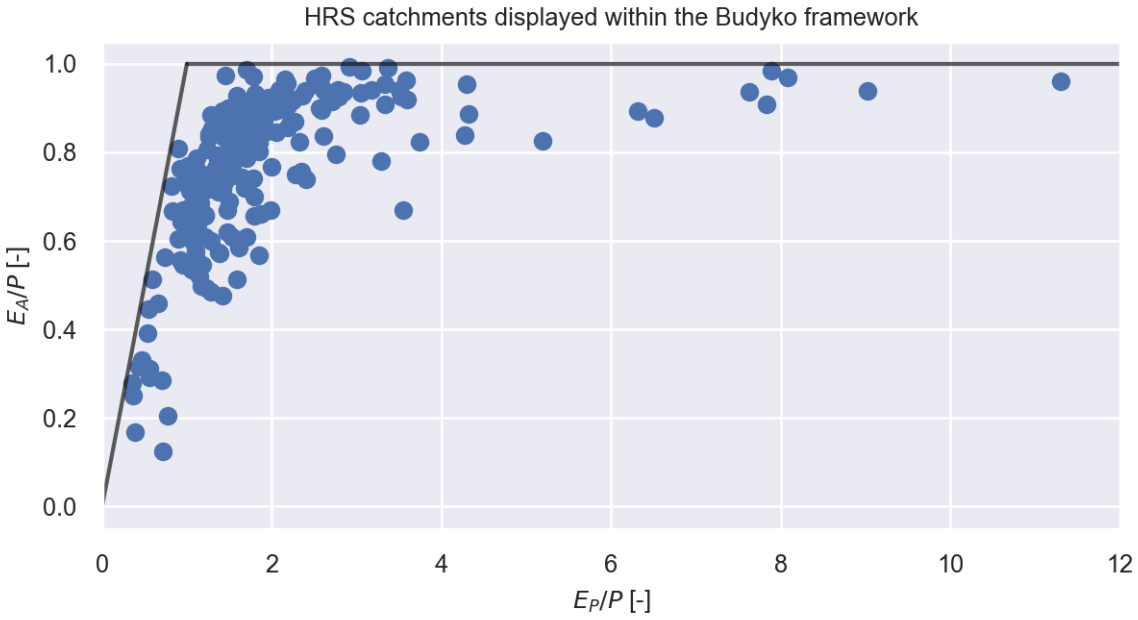

Figure 3.2: All the HRS catchments displayed in the Budyko framework

3.2.3. Land use and land cover data

Land use and land cover data consists of two datasets. These datasets are used to detect irrigation areas and forested areas in catchments.

Land use data is from Australia Government Department of Agriculture (2016). The main use of this dataset is detecting whether there is irrigation present in a catchment. This is important, because it has a large influence on the validity of the water balance.

The data is delivered as gridded data and is aggregated over the catchment. The result of this is a percentage of area of the catchment that is irrigated. As can be seen in Figure 3.3, there is not a lot of irrigation in the used catchments. Based on this no catchments will be excluded.

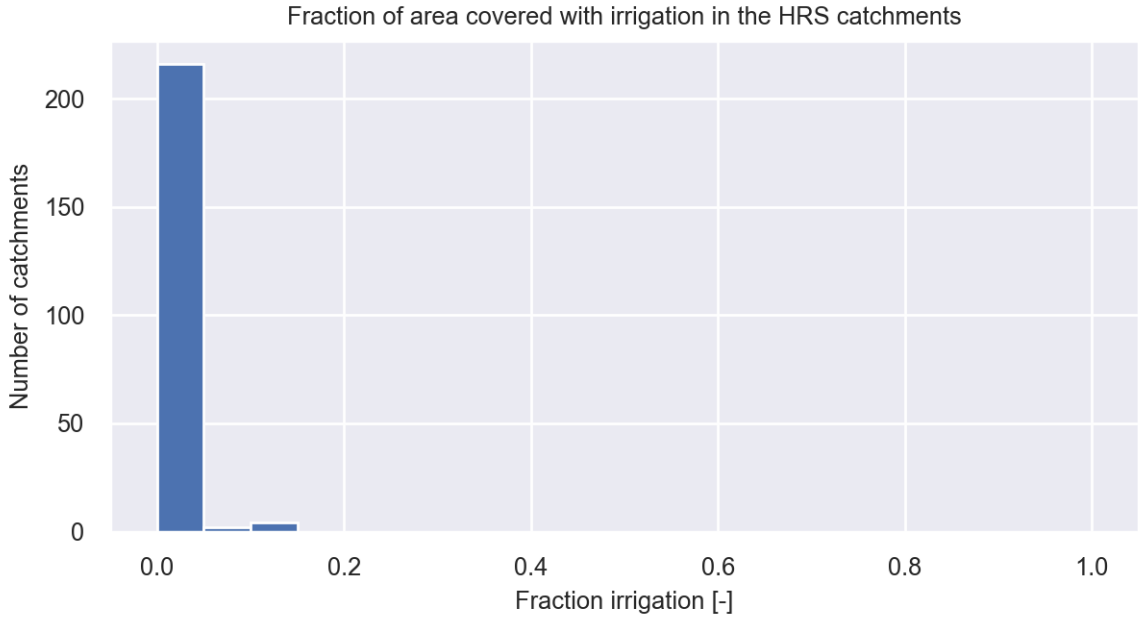

Figure 3.3: Fraction of irrigated area for each catchment. Data: Australia Government Department of Agriculture (2016)

Land cover data is from Australian Government Department of the Environment and Energy (2018). The data from this dataset is used in two ways. First of all it is used to identify the fraction of forested cover in the catchments, displayed in Figure 3.4. Secondly, it is used for identifying eucalypt forests.

Australian forests exist for a large part out of eucalypt forests. This can have an influence on the results, due to the large rooting depth of these types of trees. These can be so deep that the groundwater is reached (Enku et al., 2020). Compared to other trees that do not tap the groundwater, eucalypt trees have a higher resilience to drought. Therefore, the response to drought can be different for eucalypt forests. The distribution of the fraction of eucalypt cover for all catchments is given in Figure 3.5.

3.2.4. Climatic zones

To compare the climates for the different catchments, the Köppen climatic zones have been used. Köppen climatic zones are derived from a global dataset by Beck et al. (2018). The dataset from Beck et al. (2018) contains 30 different classes, of which 12 are present in Australia. The 12 subclasses are combined into 6 main classes, that are presented in Table 3.1.

The dataset by Beck et al. (2018) is a raster dataset, with each raster cell containing the climate class. Some catchments have multiple climatic zones within its boundaries. In this case, the climate class that is present in most cells is determined as the climate class for that catchment. Most of the catchments present in the dataset have a temperate climate with no dry season. Other frequently present climate zones are tropical climates and temperate climates with a dry summer.

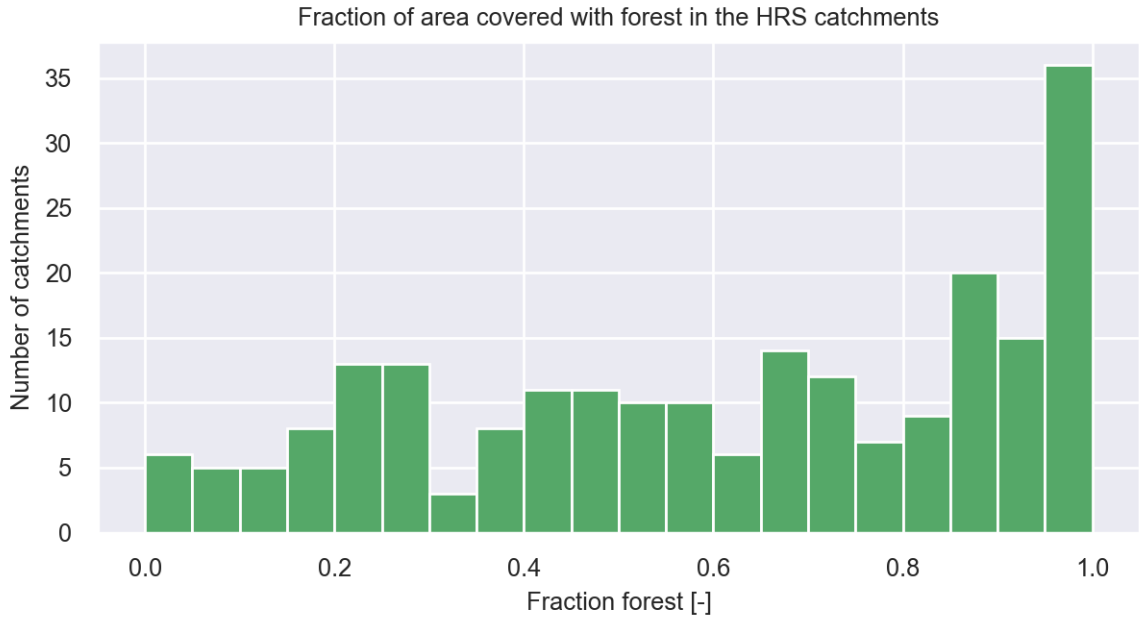

Figure 3.4: Fraction of forest covered area for each catchment. Data is from Australian Government Department of the Environment and Energy (2018)

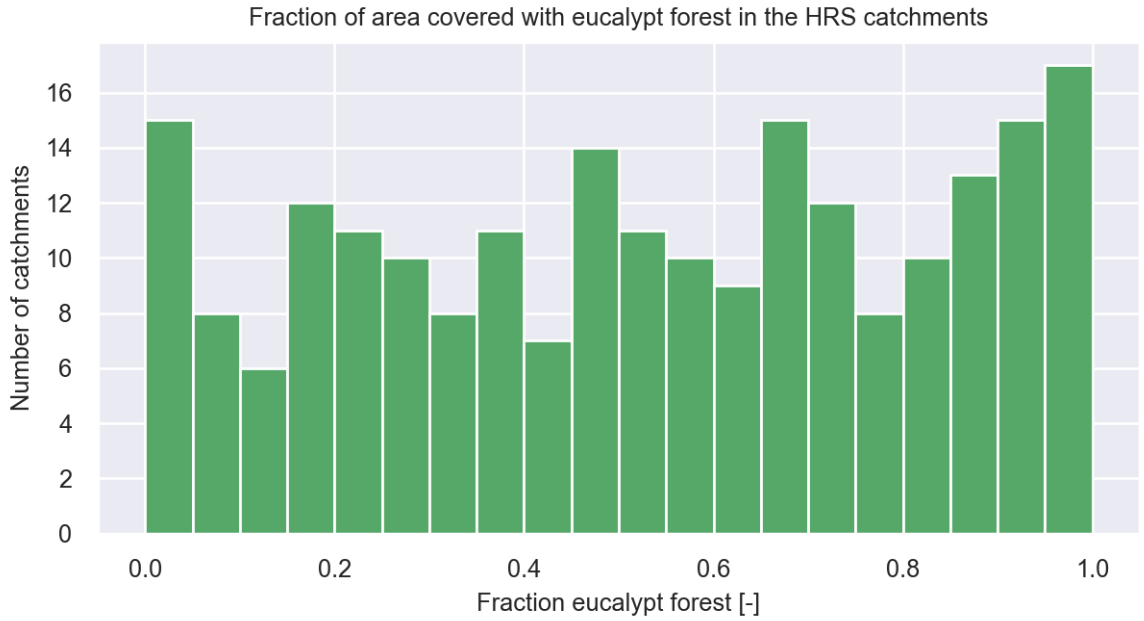

Figure 3.5: Fraction of eucalypt covered area for each catchment. Data is from Australian Government Department of the Environment and Energy (2018)

Table 3.1: Climatic zones present in Australia

Köppen classification	Name	Number of catchments
A	Tropical	28
BW	Desert	5
BS	Steppe	16
Cs	Temperate, dry summer	28
Cw	Temperate, dry winter	10
Cf	Temperate, no dry season	135

3.2.5. Additional spatial datasets

Additional spatial datasets that have been used in this research are NDVI (Didan, 2015) and Burned Area (Giglio et al., 2015) datasets. Both of these datasets are created with data from MODIS satellites. Because these datasets come from the same source, the scripts used for downloading and analyzing the data can be reused for a large part. This reduces the potential for introducing errors and the time needed for data processing.

NDVI

NDVI stands for Normalized Difference Vegetation Index and is an indicator for the presence of vegetation. The NDVI is determined by the amount of near infrared light that is reflected relative to the amount of red light (Didan, 2015). The value of NDVI is between -1 and 1, where a value of 1 indicates a large amount of dense vegetation and -1 indicates water.

The NDVI data is available in different spatial resolutions. For this analysis the coarsest resolution of 1km is chosen, to reduce the size of the data required. As the median area of the catchments is 328 km^2, a finer resolution is not deemed necessary. The temporal resolution of the data is 16 days.

NDVI data from MODIS is available from February 2000 onwards. This means that there is little or no MODIS NDVI data available from before the Millennium drought in most cases.

Data is aggregated per catchment, comparable to the way this has been done with SILO data. The mean value for each time step is used to determine the NDVI value in the catchment.

As NDVI works with reflected light, it is sensitive to cloud cover. This means that if during the overpass of the satellite clouds are present, no value for the NDVI can be determined. Quality codes are present in the data, indicating whether clouds are present in a cell. The pixels that are covered by clouds are replaced by NaN values and are not taken into account when considering the mean NDVI value. If a catchment is fully covered by clouds for a time step, this will result in a NaN value for that time step.

Burned Area

As Australia frequently experiences forest fires and these fires have an influence on vegetation (Anderegg et al., 2012), it is important to have information about forest fires in the research area. MODIS Burned Area is a dataset containing monthly data indicating whether a fire has taken place and the day on which the burning has started. The spatial resolution of this dataset is 500 meter.

The data for the burned area has been processed in a similar way to the NDVI. The difference in this case is that the exact date of the burning is not of real concern. The interest is mainly whether a fire has occurred in grid cell. Therefore, the percentage of burned area in a catchment is determined for each month. This is done by determining the number of cells that are burned and dividing this by the total number of cells in the catchment.

4

Methodology

In this chapter the methodology is described that is used to answer the research questions. Firstly, a short overview is given of how the analysis works as a whole. After this, the methods are explained separately in more detail. The Python code used in this research can be found in Appendix E

4.1. Approach

The analysis of this research consists of three steps, which will be described here in short. In the other sections, the methodology will be described in more detail. The steps that will be followed are the following:

1. Identifying droughts
2. Detecting change in rainfall-runoff
3. Detecting change in root-zone storage capacity

In Section 4.2, the identification of droughts will be explained. Identification of droughts will be done using drought indices. The results from the drought indices will be used to split the timeseries into three groups, namely before, during and after drought. This splitted timeseries is used in the next steps to detect changes in the situation after the drought relative to the situation before the drought.

In the second step, the change in rainfall-runoff will be determined. The situation before the drought is used as a baseline for the situation in the catchment. Subsequently, the situation after the drought will be compared to the baseline situation that was present before the drought. In Section 4.3 this is described in further detail.

The third step consists of detecting the changes in the root-zone storage capacity. In this section, Section 4.4, the method derived by Nijzink et al. (2016) to determine the root-zone storage of recovering systems will be used.

4.2. Drought

In the analysis it is important to have a clear definition of drought and a systematic way of determining what a drought is. In this section the used definition of droughts will be given and the way in which droughts are calculated is explained.

4.2.1. Drought index

For drought determination the Standard Precipitation Evapotranspiration Index (SPEI) has been used (Vicente-Serrano et al., 2009). The advantage of this index over the other frequently used

drought index SPI is that it takes into account both precipitation and potential evaporation. As in this case the precipitation and potential evaporation are available, the use of SPEI will give a completer overview than using the SPI.

One thing to note about the usage of the SPEI is that most catchments in the research area are water limited. An effect of this is that a change in E_P will not always be reflected by an increase in E_A due to the limited availability of water. However, daily estimates of E_A are not available and therefore, using both the potential evaporation and precipitation is considered the best option.

The calculation of the SPEI works as follows:

1. The daily data is aggregated to monthly values. If the first or last month available in the time-series is not a full month, this month will be excluded from the analysis.
2. Calculate the difference between P and E_P.
3. Take the rolling sum of the newly created timeseries for a previously determined accumulation period.
4. Group the summed values by month of the year. For each group the following steps will be taken:
   (a) Fit a general extreme value distribution through the data.
   (b) Use the percent point function to determine the percentile of calculated P - E_P values.
   (c) Use the percentile in a normal distribution with mean 0 and standard deviation 1. This will be the SPEI value for that month

The SPEI determines how dry a period is relative to the full dataset, in which positive values are relatively wet periods and negative values are dry periods. This means that it is a definition of relative dryness, but not yet of drought. A period is determined as a drought if the SPEI value is lower than -0.5. The duration of the drought will then be decided by the amount of months that this value is below -0.5.

As a first estimate an accumulation period of 36 months is used. This is comparable to the rolling mean of 3 years used in Saft et al. (2015). A comparison between SPEI values for an accumulation period of 12 and 36 months is displayed in Figure 4.1.

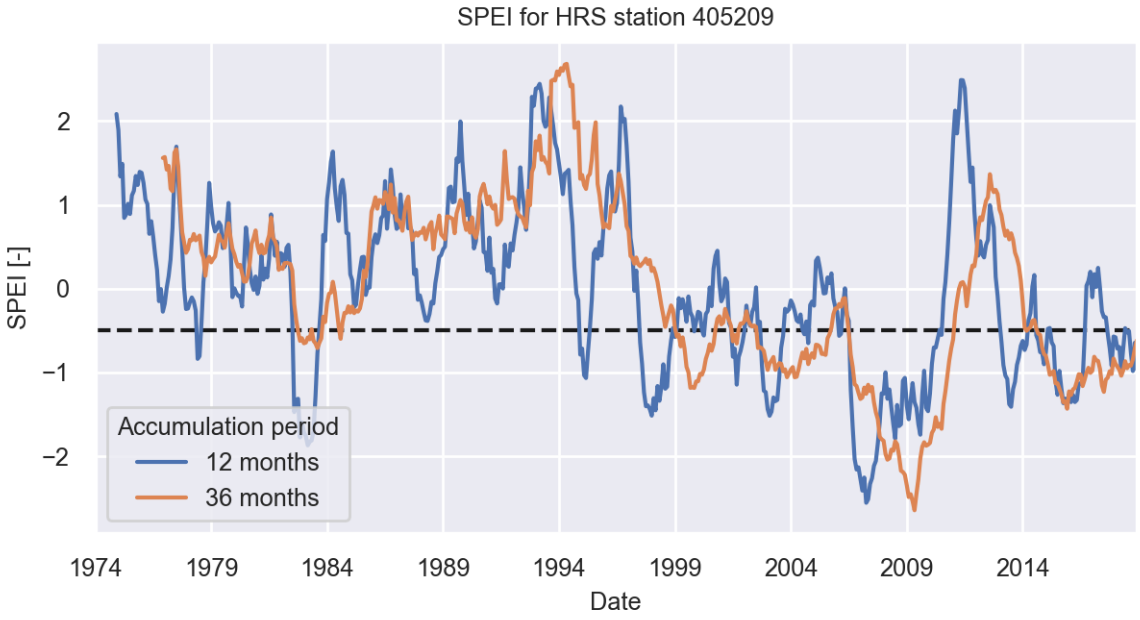

Figure 4.1: SPEI comparison for an accumulation period of 12 and 36 months for station 405209. The dashed black line is the drought limit of -0.5.

An advantage of the accumulation period of 36 months is that this method reacts less quickly than the SPEI with an accumulation period of 12 months. For long-term droughts this prevents a short, relatively wet period to end the drought. A disadvantage, that can be seen in Figure 4.1 is that the drought can start before the 36 month SPEI has a value below -0.5 or that due to the long accumulation period heavy rainfall after a dry period is detected late.

To prevent these disadvantages from having a large effect on the results, the 36 month SPEI is used for a rough estimation of duration and timing of the drought. Subsequently, the 12 month SPEI is used to determine the actual start and end of the drought. The beginning of the drought would in that case be the beginning of the 12 month period when the SPEI is first below -0.5 and the end would be when the SPEI returns back above -0.5.

4.2.2. Timeseries

To compare the different periods, before and after drought, the full timeseries are split into three different shorter timeseries:

- Before drought
- During drought
- After drought

In this research, one drought period will be looked into per catchment. The drought period that will be looked into is the period where the duration of the drought is the longest. If there are multiple droughts in a catchment that are equally long, the first drought occurrence is analysed.

For the period before and during the drought all available data is used. For the period after the drought, the data up to 10 years after the drought has ended is taken into account. For most catchments that are affected by the Millennium drought this means that all available data is used, but for catchments affected by earlier droughts, some data is not used.

Furthermore, to make it easier to compare different catchments, the drought period is clipped to hydrological years. This is done by finding the closest start of a hydrological year for both the start and end date of the drought. The start and end date will than be set to the start of the hydrological years.

An important assumption that is made in this analysis is that the situation before the drought is static, meaning there are no large changes in rainfall-runoff relationship during this period.

4.3. Methods for change detection in rainfall-runoff

In this section the methods that are used to detect a change in rainfall-runoff will be described. The initial steps that are taken are done separately for each catchment.

4.3.1. Basic idea

Determining whether a change in rainfall-runoff has taken place in a catchment will be done using the Equation of Fu (Equation 2.1). The situation before the drought will first be investigated. This is done by using bootstrapping samples from the timeseries before the drought. The ω values for these samples will be determined, which will give an idea about the situation before the drought. The situation that is present after the drought will be compared to the samples that are taken before the drought. This is done for differing sample lengths, from 1 year up until 7 years.

As described in Chapter 2, the Budyko relationship is non-linear. This also means that a certain absolute difference in evaporative index at high aridity indices are more significant than the same difference at an aridity index close to 0. To compare between different catchments, which do not all have the same aridity, using absolute differences will result in larger differences in catchments with an aridity index close to 0. This is the reason that absolute differences are not used, as is done in the method by Jaramillo et al. (2018), but the equation of Fu is used and the ω values are compared before and after the drought.

4.3.2. Expectations

As stated in Chapter 1, the expected result will be that the runoff ratio in a catchment increases due to a decrease in vegetation. This would mean that given a certain value of the aridity index, the evaporative index would decrease. In the previous section the basic idea of the method is described. In this method, the equation by Fu (Zhang et al., 2004) is used to determine the changes in the rainfall-runoff relationship. This equation is comparable to the other frequently used equation of Choudhury (Yang et al., 2008).

In Figure 4.2, a comparison is given for different ω values. As displayed in this Figure, the value of the evaporative index increases with increasing ω, if the aridity index remains constant. If the aridity index in a catchment changes and the evaporative index changes along the same line of the Fu equation, the change is assumed to be purely due to climatic changes. However, if the evaporative index does not change along the same line, so the ω value becomes lower or higher, the catchment characteristics are assumed to have changed.

Given the definition of the Fu equation and the hypothesis that the runoff ratio in catchment increases, this would mean that after the drought the ω value would decrease if the hypothesis is true. If the ω value does not decrease, the hypothesis can not be proven.

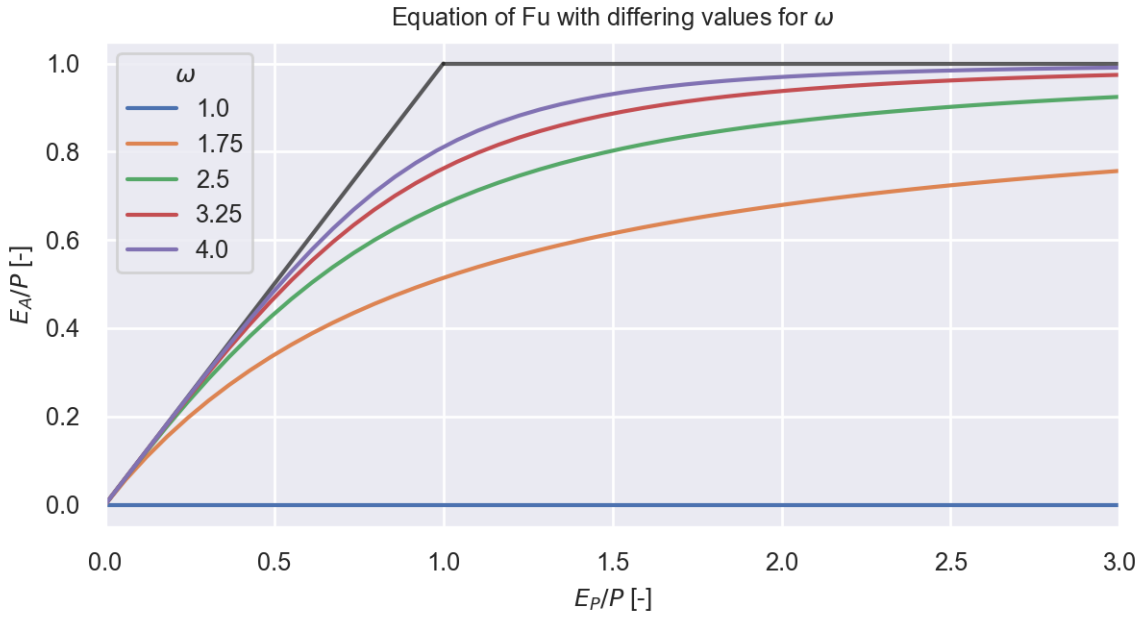

Figure 4.2: The Budyko framework for different values of ω

4.3.3. Sampling

Sampling is done based on the bootstrap methodology. What this means is that a random sample is taken of length N, in which N is the number of years after the drought that the sample will be compared to. This sampling is done using replacement. The advantage of the bootstrapping methodology is that few assumptions need to be made about the underlying data (Kundzewicz and Robson, 2004).

Within years there is a significant influence of seasonality, meaning that there is autocorrelation between data points. Autocorrelation means that there is a relation between points at different timings (Kundzewicz and Robson, 2004). If there is for example a rainy season, the precipitation values at time t are likely to be close to the values of the precipitation value at time $t+365$. The same is the case with potential evaporation. In the summer the potential evaporation is always

higher than the potential evaporation in the winter, so if the value for E_P is high at time t, it is likely to be high at time $t+1$.

To reduce the effects of autocorrelation, yearly data is used instead of daily data. This means that with sampling, full years are chosen instead of days. In this research the length of samples varies from 1 up to 7 years. In case of a sample length of 5 years, 5 random years will be chosen from the underlying dataset. This will be done for all 1000 samples.

The samples will in that case look as follows:

$$[[1964, 1971, 1963, 1993, 1992], \ldots, [1983, 1962, 1951, 1960, 1996]]$$

For each sample length 1000 samples are taken. For each sample, the sum of precipitation, potential evaporation and discharge is determined for all the years. Using this, the aridity index and evaporative index of the sample can be determined. With these, the sample can be positioned within the Budyko framework.

Another possibility which has not been used is to use samples of consecutive years, instead of samples of random years. The advantage of this method is that there are consecutive years that happened, opposed to the sum of random years that are used with the bootstrapping method. This will probably lead to a lower total storage error.

However, there are some disadvantages to this method. First of all, the years at the beginning and the end of the timeseries will be used a lot less. For example, the first year in the series will be only taken into account 1 time, opposed to N times for the years in the middle of the timeseries. Therefore, more weight is given to the middle of the timeseries for the consecutive years method. Secondly, the number of datapoints in case of the consecutive years method is limited. The bootstrapping method can be used to derive confidence intervals of the underlying target (Guo et al., 2019), which can be used to determine whether the after drought situation is within these confidence bounds.

4.3.4. Determination of ω

In the previous subsection, the determination of the aridity index and evaporative index for each sample is explained. With these known, the equation of Fu (Zhang et al., 2004), given in Equation 4.1, can be used to determine the ω value. This will give an indication how much water will be used for evaporation given a certain level of aridity.

$$\frac{E_A}{P} = 1 + \frac{E_P}{P} - \left(1 + \left(\frac{E_P}{P}\right)^{\omega}\right)^{\frac{1}{\omega}} \tag{4.1}$$

To find the ω value belonging to the evaporative index and aridity index, the function in 4.1 is minimized. The full minimization equation is given in Equation 4.2. This function is squared so that the minimum value will be found when the left and right side of Equation 4.1 are equal to each other. In this case the value of Equation 4.2 will be equal to 0. If it is not squared, the minimum is found when the value of the term with ω is largest. Using a squared function ensures that the minimization function returns the ω value where the left and right term of Equation 4.1 are equal to each other.

$$\left(1 + \frac{E_P}{P} - \left(1 + \left(\frac{E_P}{P}\right)^{\omega}\right)^{\frac{1}{\omega}} - \frac{E_A}{P}\right)^2 \tag{4.2}$$

Besides the samples from before the drought, the ω value has also been determined for the timeseries after the drought. After the drought, one sample is used. This is the sample directly after the drought period. The length of the sample is equal to the length of the samples that it is compared with, so it differs from 1 to 7 years.

In a small amount of cases a sample is not within the energy or water limit. For the complete timeseries a test has been performed whether catchments are within the bounds of the Budyko framework, as described in Section 3.2.2. However, with a shorter length of the dataset the data is not always within these bounds anymore. For these samples, the Fu equation can not be fitted to the data, as this equation is only valid within the Budyko limits. However, if this data point is removed, the information regarding the high evaporative index from this sample will not be considered. Therefore, it has been decided to take these data points into account with an ω value of 20. This ω value is high and therefore it is unlikely that the sample after drought will be higher than this value.

4.3.5. Empirical distribution of ω

Using the obtained ω values for all different samples, a distribution for these ω values can be generated. The distribution of the ω values give an idea of the range of the rainfall-runoff relationship before the drought. Given that after drought there may be a different aridity index, it is hard to compare actual evaporative index values. Using the equation of Fu makes sure that values can be compared, even with differing aridity indices.

The distribution generated by all the values before the drought is an empirical distribution, which is given in Figure 4.3. This distribution can be used to generate 5% and 95% confidence curves for the Budyko framework. This gives an idea what the conditions in the catchment were before the drought. A visual example of this is given in Figure 4.4.

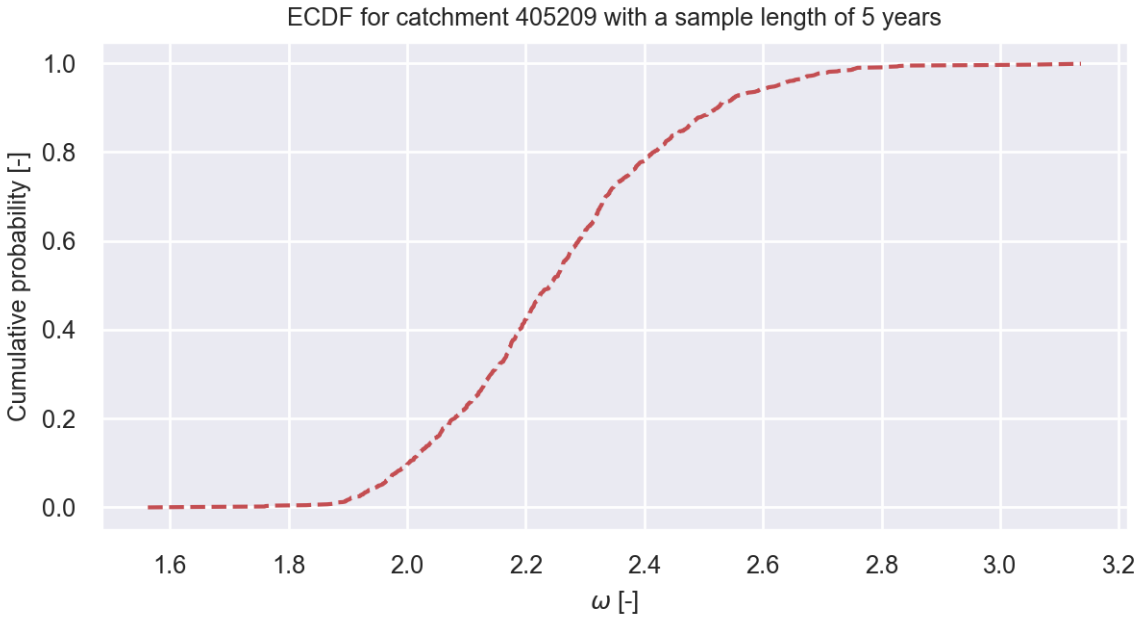

Figure 4.3: The empirical cumulative distribution of ω values for catchment 405209. In this case the sample length is 5 years.

The distribution that is created by this method can be compared to the ω value that is found after the drought. This gives a position on the cumulative distribution function, which describes how the rainfall-runoff relationship that is found after the long-term drought is related to the rainfall-runoff relationship observed before the drought. The way in which this is calculated is by determining the number of samples with an ω value smaller than the ω value after the drought. This value will be divided by the total number of samples. The name for this value will be $F(\omega_{after})$. This is done for each catchment and all the different sample lengths.

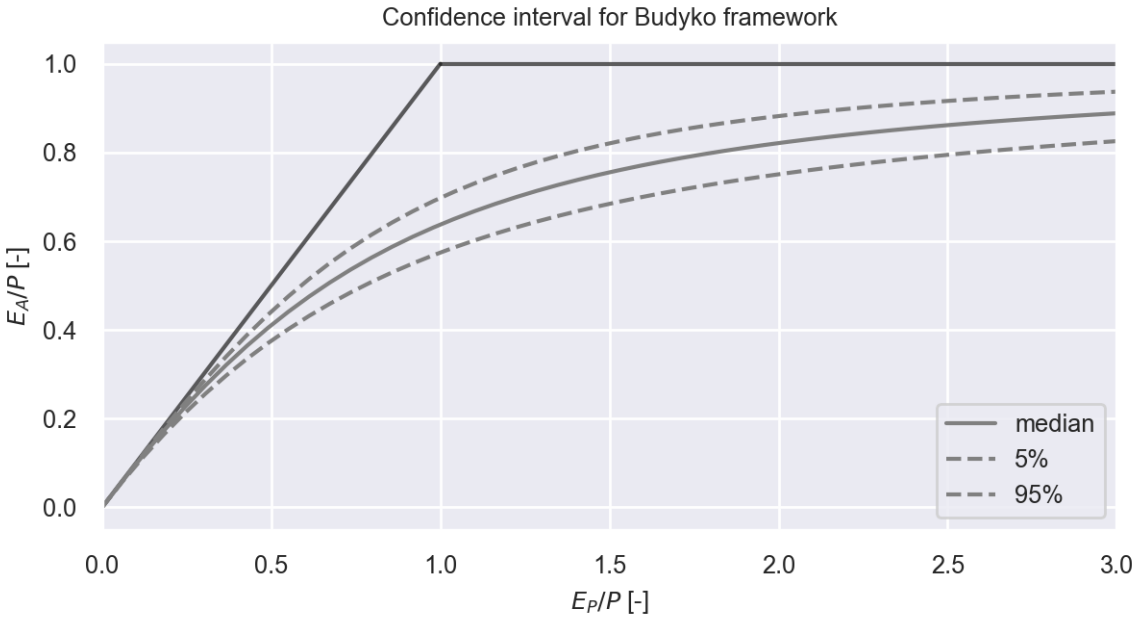

Figure 4.4: The Budyko framework for catchment 405209. In this case, the Fu equation is displayed for the median value of ω as well as for the 5 and 95 percentiles of ω

4.3.6. Factors relating to change in rainfall-runoff

To determine whether different responses in catchments can be explained, the values found for $F(\omega_{after})$ will be compared to several different factors which could have a relation to the change. Factors that will be looked into are:

- Drought severity
- SPEI after drought
- Aridity index before drought
- Climatic zone
- Seasonality
- NDVI
- Forested cover
- Eucalypt cover

Some factors that need additional explanation are discussed below.

Seasonality index

The seasonality index is calculated based on the method described by Gao et al. (2014). The seasonality index that is used is the seasonality of the precipitation. For the calculation of the seasonality index, two factors need to be determined, namely the mean annual precipitation and the mean precipitation for each month of the year. If these are known, the seasonality index can be determined using Equation 4.3, in which t is the number of the month (January = 1, December = 12).

$$SI = \frac{1}{\overline{P_a}} \sum_{t=1}^{12} \left| \overline{P_m}(t) - \frac{\overline{P_a}}{12} \right| \tag{4.3}$$

The seasonality index is 0 in case of no seasonality. In that case $P_m = \frac{P_a}{12}$ for each month. In the case where all precipitation falls in one month, the seasonality index is $1\frac{5}{6}$. This means that the catchment is very seasonal. In most cases the value of the seasonality will be in between these two values.

The calculation of the seasonality index is done based on the complete dataset, meaning time-series before, during and after drought are taken into account.

Seasonality timing index

The above mentioned seasonality index only takes into account the timing of the precipitation. To combine both precipitation and potential evaporation, the dimensionless seasonality timing index is used (Berghuijs et al., 2014; Berghuijs and Woods, 2016).

Compared to the seasonality index, the value of seasonality timing index can be both positive and negative, in which the absolute value indicates the amount of seasonality and the sign indicates the timing of the seasonality. A negative value indicates that the precipitation is mostly winter-dominant, while a positive value indicates a summer-dominant precipitation regime.

NDVI

The difference in NDVI is calculated as the difference between the NDVI 3 years before the drought and the NDVI 3 years after the drought. In this case the NDVI before the drought is taken as a baseline, assuming that normal vegetative conditions are in place. Therefore, the difference in NDVI is divided by the mean NDVI before the drought. This will be the relative difference in NDVI. If the drought has an influence on the NDVI, it is expected to be lower, following the hypothesis of lower vegetative cover.

The relative difference in NDVI is calculated as follows:

$$\Delta_r NDVI = \frac{NDVI_{after} - NDVI_{before}}{NDVI_{before}} \tag{4.4}$$

A problem with the MODIS NDVI data is that it is only available from 2000 onwards, meaning that it is not possible to calculate the NDVI difference for the catchments which longest drought was before the Millennium drought.

Drought intensity and drought severity

Two factors that are considered regarding the conditions during the drought are the drought intensity and the drought severity. The drought intensity is defined as the minimum SPEI value that is present during the drought. The drought severity combines the duration and intensity of the drought. It is the summed value of the 12 month SPEI values during the drought (McKee et al., 1993). A short, intense drought can in this case have a larger value than a longer, less intense drought.

Kolmogorov-Smirnov Test

To compare low and high values of $F(\omega_{after})$, the two sample Kolmogorov-Smirnov test is used. The Kolmogorov-Smirnov test is used to determine whether two samples are from the same distribution. This test uses no assumption on the distribution of the underlying data (Young, 1977). The null hypothesis is that the two distributions are from the same distribution. The alternate hypothesis is that the two samples come from a different distribution.

4.4. Methods for determining change in the root-zone storage capacity

In this section the methods that are used for detecting a change in root-zone storage capacity are explained. The methods that are used in this section will be used to answer the second research question. First, an introduction is given of the model that is used and its fluxes are described, after which a description is given of how the root-zone storage capacity is determined and finally a method is introduced to compare root-zone storage capacities before and after a drought.

4.4.1. Bucket model

The model that is used in the determination of root-zone storage capacities can be described as a bucket model. In Figure 4.5, the basic model outline for the determination of the root-zone storage capacity is displayed. The way in which the fluxes in the model are determined, is discussed in later sections. The model consists of two reservoirs namely:

- Interception reservoir
- Root-zone storage reservoir

The interception reservoir has one incoming flux and two outgoing fluxes. The incoming flux is the precipitation (P) and the outgoing fluxes are the interception evaporation (E_i) and the effective precipitation (P_e). The maximum volume of the interception reservoir is I_{max}

The effective precipitation is an influx into the root-zone storage reservoir, which has a maximum storage capacity S_R. The outgoing fluxes are the evaporative flux (E_t) and the discharge (Q). The discharge does not always turn into streamflow immediately, as it will first go to deeper groundwater layers.

Initially, the value for S_R is an unknown value and has to be determined. The way in which this is done is by assuming that in the beginning the storage in the root-zone storage reservoir will be equal to the value of S_R. In that case, any amount of effective precipitation that will not evaporate, will turn into runoff. If more water evaporates than the effective precipitation, the storage in the reservoir will decrease.

As the value of S_R is not yet known, it is initially set as being infinitely large. The decrease in the reservoir relative to the initial storage will be called the deficit. This is the amount of water that should be in the reservoir to accommodate the fluxes present in the catchment.

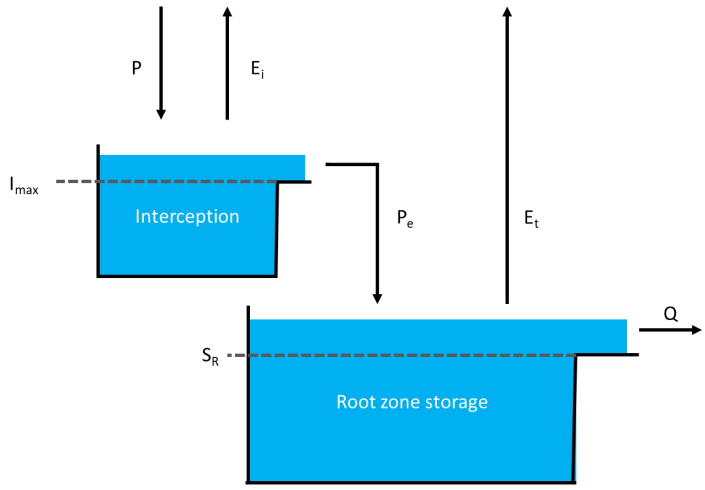

Figure 4.5: Basic display of the used model for the root-zone storage determination

The model presented is simplified, as it assumes all effective precipitation will infiltrate into the soil and ignores processes like Hortonian overland flow.

4.4.2. Determination of fluxes

To determine the deficit, the fluxes present in the model have to be known. The fluxes that will be determined are the interception evaporation, the effective precipitation and the transpiration.

By determining the transpiration, the value for the other two fluxes can also be determined. The transpiration in a catchment is determined in three steps, namely:

1. Determine the daily potential evaporation
2. Determine the average daily transpiration
3. Determine the daily transpiration

Daily potential evaporation

In Section 3.2, the used data sources are described. One of the datasets that is used is potential evaporation. However, this potential evaporation is available to both interception and transpiration. It is assumed that transpiration only takes place when the interception bucket is completely empty. The amount of water present in the interception bucket in the described bucket model is determined with Equation 4.5. The amount of evaporation used for interception is determined with Equation 4.6. It is assumed that if there is capacity for interception evaporation, this will be evaporated. This amount will be subtracted from the initial potential evaporation to determine the residual potential evaporation available to transpiration, which is also given in Equation 4.8.

$$\frac{dS_i}{dt} = P - E_i - P_e \tag{4.5}$$

$$E_i = \begin{cases} E_P & if \quad E_P dt < S_i \\ \frac{S_i}{dt} & if \quad E_P dt \leq S_i \end{cases} \tag{4.6}$$

$$P_e = \begin{cases} 0 & if \quad S_i \leq I_{max} \\ \frac{S_i - I_{max}}{dt} & if \quad S_i > I_{max} \end{cases} \tag{4.7}$$

$$E_{P,res} = E_P - E_i \tag{4.8}$$

Average daily transpiration

The average daily transpiration is determined using the water balance method, in which the storage change is neglected. This assumes that the precipitation that is available is equal to the sum of the discharge and evaporation. As the effective precipitation can be calculated, using the method described in the above section, all necessary data is available. The mean daily evaporation can therefore be determined with Equation 4.9.

$$\overline{E_t} = \frac{\sum_{t=0}^{T} P_e(t) - Q(t)}{T} \tag{4.9}$$

In this equation T is the total amount of time steps available, which is the complete timeseries before the drought. The result of this will be the average daily transpiration in the catchment in mm/day.

Daily transpiration

The daily value for the transpiration is determined by scaling the mean transpiration to the potential evaporation. For potential evaporation, daily values are available. The average daily value for potential evaporation can be determined using Equation 4.10. The found value for the mean potential evaporation is used in Equation 4.11 to determine a daily estimate for the transpiration. It should be noted that this is an estimation of the value for E_t and the actual value for E_t can be different.

$$\overline{E_{P,res}} = \frac{\sum_{t=0}^{T} E_{P,res}(t)}{T} \tag{4.10}$$

$$E_t(t) = E_{P,res}(t) \frac{\overline{E_t}}{\overline{E_{P,res}}} \tag{4.11}$$

4.4.3. Interception capacity

An important parameter in determining the transpiration is the interception capacity in the catchment. The water in the interception reservoir is evaporated before any other evaporation takes place. Furthermore, the interception reservoir prevents part of the water from reaching the soil.

In general, a larger I_{max} gives a smaller deficit. The reason for this is that the total leftover capacity for evaporation is smaller in case of a higher interception. Therefore $\overline{E_t}$ is smaller. As this is scaled with the value of potential evaporation, the value of E_t will be smaller. Another effect of a larger interception capacity is that the effective precipitation is smaller. However, in the dry months this value will be relatively small anyway. Therefore the maximum value for deficit will be smaller in case of a large interception capacity compared to a case with small interception capacity.

In this research, the interception capacity is 2 mm for each catchment. This value is based on the research by Nijzink et al. (2016), in which the interception capacity that has been used is between 1 and 5 mm.

4.4.4. Yearly deficit

The precipitation deficit is determined using the method derived by Nijzink et al. (2016). A daily precipitation deficit is determined by subtracting the effective precipitation from the determine evaporation, calculated with Equation 4.12. The daily deficit is used in determining the total deficit, calculated with Equation 4.13. The total deficit starts at 0 at t = 0. For each hydrological year, the maximum deficit that is present in that year is determined. An example of the deficit is displayed in Figure 4.6.

$$D(t) = E_t(t) - P_e(t) \tag{4.12}$$

$$D_{tot}(t) = \max(D_{tot}(t-1) + D(t), 0) \tag{4.13}$$

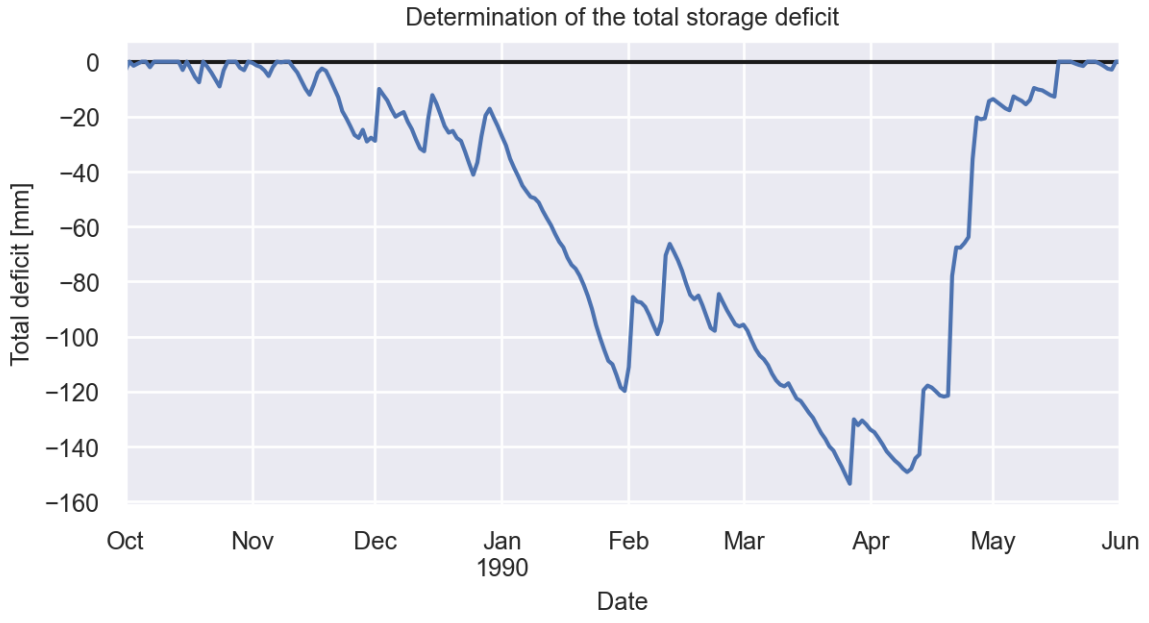

Figure 4.6: The yearly deficit for a catchment

A problem that can occur with this method is that in dry years the cumulative deficit will not return to zero in a hydrological year. When a Gumbel distribution is used, a yearly maximum deficit value is required. If for the next year the maximum deficit is used as described above, this will not be in

accordance with the physical world. The reason for this is that the deficit in the previous year is also taken into account in the next year. To overcome this a method has been used to determine the deficit of the hydrological year.

In this method the yearly maximum value is determined first. The day of occurrence of this maximum value is used to clip the timeseries and determine the minimum value that occurred before this. Consecutively, the storage deficit is determined by subtracting the minimum value from the maximum value.

In summary, the process for determining the yearly storage deficit is as follows:

1. Determine the deficit for the whole timeseries
2. Split the timeseries in hydrological years. For each of these years:
   (a) Determine the value and the date of occurrence of the maximum deficit
   (b) Clip the hydrological year to the date of occurrence
   (c) Determine the minimum value in the new timeseries
   (d) Subtract the minimum value from the maximum value

A problem that was detected when using method is that the maximum yearly deficit sometimes occurred around the same time as the start of the hydrological year. Due to this the maximum value of the hydrological year was either very close to the start of the hydrological year, causing the minimum to be high as well, or near the end of the hydrological year. This also has the effect that dry years can be taken into account twice.

To overcome this, a root-zone year has been defined. This is done by determining the maximum deficit for each month in the timeseries. Subsequently these values will be summed by month of the year. The month where this total deficit over all years is minimal will be chosen as the start of the root-zone year. This is done because the chance that the deficit is largest in this month is small.

4.4.5. Long-term root-zone storage capacity

The yearly deficits that have been found are used to determine the long-term root-zone storage capacity S_R using the timeseries before drought. In earlier studies it has been found that the root-zone storage capacities are evolving to overcome deficits of 10 - 20 years (de Boer-Euser et al., 2016; Gao et al., 2014). Therefore, the found yearly deficits were fitted to a Gumbel distribution. The value of S_R is the value of the fitted Gumbel distribution with a return period of 20 years.

4.4.6. Recovery of root-zone storage capacity

The hypothesis of this research is that during drought the root-zone storage capacity will decline. After the end of the drought, this storage capacity should restore to pre-drought levels. This restoration process is described in Nijzink et al. (2016).

The way in which recovery was determined in his research is by determining the water balance for a 2-year period. It is assumed that for this period the change in storage is negligible. The amount of precipitation that has evaporated can be calculated in the same way as is done in the determination of long-term S_R.

The evaporation will be scaled to the potential evaporation in the two-year period. After this is done, the second year will not be considered anymore.

For the first year, the deficit is calculated in the normal way. This will return a maximum deficit. As the deficit in this year starts at zero, the minimum deficit will always be zero, so the maximum deficit in a year is also the cumulative yearly deficit.

In this research the period that is used to determine the water balance is 3 years, compared to the 2 years used by Nijzink et al. (2016). This decision is based on the difference that were found in determined transpiration using different lengths for the water balance, the results of which can be found in Figure 4.7. In this figure, the determined E_t values are compared. Because the water

balance is determined using multiple years of data, the evaporation for a year is also determined multiple times with differing data.

In reality, the evaporation for the same year should be equal. As can be seen from Figure 4.7, this is not the case, either due to an violation of the assumption of no storage change, measurement errors or an imperfect assumption in converting the potential evaporation to transpiration. A water balance of 2 years gives a large difference between the two different determined E_t values. In the case of a water balance of 3 years, these differences that are present are already a lot smaller. This is the reason that a water balance of 3 years has been chosen in the determination of the $S_{R,1yr}$ values.

4.4.7. Identification of change in root-zone storage capacity

To identify if there is a change present in the root-zone storage capacity after a drought, the situation before drought is compared to the situation after the drought.

Because the root-zone storage capacity after drought is assumed to be non stationary, $S_{R,1yr}$ has to be used in this period. In order to prevent the introduction of methodological inconsistencies, $S_{R,1yr}$ is also used for the situation before the drought. The way in which this is done is by determining the value for $S_{R,1yr}$ for all years as was described in Section 4.4.6, both before and after the drought.

The usage of $S_{R,1yr}$ in catchments under changing conditions has been done before by Nijzink et al. (2016). This study showed that after deforestation, a change in $S_{R,1yr}$ was present, with lower values for $S_{R,1yr}$ in catchments with a shift in vegetation, compared to catchments that did not have a change in vegetation. After recovery has taken place, a new equilibrium was found. Therefore, if there is a die-off in vegetation, it is expected that values of $S_{R,1yr}$ after the drought decrease relative to the situation before the drought.

The root-zone storage capacities before and after drought are compared in the following way:

$$\Delta S_{R,1yr} = S_{R,1yr,after} - S_{R,1yr,before} \tag{4.14}$$

In this equation, the values for $S_{R,1yr,before}$ and $S_{R,1yr,after}$ are the median values of the determined $S_{R,1yr}$ values for the different periods. The median value is used to get an idea about the $S_{R,1yr}$ values. As there are sometimes outliers present in the distribution of $S_{R,1yr}$, using the mean could give a heavy weight to these outliers. Therefore, the median is used as the better option.

For the timeseries after the drought, the full timeseries after drought as described in Section 4.2 is used. This means that if 10 years are available this is used. However, as 3 years are needed for the determination of the transpiration, only a maximum of 8 years are considered regarding the value for $S_{R,1yr}$.

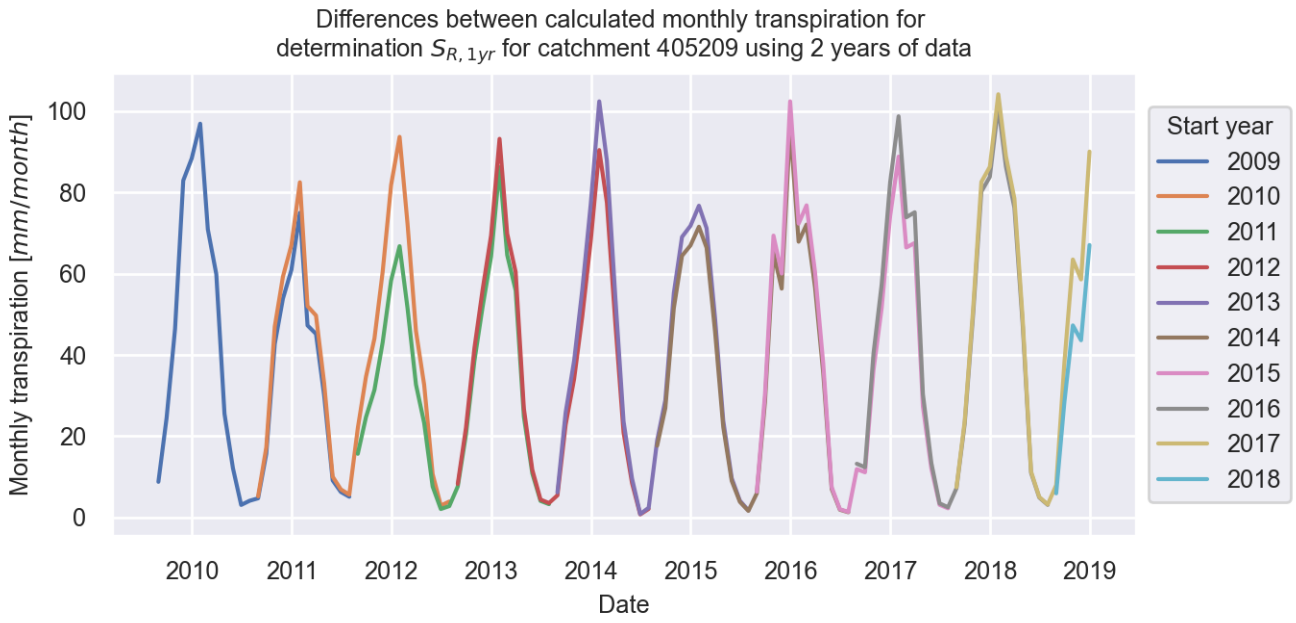

(a)

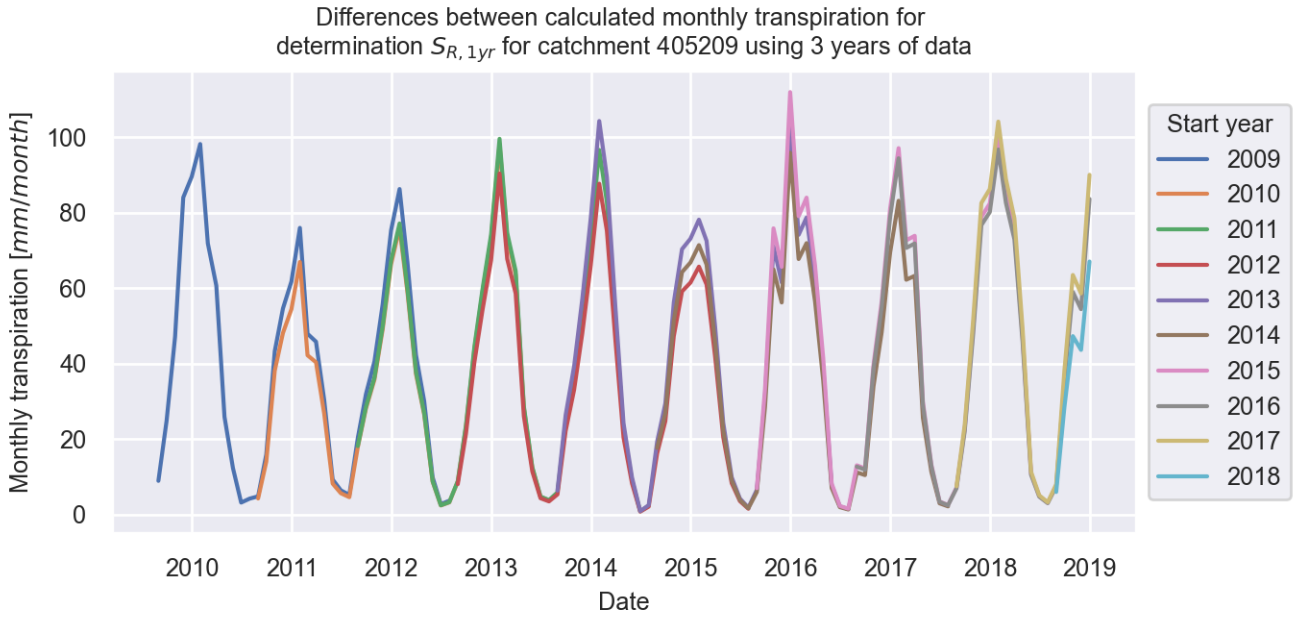

(b)

Figure 4.7: The monthly estimated transpiration after the drought for catchment 405209 using a water balance of (a) 2 years and (b) 3 years

5
Results

In this section the results are discussed. First, the drought identification is shown, after which the results of the change in rainfall-runoff are given. This is followed by the results of the root-zone storage capacity. In the last section, the results of the change in rainfall-runoff and change in root-zone storage capacity are combined.

5.1. Drought identification

The drought is identified using the SPEI as described in Chapter 4. Catchments where the number of days with available data after the drought is less than 1500 days are excluded from further analysis. This is the case for 24 of the 220 catchments. The number of catchments that are analysed is therefore 196. The drought in a catchment is determined to be during the Millennium drought if the start of the drought is later than 1995. In 150 of the 196 catchments the longest drought is during the Millennium drought. In 46 catchments the drought starts earlier.

The median duration of the identified droughts is 1826 days. In Figure 5.1 the distribution of the drought length is displayed. There are two peaks present in the drought duration, one is with a duration of 4 to 5 years and one with a duration of 8 years.

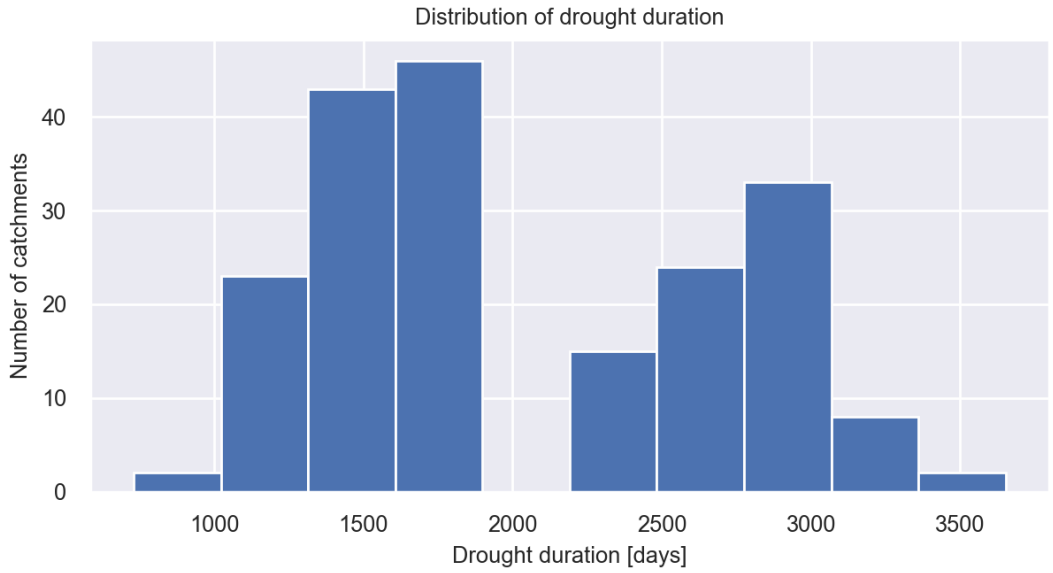

Figure 5.1: The distribution of the longest determined drought durations for the 196 catchments used in the analysis.

5.2. Results of detecting rainfall-runoff change

In this section the results regarding the rainfall-runoff relationship are discussed. First the shifts in rainfall-runoff relation are shown, after which several factors that may have a link to the found shifts are displayed.

5.2.1. Distribution of change rainfall-runoff relationship

The after drought rainfall-runoff relationship is investigated using the variable $F(\omega_{after})$, which is explained in Section 4.3.5. This variable indicates how the runoff ratio after drought relates to the runoff ratio before the drought.

In case of a decrease in runoff ratio after the drought compared to the period before drought, a high value of $F(\omega_{after})$ is present. Likewise, an increase in the runoff ratio is indicated by a low value of $F(\omega_{after})$. In the case that there is no change in the rainfall-runoff relationship, the ω value after drought relates well to the ω values before the drought. This means that $F(\omega_{after})$ will have a value around 0.5.

In Figure 5.2, the distribution for the value of $F(\omega_{after})$ for all the different catchments is given. This is done for different sample lengths, varying from 1 up until 7 years, as explained in Section 4.3.3. It is noticeable that in case of a short sample length, 1 and 2 years, there are a lot of catchments with a very high $F(\omega_{after})$ and few catchments with a low value of $F(\omega_{after})$.

When the length of the sample increases, the number of catchments with a value of $F(\omega_{after})$ larger than 0.9 decreases, from 72 catchments in the case of a sample length of 1 year to 57 catchments in the case of a sample length of 7 years. On the other hand, the number of catchments with a value of $F(\omega_{after})$ less than 0.1 increases, from 14 catchments in the case of one year samples to 28 catchments in case of seven year samples.

The distribution of $F(\omega_{after})$ shown in Figure 5.2 indicates that there are more catchments where after the drought a decrease in the runoff ratio can be observed than catchments where an increase in the runoff ratio can be found. However, for all different sample lengths, the number of catchments that are in between these high and low values of $F(\omega_{after})$ is higher than the number of catchments with extreme values.

In the remainder of this study, the focus will be mainly on comparing catchments with extreme values of $F(\omega_{after})$. This is done to determine whether a reason can be given for the large differences that are found in the catchment response after a long-term drought.

The correlation matrix for comparing the correlation in $F(\omega_{after})$ for different sample lengths can be found in Figure 5.3. The correlation matrix shows that catchments with a sample length larger than 3 years generally show a good correlation. This means that the values found for $F(\omega_{after})$ show a good relation for differing sample lengths. Furthermore, the correlation coefficient increases with decreasing difference in sample length. Catchment with a short sample length of 1 and two years show a poorer correlation with other sample lengths. This is not surprising, as the number of catchments with a high value of $F(\omega_{after})$ are a lot higher in the case of a shorter sample length than for longer sample lengths.

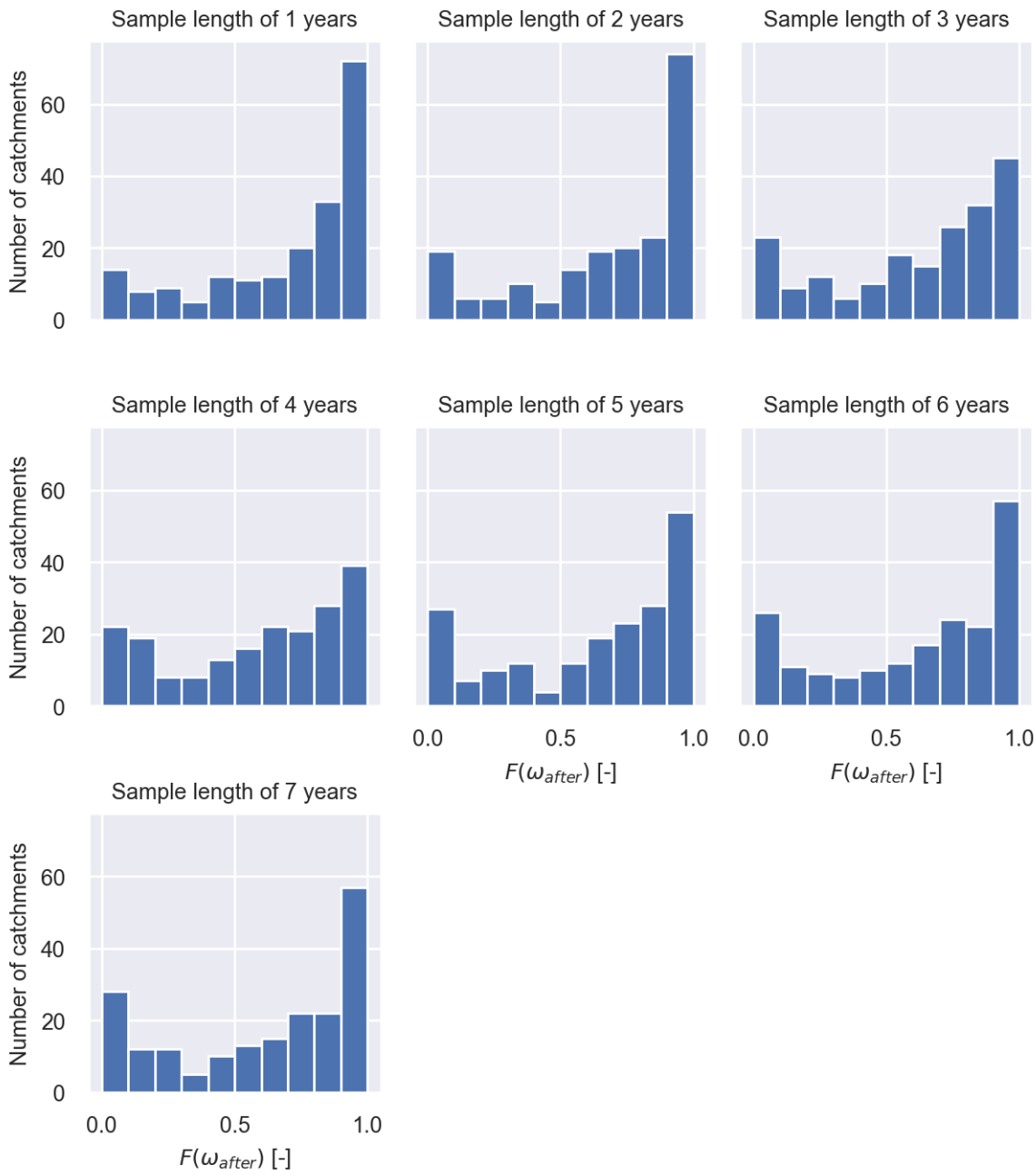

Figure 5.2: Distribution of $F(\omega_{after})$ for different sample years

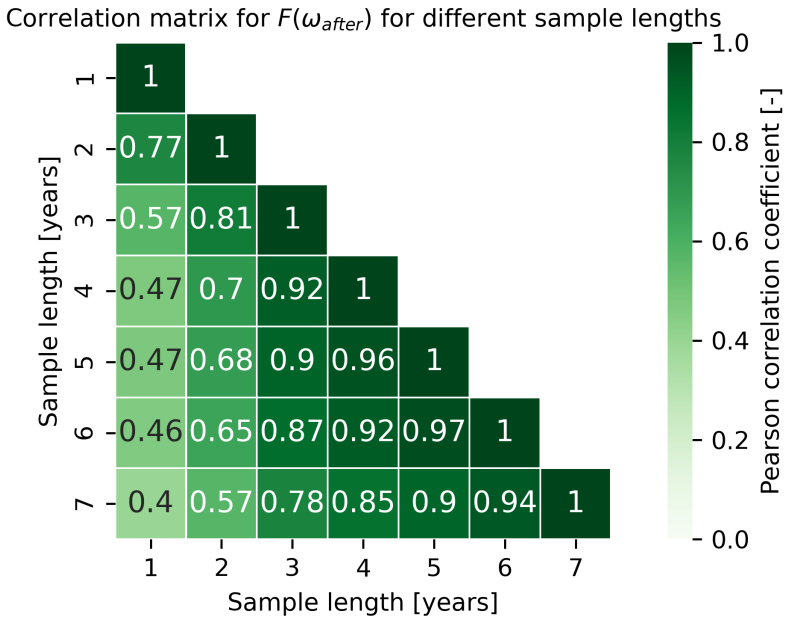

Figure 5.3: Correlation of $F(\omega_{after})$ for different sample lengths using the Pearson correlation coefficient.

5.2.2. Changes in rainfall-runoff in Budyko framework

In this section, the changes in the rainfall-runoff relationship that have been found with $F(\omega_{after})$ will be given with the changes that are found in the Budyko framework.

This investigation has only been performed for a sample length of 5 years. The decision to use a sample length of 5 years has been made on the basis of a trade off between having enough random samples and having a short time period after the drought. Furthermore, looking at the correlation matrix in Figure 5.3, the results for this sample length have a good correlation with other sample lengths.

To compare high and low values of $F(\omega_{after})$, the catchments are divided into three groups. The low bound is set at a value for $F(\omega_{after})$ of 0.1 and the high bound is set at 0.9. More information about the three groups that are formed can be found in Table 5.1.

Table 5.1: The three groups that are used in the analysis, with the number of catchments that are in each group. The number of catchments is based on a sample length of 5 years.

Name	Condition	Number of catchments
Low	$F(\omega_{after}) < 0.1$	27
Medium	$0.1 \leq F(\omega_{after}) \leq 0.9$	115
High	$F(\omega_{after}) > 0.9$	54

The movement of catchments within the Budyko framework from the period before the drought to the period after drought is displayed in Figures 5.4 and 5.5 for catchments with a low value for $F(\omega_{after})$ and catchments with a high value of $F(\omega_{after})$. In both Figures, the full timeseries before and after drought are used to determine the aridity index and the evaporative index.

Figure 5.4 shows the movement for catchments with a low value of $F(\omega_{after})$. This Figure shows that catchments in this group have a lower evaporative index after the drought than before the drought. Oftentimes the aridity index also decreases, but this is not always the case.

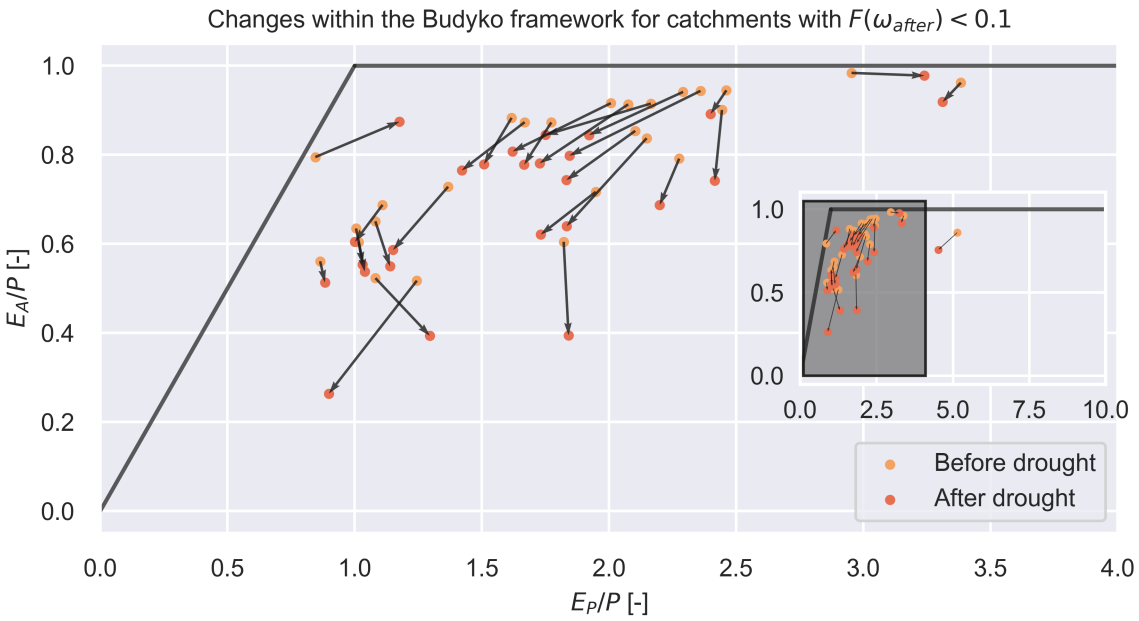

Figure 5.4: Changes within the Budyko framework before and after the drought for catchments with a value of $F(\omega_{after}) < 0.1$. The arrow displays the change. The sample length is 5 years.

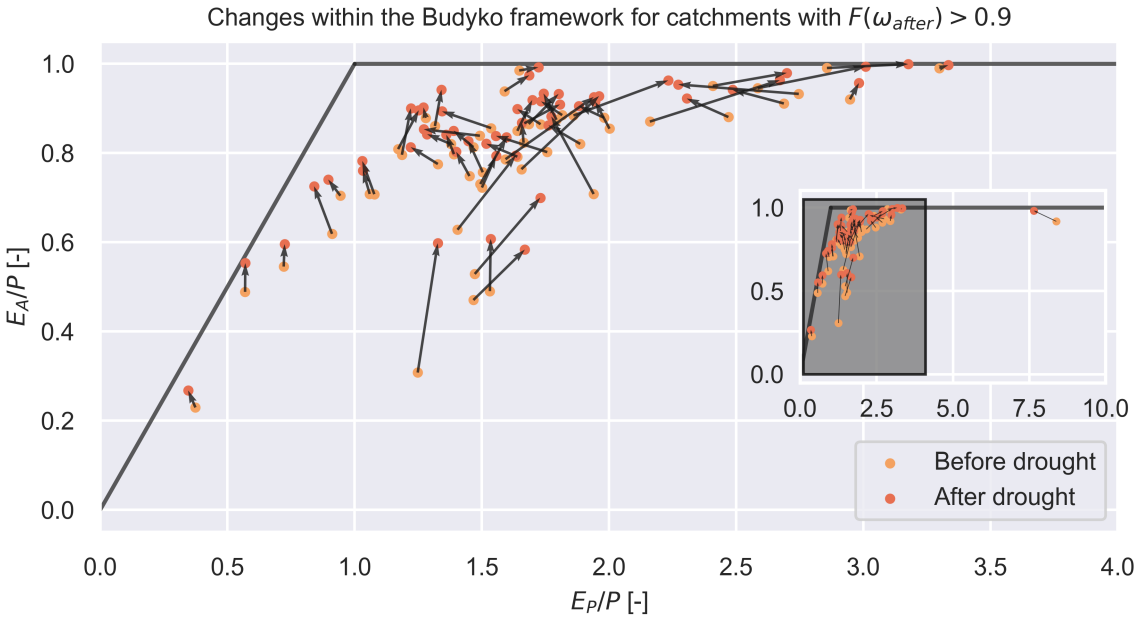

Figure 5.5: Changes within the Budyko framework before and after the drought for catchments with a value of $F(\omega_{after}) > 0.9$. The arrow displays the change. The sample length is 5 years.

In Figure 5.5, the movement in the Budyko framework is displayed for catchments with a high value of $F(\omega_{after})$. In this case the evaporative index increases over the drought period. The change in aridity index differs from decreasing to increasing.

The above Figures show that the evaporative index does indeed decrease for catchments with a low value of $F(\omega_{after})$ and increase for catchments with a high value of $F(\omega_{after})$. However, the magnitude of the changes in evaporative index differ.

To get a better idea about the magnitude of the change, the change in evaporative index is compared to the value of $F(\omega_{after})$ for each of the 196 catchments. The change in evaporative index is defined as is stated in Equation 5.1, in which EI is the evaporative index.

$$\Delta EI = EI_{after} - EI_{before} \tag{5.1}$$

A negative value for ΔEI therefore indicates that the evaporative index has decreased over the drought period.

In Figure 5.6 the change in evaporative index for different values of $F(\omega_{after})$ is presented. This Figure shows that when the value of $F(\omega_{after})$ is low, the evaporative index does indeed decrease in most cases, meaning that there is an increase in runoff ratio. Likewise, the value of the evaporative index does increase when the value of $F(\omega_{after})$ is high. Furthermore, this Figure shows that the most extreme negative and positive changes in evaporative index are found when the value of $F(\omega_{after})$ is respectively close to 0 or close to 1.

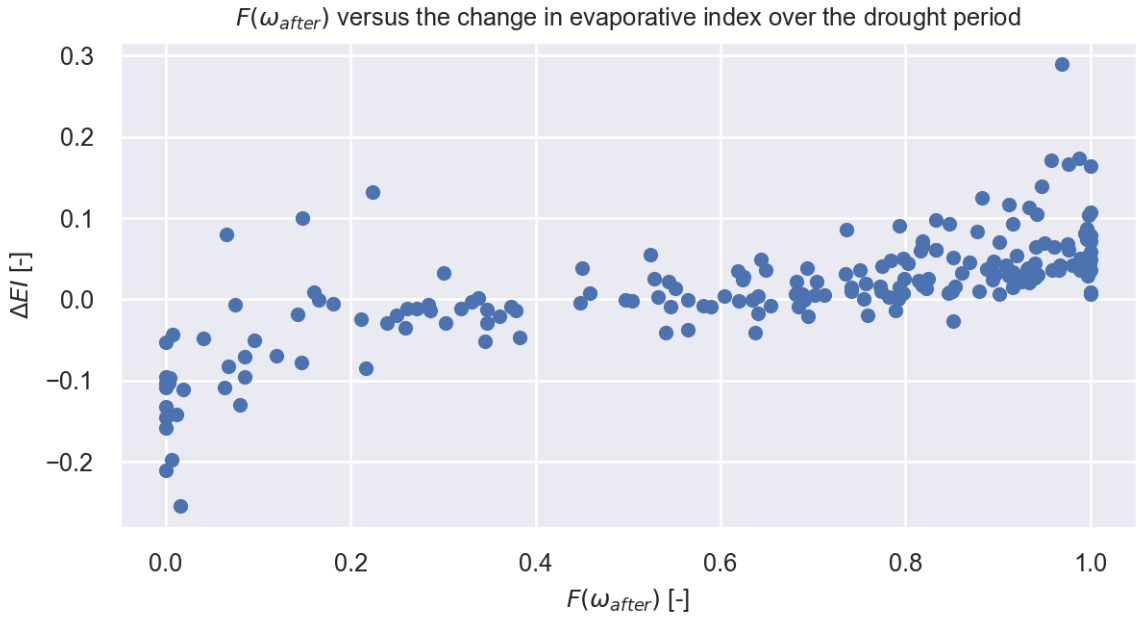

Figure 5.6: $F(\omega_{after})$ versus the change in evaporative index in case of a sample length of 5 years. Each blue dot represents a catchment. A negative change in evaporative index indicates a decrease in evaporative index over the drought period, while a positive value indicates that the evaporative index has increased.

In Table 5.2 the number of catchments for different groups of change in evaporative index are displayed. This Table gives an insight into the magnitude of change in the catchments. The spread in change in evaporative index is between -0.25 and 0.29. This indicates that in the most extreme catchments there is an in- or decrease of runoff between 20 and 30% of the precipitation. In most cases, this change is less than 10% of the total precipitation.

Table 5.2: Change in evaporative index over the drought period

Group	Number of catchments
-0.3 < $\Delta EI \leq$ -0.2	2
-0.2 < $\Delta EI \leq$ -0.1	13
-0.1 < $\Delta EI \leq$ 0.0	55
0.0 < $\Delta EI \leq$ 0.1	113
0.1 < $\Delta EI \leq$ 0.2	12
0.2 < $\Delta EI \leq$ 0.3	1

5.2.3. Investigation of factors affecting a change in rainfall-runoff

To identify whether the differences of the rainfall-runoff response in relation to a drought can be explained, several different factors have been investigated. In this section these results are presented.

Like in the previous section, this analysis is performed for a sample length of 5 years. The groups that are used can be found in Table 5.1.

The results are compared for different variables, which can be summarized as follows:

- Climatic conditions
  - Drought severity
  - SPEI after drought
  - Aridity index before drought
  - Climatic zone
  - Seasonality
- Land Use / Land cover
  - NDVI
  - Forested cover

For each of these variables, the 2-sample Kolmogorov-Smirnov test has been performed. The 2 samples that are compared for the Kolmogorov-Smirnov test are the group with a low value of $F(\omega_{after})$ and the group with a high value of $F(\omega_{after})$.

Climatic conditions

In this section the results related to climatic conditions before, during and after the drought are displayed. Besides the results presented in this section, additional plots related to climatic conditions can be found in Appendix A.

Drought characteristics

In Figure 5.7, the distribution of the drought severity, described by the sum of the SPEI over the drought duration, is shown for each group. In this Figure, it is noticeable that the higher values for drought severity are in the group with a low value for $F(\omega_{after})$. This is also reflected in the p-value for the Kolmogorov-Smirnov test, which is <0.001.

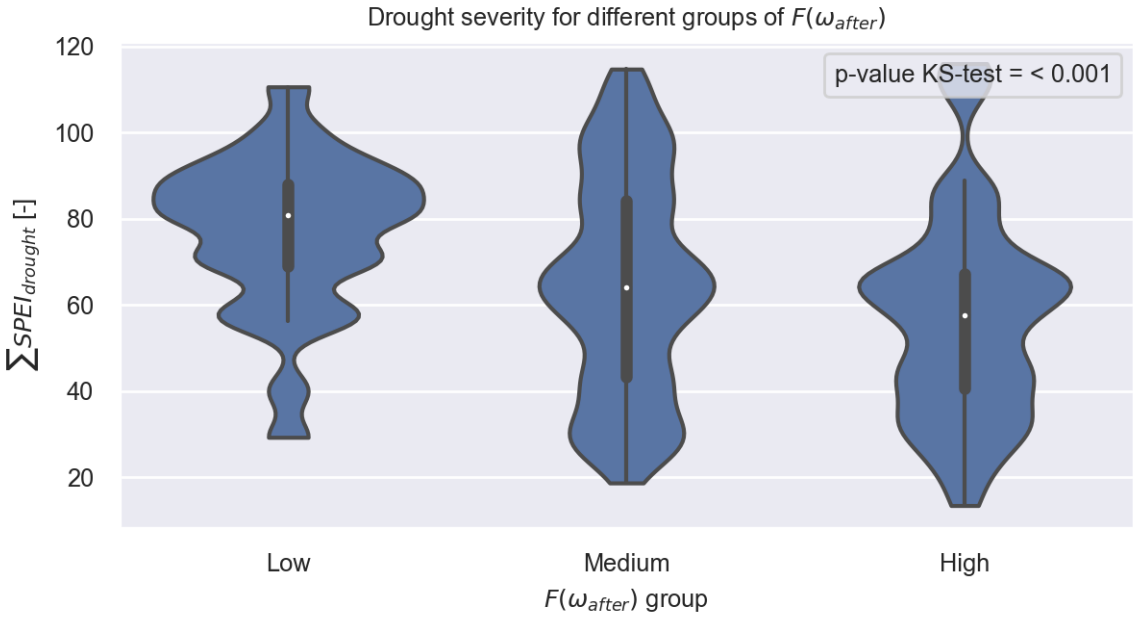

Figure 5.7: The drought severity for the different groups of $F(\omega_{after})$

When comparing only the intensity for the different groups, which is shown in Figure A.1 in Appendix A, there is no clear difference between different values of $F(\omega_{after})$. For all different groups the maximum intensity has a median value of 2.5. The spread of the data is also very comparable, with the 25 and 75 percentiles at similar levels. As a consequence, the p-value for the KS-test is very high, 0.915.

Looking at only the drought length, displayed in Figure A.2 in Appendix A, it is noticeable that the higher values for drought length are in the group with a low value for $F(\omega_{after})$. Where the drought length for both the groups with a medium and a high value for $F(\omega_{after})$ is mostly concentrated below 2000 days, the drought length in case of a low value for $F(\omega_{after})$ is mostly clustered between 2000 and 3000 days. There seems to be a second group in the case of a low value for $F(\omega_{after})$, which is a group between 1000 and 2000 days.

Another thing worth to mention, is that the value for drought length is not a continuous variable, like the other variables mentioned in this section. As the droughts start and end at the beginning of a hydrological year, the number of possibilities is not very large, from a minimum of 3 years up to a maximum drought length of 10 years.

Mean SPEI after drought

The mean value of the SPEI after drought is the mean value of the 12 month SPEI for 3 years after the drought. In Figure 5.8, the distribution for the mean SPEI is displayed for each of the three groups.

In most cases, the mean SPEI of the catchment is larger than 0, meaning that the period after the drought is relatively wet. However, some catchments do have a mean SPEI value lower than 0, meaning the period after drought is relatively dry. There is not one group for which this is the case especially, but the spread seems to be present in all three groups. This also results in a high p-value for the KS-test, indicating that there is no difference between the distribution of the mean SPEI of the different groups.

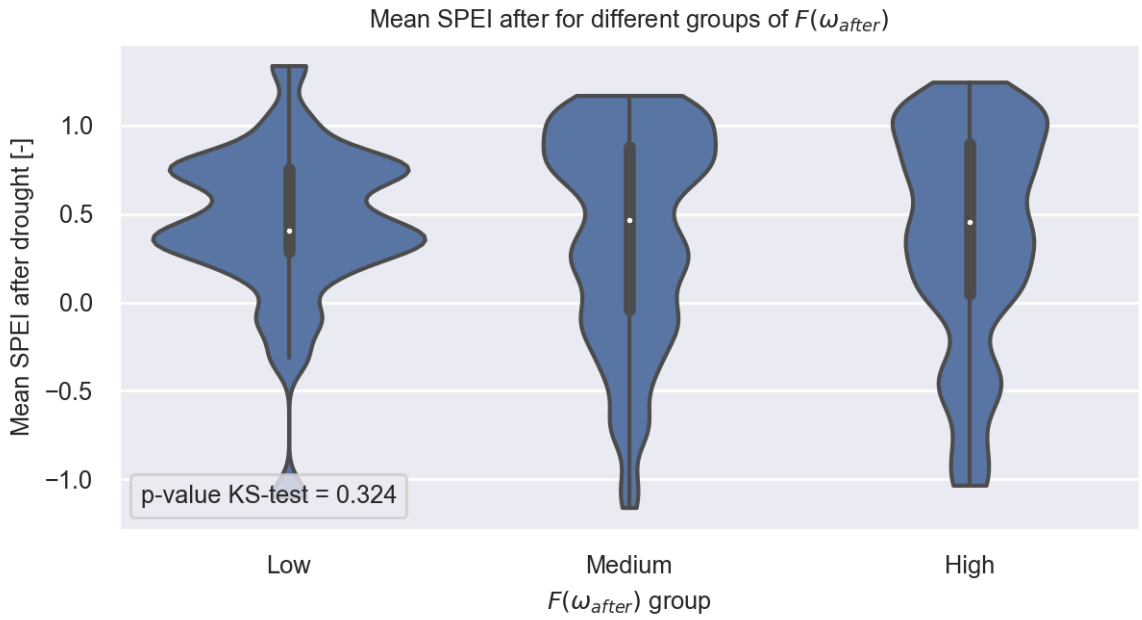

Figure 5.8: Mean SPEI after the drought

Aridity before drought

In Figure 5.9 the aridity index before the drought is compared for the different groups. As can be seen in the Figure, there are some outliers in the aridity index, with values over 10. Besides these outliers, most of the data is concentrated between 0 and 3.

The values in the group with a low value for $F(\omega_{after})$ seem to be concentrated in two areas, with aridity indices around 1 and a little over 2, while the data for the other two groups is concentrated below an aridity index of 2. Furthermore, there are few catchments with a wet climate in the group with a low $F(\omega_{after})$. The lowest aridity index before the drought for this group is 0.85, while for the medium and high groups this is 0.36 and 0.37. Despite this, the p-value for the KS-test is not very low, with a value of 0.079. This means that it is not very certain that the aridity between groups is different.

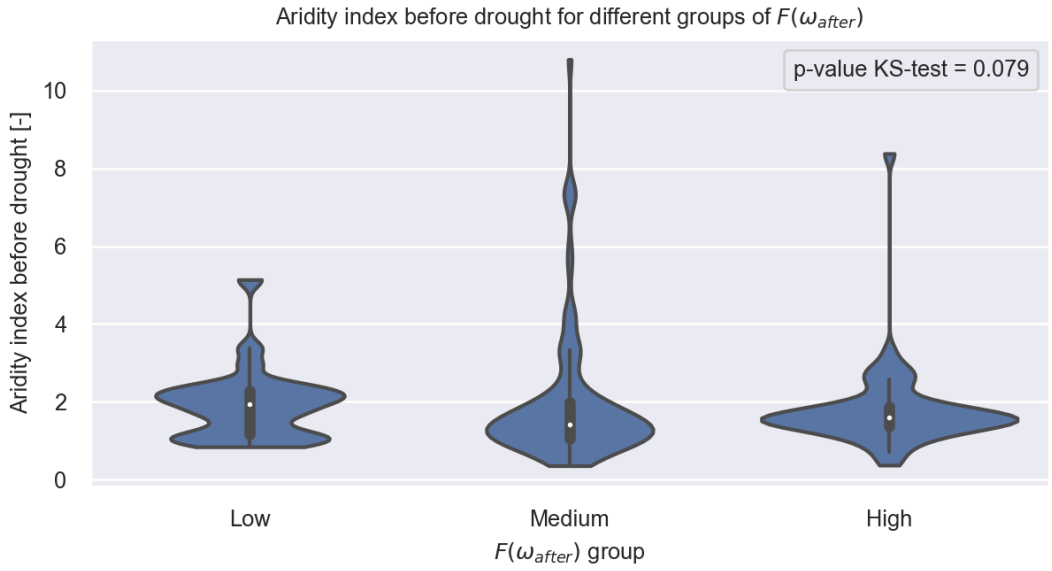

Figure 5.9: Aridity index before the drought

Climate zone

In Figure 5.10, the different climate zones are shown and the distributions of $F(\omega_{after})$ are shown. As stated in Chapter 3, the number of catchments that have a desert or temperate climate with no dry winter is limited. Noticeable in this Figure is that there are some distinctions between climate zones when looking at the value for $F(\omega_{after})$. Especially the temperate climate zone with a dry summer has high values for $F(\omega_{after})$, while temperate zones with a dry winter have, on average, a low value for $F(\omega_{after})$.

In the case of catchments with a tropical or a temperate climate without dry season, the values for $F(\omega_{after})$ are a lot more spread out. However, values for $F(\omega_{after})$ are on average lower in a tropical climate than in a temperate climate without a dry season.

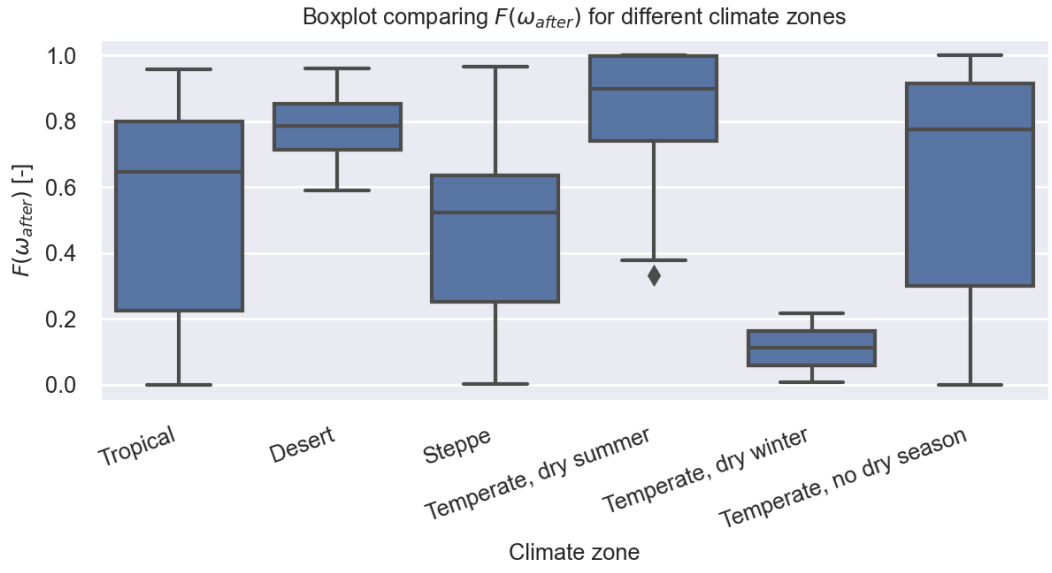

Figure 5.10: Boxplot climate zones

These results indicate that the seasonality and timing of the precipitation are important in the response of the catchment to the drought. Therefore, the three groups are compared using the value of the seasonality timing index, which is displayed in Figure 5.11.

These results are in line with what was found for the division in climate zones, as catchments with a negative value for the seasonality timing index, in which the precipitation largely winter based and the summer is a dry period, seem to more often have a higher value for $F(\omega_{after})$ than catchments with a positive value for the seasonality timing index, which have a dry winter period. In case of a low value for $F(\omega_{after})$ there is a large group of catchments with a high seasonality with precipitation in the summer. There is also a small group of catchments that are less seasonal, with a concentration of precipitation in the winter. The differences in the two groups are also reflected in the p-value for the Kolmogorov-Smirnov test, which is low with 0.001.

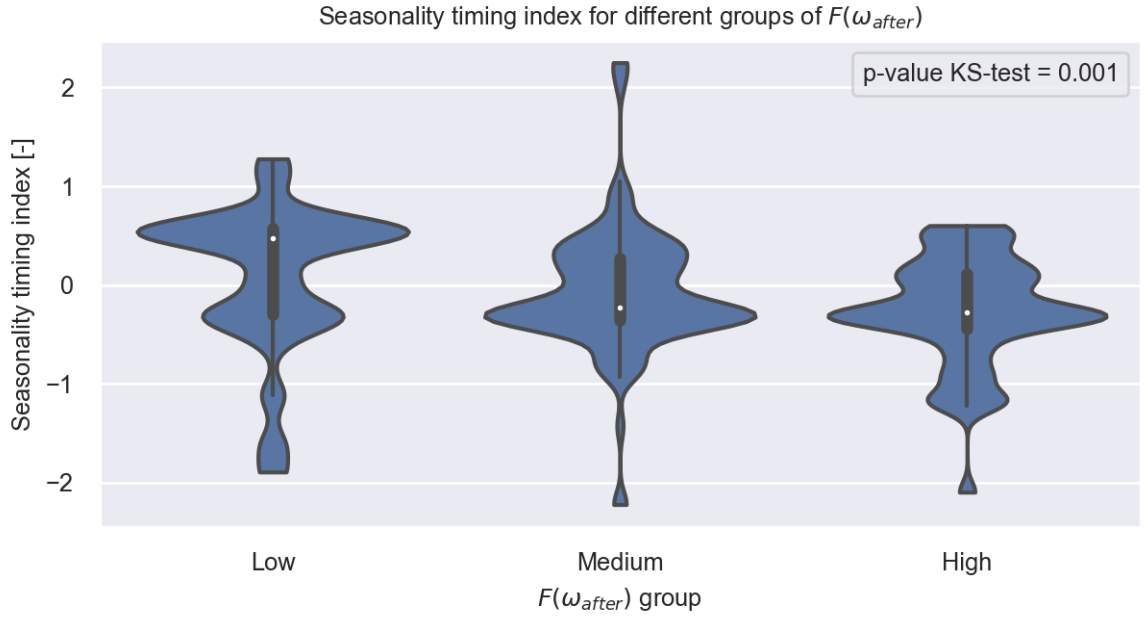

Figure 5.11: Violinplot Seasonality Timing

When only looking at the seasonality, displayed in Figure A.3 in Appendix A, there is oftentimes a higher seasonality in case of a low value of $F(\omega_{after})$. However, the p-value for the Kolmogorov-Smirnov test is not as low as for the combined seasonality timing index, with a value of 0.013. This indicates that both seasonality and timing play a role in the differences that are found.

Land use / land cover

As the expectation is that a change in vegetative cover has a large influence in the way a catchment responds to drought, the land use and land cover are expected to play a role in the changes that are found in catchments. In this section, several factors related to land use and land cover are presented.

Besides the results shown in this section, additional plots related to land use / land cover are given in Appendix B.

Forest cover

In Figure 5.12, the distribution of the forest cover for the different catchments is displayed per group. In both the high and low group, there are a large amount of catchments that have a high fraction of forest cover, close to 1.0. The medians of the two groups are also similar. However, in catchments that see a decrease in ω, there is also a group of catchments with low forest cover.

In the case of a medium $F(\omega_{after})$, the forest cover is distributed more evenly, with more catchments with a small amount of forest cover. The resulting median value is lower than the median of the other two groups.

The division for Eucalypt cover, which can be found in Figure B.1, shows a very similar pattern. In both cases the p-value for the KS-test is high, 0.237. One thing to note is that the median fraction of eucalypt cover in case of a low value of $F(\omega_{after})$ is 0.42, while this is 0.59 for the fraction forest cover. In case of a high value for $F(\omega_{after})$, medians are 0.68 and 0.65 for forest cover and eucalypt cover.

This could indicate that the fraction of forest cover that is eucalypt forest plays a role. However, when looking at the fraction of forest that is eucalypt trees, no clear differences are visible. A lot of catchments have close to 100% eucalypt trees, resulting in a p-value of 0.43 for the KS-test.

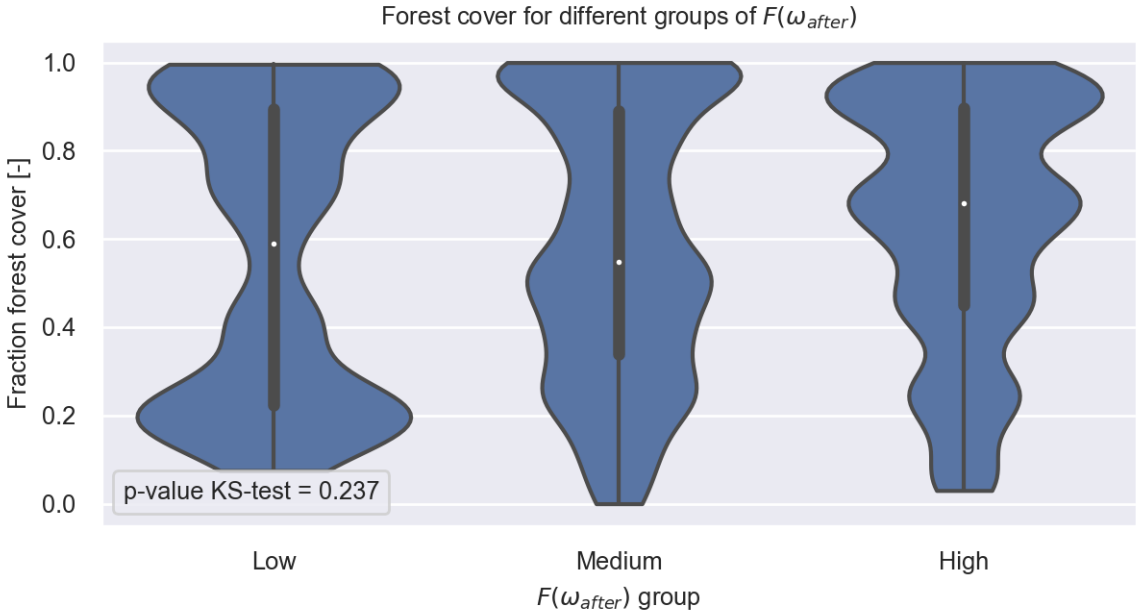

Figure 5.12: Violinplot for forest cover

NDVI

In Figure 5.13, the relative difference in NDVI is compared for the different groups. As stated in Chapter 4, NDVI data is only available from 2000 onwards. This means that it is possible to determine the NDVI difference for 143 of the 196 catchments. The number of catchments with a low $F(\omega_{after})$ is 22 and the number of catchments with a high value of $F(\omega_{after})$ is 40.

As shown in Table 5.3, the median values for the three different groups are close to each other. Furthermore, the value for the 25 and 75 percentile are similar. This results in a high KS-test p-value of 0.812.

Table 5.3: Statistics for the value of $\Delta_r NDVI$ for the different groups of $F(\omega_{after})$

Group	Min	Median	Max
Low	-0.105	0.050	0.259
Medium	-0.192	0.029	0.225
High	-0.047	0.026	0.149

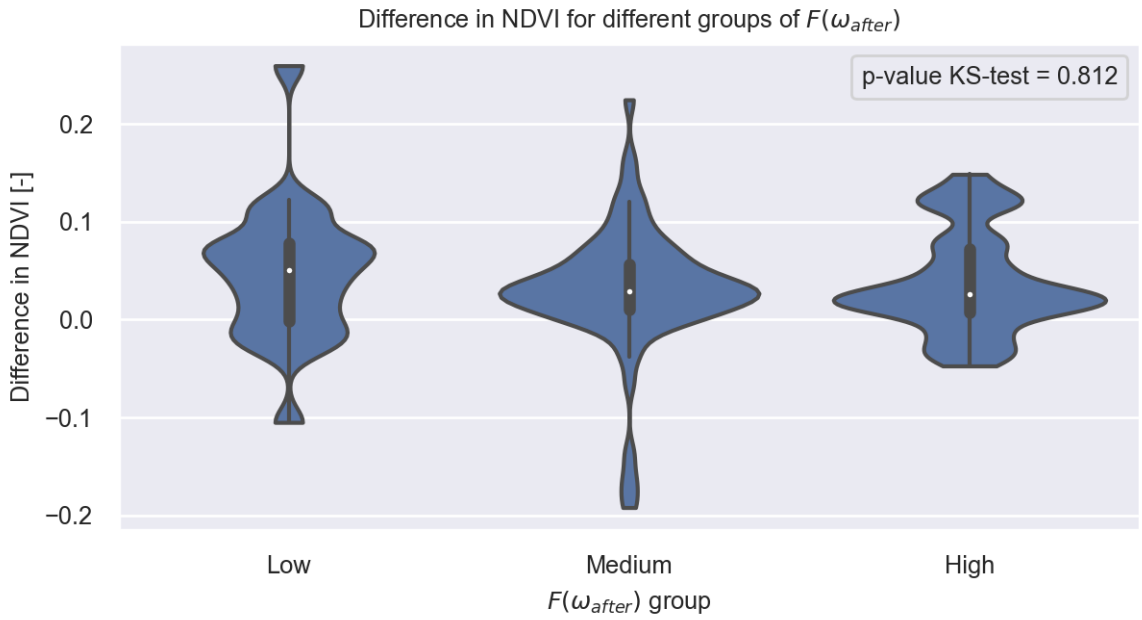

Figure 5.13: Difference in NDVI

5.3. Results of detecting root-zone storage capacity change

In this section the results regarding the root-zone storage capacity are discussed. First, the results of the mass curve technique are displayed, after which the results regarding $\Delta S_{R,1yr}$ are given.

5.3.1. Pre-drought root-zone storage capacity

In Figure 5.14, the distribution of the determined root-zone storage capacities are shown, determined with the mass curve technique. The root-zone storage capacities have been determined with the timeseries before the drought, as the hypothesis is that the values of the root-zone storage capacity change during the drought.

The value of S_R differs between catchments. Most of the catchments have a root-zone storage capacity between 200 and 400 mm. There are, however, some extremes, with storage capacities over 1000 mm.

In Figure 5.15, the spatial distribution of S_R is displayed. It can be seen that the value of S_R is higher in the northern areas of Australia, and oftentimes low in the center of Australia. The center of Australia is more desert-like and has less vegetation. It is therefore logical that the values of S_R are lower in this area.

5.3.2. Change in root-zone storage capacity

The value of $\Delta S_{R,1yr}$ has been determined for every catchment using the method described in Chapter 4. The results for all the catchments that are taken into account during the analysis are presented in Figure 5.16.

Most of the values of $\Delta S_{R,1yr}$ are close to 0, indicating that there is little change in the root-zone storage capacity. However, the number of catchments where the value of $\Delta S_{R,1yr}$ is larger than 0 is comparable to the number of catchments with a $\Delta S_{R,1yr}$ smaller than 0. In Table 5.4 statistics are presented. The median value of $\Delta S_{R,1yr}$ is close to 0.

In Figure 5.17 the value of $\Delta S_{R,1yr}$ is displayed spatially. The largest declines in root-zone storage capacities determined with this method are visible in the southeast and in the southwest of Australia. In Tasmania and in northern areas, the value of $\Delta S_{R,1yr}$ is positive more often.

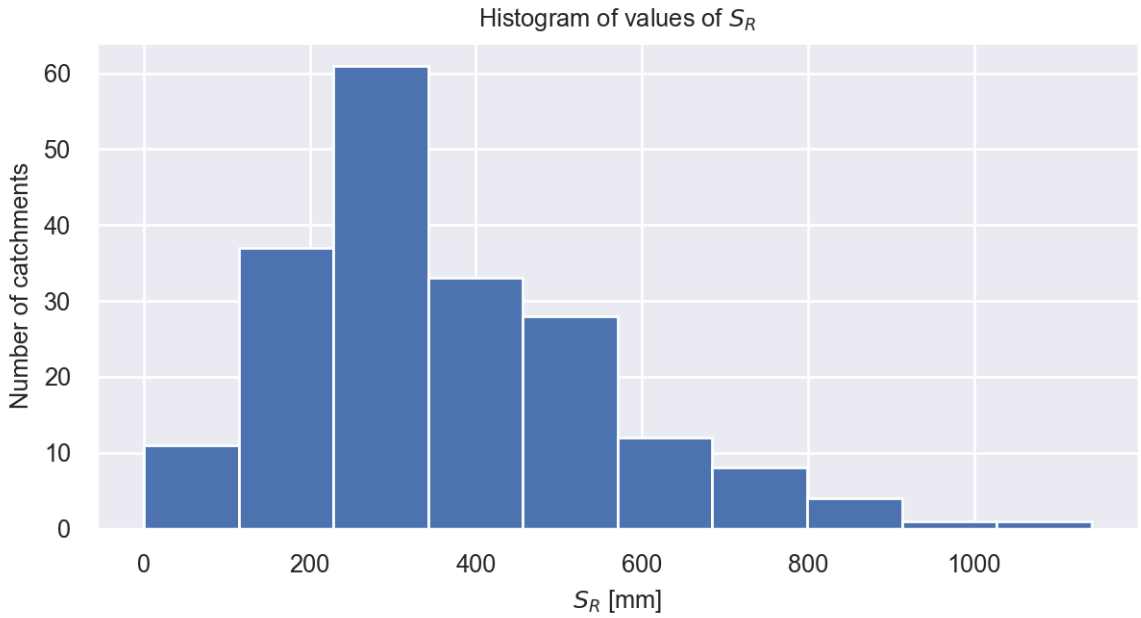

Figure 5.14: Histogram for the determined values of the pre-drought S_R

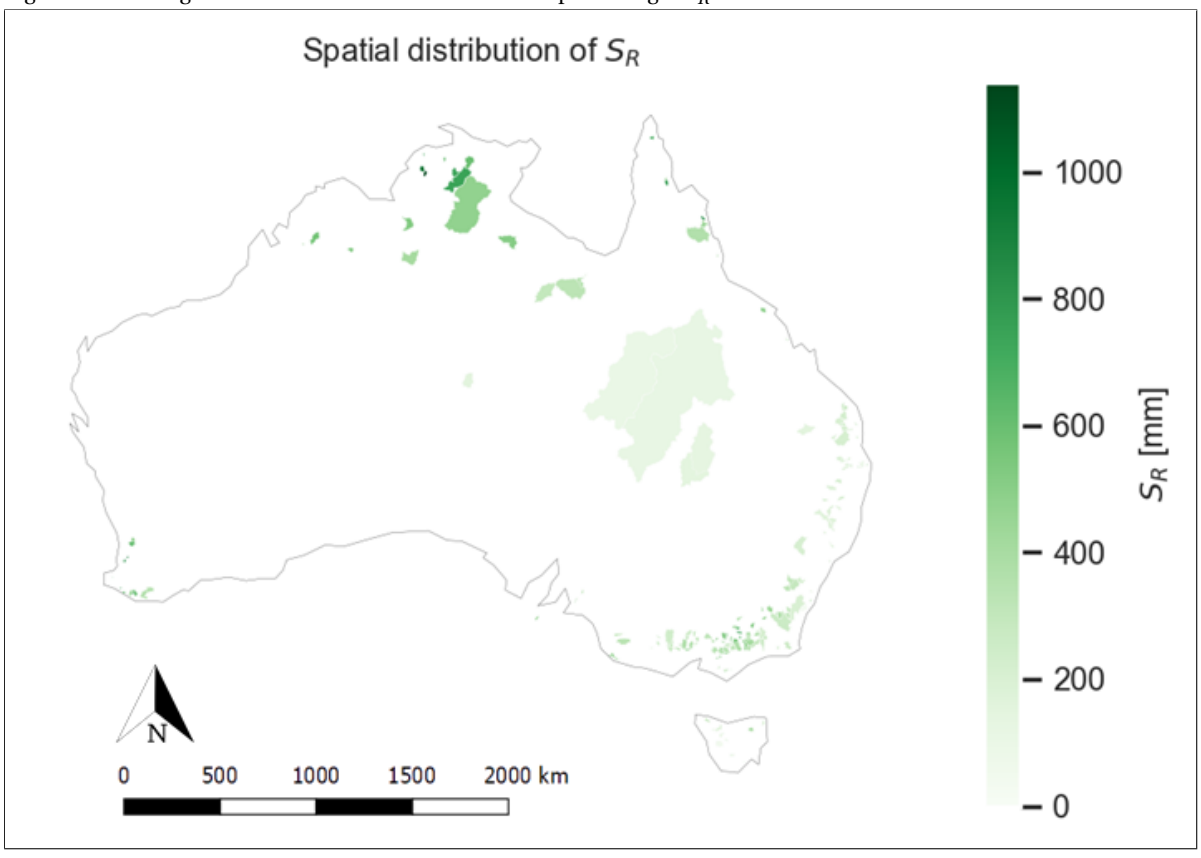

Figure 5.15: The spatial distribution of S_R

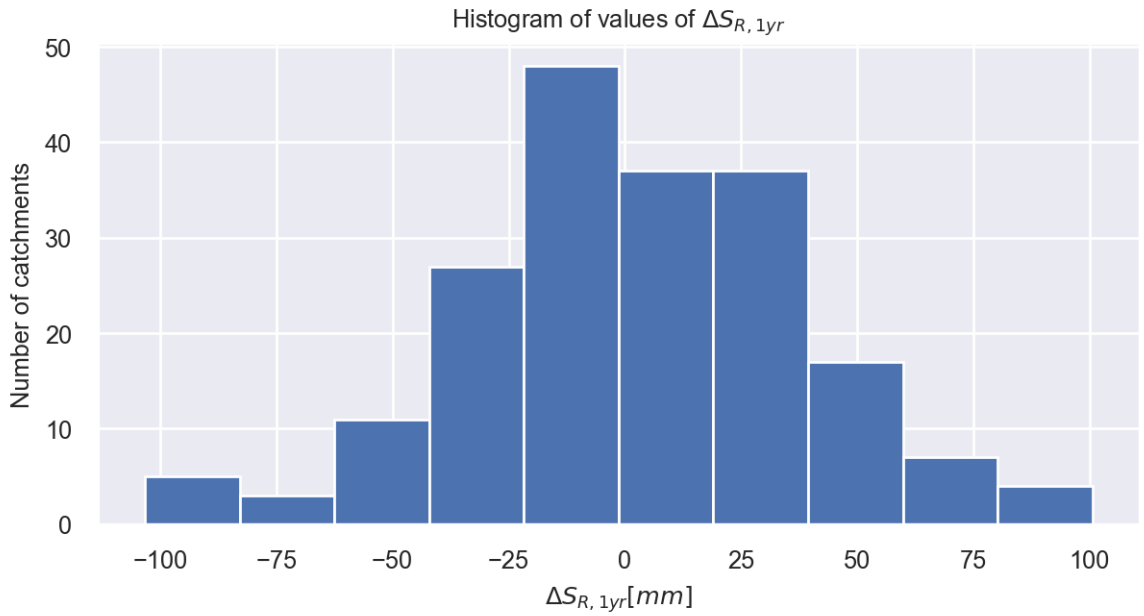

Figure 5.16: Histogram for the determined values of $\Delta S_{R,1yr}$

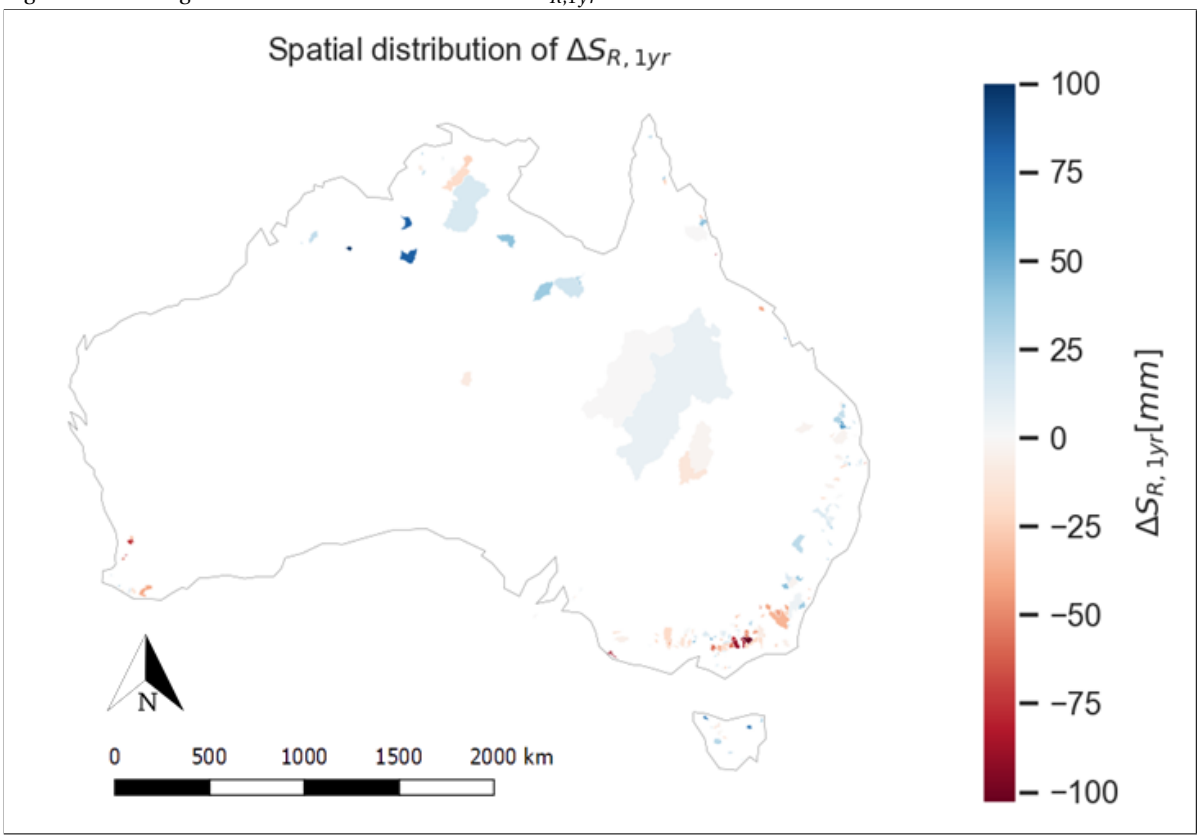

Figure 5.17: The spatial distribution of $\Delta S_{R,1yr}$

Table 5.4: Statistics for the value of $\Delta S_{R,1yr}$

Statistic	Value
$\Delta S_{R,1yr} < 0$	99
$\Delta S_{R,1yr} > 0$	97
Min	-103.29 mm
Median	-0.17 mm
Max	100.59 mm

5.4. Combined results

In this section, the results for $F(\omega_{after})$ and $\Delta S_{R,1yr}$, which have been discussed in the previous sections, will be brought together. The goal of this is to investigate whether the changes that are found in Section 5.2 can be linked to a change in the root-zone storage capacity.

In Figure 5.18 the distribution of the determined value of S_R is displayed for the three different groups. In case of a low value of $F(\omega_{after})$, the values for S_R are mostly concentrated a little above 200 mm. This is also the root-zone storage capacity that is most often present in all investigated catchments. Furthermore, it is noticeable that there are no catchments with a small root-zone storage capacity in this group.

When looking at the other two groups of $F(\omega_{after})$, the S_R are more spread out, meaning that there are more catchments with a high and a low value of S_R. However, also in this case, most catchments have a value of S_R between 200 and 400 mm.

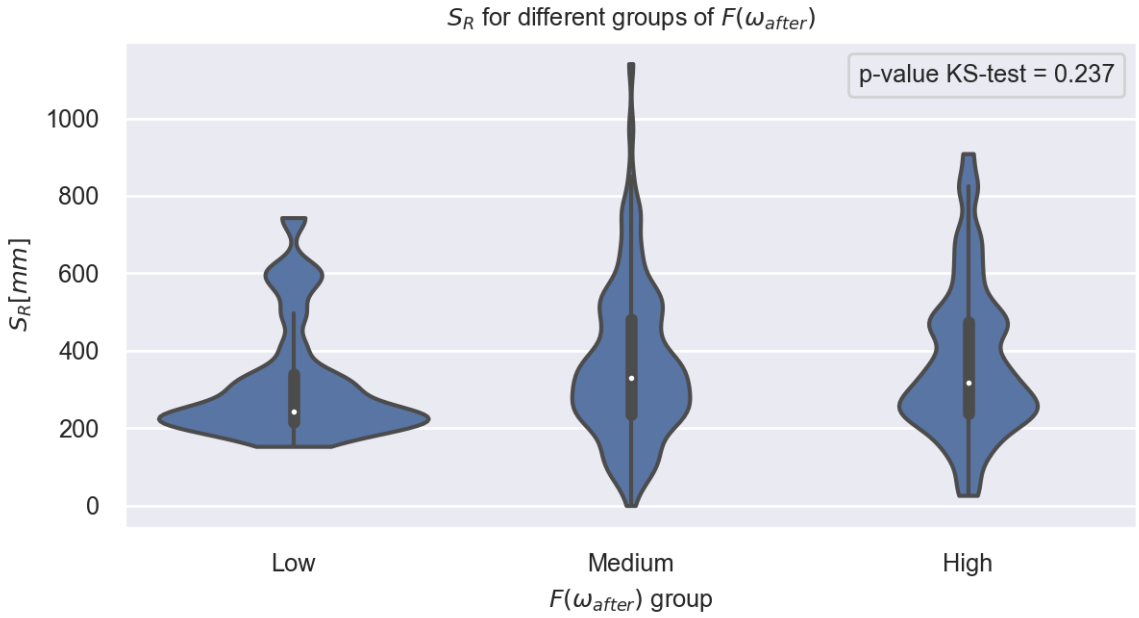

Figure 5.18: Violinplot linking the found value of S_R with the changes found in the rainfall-runoff relationship

In Figure 5.19 the results for combining the change found in rainfall-runoff relationship and the value found for $\Delta S_{R,1yr}$ are displayed. The catchments that were used are the 196 catchments that have been used in the previous sections.

The results from Figure 5.19 show that there is a difference between the values that are found for $\Delta S_{R,1yr}$ in case of low values for $F(\omega_{after})$ and high values of $F(\omega_{after})$. In general, the value of $\Delta S_{R,1yr}$ is larger when the value of $F(\omega_{after})$ is high. This results in a median that is quite different

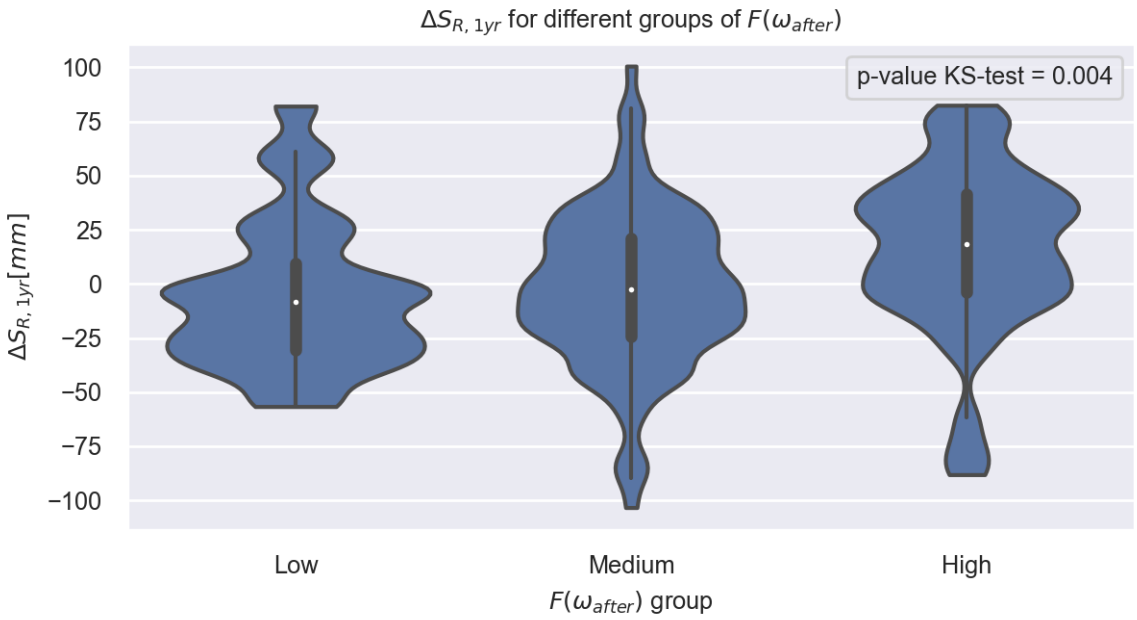

Figure 5.19: Violinplot linking the changes found in the rainfall-runoff relationship to the change in root-zone storage capacity.

for the three groups, as can be seen in Table 5.5. However, the spread is quite large in all three cases, with all groups having a minimum value below 0 and a maximum value above 0. The resulting p-value for the KS-test is low, with a value of 0.004. This indicates that there is a difference in $\Delta S_{R,1yr}$ between catchments with a high value of $F(\omega_{after})$ and catchments with a low $F(\omega_{after})$.

Table 5.5: Statistics for the value of $\Delta S_{R,1yr}$ for the different groups of $F(\omega_{after})$

Group	Min [mm]	Median [mm]	Max [mm]
Low	-56.63	-8.39	82.11
Medium	-103.29	-2.49	100.59
High	-88.08	18.30	82.52

6

Discussion

In this chapter, the results that have been found in the previous section will be discussed. Furthermore, a link will be made to the current literature.

6.1. Drought detection

In this research one drought period has been considered per catchment, which was defined as the longest drought period in the timeseries for that catchment. The results showed that the SPEI after the drought did not have an effect on the rainfall-runoff relationship after the drought. There could however be some effects of shorter droughts during the period before the longest droughts. A way that this can be tested is by using the variance of the SPEI before the drought. If dry periods occur frequently, this variance will be higher.

Furthermore, in this research a value of -0.5 has been used as a boundary value for drought detection. This value relates to approximately the driest 30% of the timeseries. Using a different boundary value for the SPEI could result in differing drought durations. Especially for catchments where the 36 month SPEI does shortly go over this boundary value before returning below -0.5, a change in boundary value could have a large effect. A possible extension could therefore be to add droughts together if there is a short time between two droughts determined with the method used in this research.

6.2. Rainfall-runoff relationship

The results regarding the change in rainfall-runoff relationship showed a diverse image. In the majority of the analysed catchment no clear change has been found.

Interesting is that in most catchments where a change was found, the runoff ratio appears to have decreased. This is opposed to the hypothesis that an increase in runoff ratio would be present.

To make sure that the differences found from the expectation are not due to inconsistencies in the used method, the results using the method for detecting rainfall-runoff change described in this research have been compared with the results using the method of Jaramillo et al. (2018). The only adjustment that has been made in this method is that the equation of Fu is used instead of Choudhoury. In case of the sampling method, a 5 year period is used, while for the method of Jaramillo the full after-drought timeseries is used. In Figure C.1 in Appendix C the comparison can be found. Overall results are comparable, with a clear relation (r^2 = 0.5) between the value of $F(\omega_{after})$ and $\Delta(E/P)_r$ introduced by Jaramillo et al. (2018). Catchments where a low value of $F(\omega_{after})$ is found also show a decrease in $\Delta(E/P)_r$, which both indicate an increase in runoff ratio due to non-climatic circumstances. Catchments where the value for $F(\omega_{after})$ is high have a positive value for $\Delta(E/P)_r$. This seems to indicate that the method used in this research is valid and the results are logical.

6.2.1. Difference in response between short and long sample lengths

In this research, differing time periods after a drought have been investigated. Results for different time periods after the drought showed varying results.

In the results it was shown that for a short period after the drought, there are few catchments that have a low value for $F(\omega_{after})$ and a high number of catchments with a high value for $F(\omega_{after})$. This indicates that in the first year after a long-term drought the evaporative index increases, given a similar aridity index. This is opposed to the hypothesis that the runoff in a catchment increases after a long-term drought. In the longer term, the number of catchments with a low value of $F(\omega_{after})$ increases, indicating an increase in the runoff ratio. This starts to show at a sample length of two years, but becomes clearer with sample lengths of 6 and 7 years.

In this analysis, the time period of the drought has been determined using the meteorological drought. Yang et al. (2017) has shown that the hydrologic recovery after drought can significantly lag behind the meteorological recovery. The mean time lag is 7 to 11 months. This lag in recovery has the effect that the runoff ratio shortly after drought is smaller. This could explain the differences found between the situation 1 and 2 years after the drought and the situation after 6 and 7 years. The lag in hydrological drought restoration will have a larger effect in the first years after the drought than it will have on a longer timescale.

6.2.2. Reasons for changing rainfall-runoff relationship

For all considered time periods, a high value of $F(\omega_{after})$ was more often found than a low value. This indicates that a decrease in runoff ratio is present more frequently than expected. In this section possible explanations will be discussed.

A reason that a decreased runoff ratio is more often observed in this research could be that a trend in the runoff ratio has not been considered. The assumption of a static situation before the drought implicitly assumes that a step change takes place. Declining trends in total annual runoff in Australia have been found, using a Mann-Kendall trend test (Zhang et al., 2016). The trends that were found regarding the runoff were consistent with changes found in annual total rainfall. The found trend in runoff is largely attributed to this trend in rainfall. Ajami et al. (2017) investigated 166 HRS catchments for trends in the period 1984 - 2005. A trend in runoff ratio was found for 20 catchments using a Mann-Kendall test. In 19 out of 20 catchments, the trend in the runoff ratio was decreasing. Change point detection was not investigated in this case. In 17 of the 20 catchments that were found, an increase in fractional vegetative cover was present. This seems to indicate that a decreasing trend regarding runoff ratio in Australia is more common than increasing trends regarding the runoff ratio. This decreasing trend regarding runoff ratio present in catchments in Australia could explain that most catchments that were found to have a change in this research showed a high value for $F(\omega_{after})$.

Previous research has shown that a possible reason for a declining runoff ratio in catchments in south-west Australia is a falling groundwater table (Chiew et al., 2014; Kinal and Stoneman, 2012; Potter and Chiew, 2011). The effect of these falling groundwater tables is a disconnection between the groundwater and the surface water. The consequence of this disconnection is a decrease in groundwater flow, resulting in a decreased annual runoff. These effects were mostly present during the Millennium drought and it was expected that the effect of groundwater disconnection would reduce after one or more wet years (Petheram et al., 2011).

The effect of groundwater disconnection seems to be mostly present in catchments with moderate rainfall and little height differences. Catchments where the height differences are larger and where the amount of precipitation is smaller are less prone to changes due to disconnection of groundwater and streamflow (Chiew et al., 2014). Incorporating topography was not within the limits of this study. It is therefore not possible to determine whether the catchments that were found to

have a decreased runoff ratio in this study have little height differences. However, in further studies it may be interesting to take the topography of the catchments into account to investigate the effect of slopes.

Other possible causes for a decrease in runoff ratio are linked to changed climatic conditions. In a modelling experiment performed by Potter and Chiew (2011) for one catchment, a reduction in runoff was partly attributed to decreased interannual variability and changed seasonality of precipitation. The changed seasonality is caused by a higher reduction in precipitation during the autumn and winter months than in summer months (Chiew et al., 2014).

In this study it was found that a decrease in runoff ratio was mostly present in catchments in which precipitation is out of phase with the potential evaporation, and therefore most precipitation occurs during the autumn and winter months in these catchments. Even after the Millennium drought has ended, the precipitation in the cool months has remained below average (Chiew et al., 2014). This reduction in autumn and winter rainfall could be a cause for the observed reduction in runoff ratio in catchments with a dominant cool month precipitation regime.

Climate models indicate that the reduction of rainfall in the cool season can progress into the future (Post et al., 2014). The observed reductions in runoff ratio may therefore be long-term changes.

6.2.3. Rainfall-runoff change methodology

The bootstrapping method used in this research is essentially a data-driven method. A result of using the bootstrapping samples is that the storage assumption in the water balance might be violated. Normally, using consecutive years, the storages at the start of the hydrological year is equal to the storage at the end of the previous hydrological year. Using the bootstrapping samples, this will most likely not be the case. Therefore, a storage error may be introduced here. The direction of this storage error can either be positive or negative. However, these differences in storage can cancel each other out. Having positive storage changes for each sample would result in an underestimation of E_A and therefore a lower evaporative index and lower ω. Similarly, negative storage changes will result in a higher evaporative index and ω. Oftentimes, the annual storage change is however assumed to be small. Therefore, the error that is introduced will probably be limited.

In case of using a sample length of 1 or 2 years, the number of unique samples is limited. In case of 1 year, the number of unique samples is equal to the number of years before the drought. The use of bootstrapping may not be very useful in this case, as the same sample will be generated often. In case of a limited number of unique samples, it may be better to use each unique sample once and generate the distribution using these samples, instead of using the bootstrapping method. Furthermore, the spread in ω seems to decrease with an increasing sample length. In Appendix D, the 5 and 95 percentile of ω and the difference between these two values have been displayed for a sample length of 1 and 7 years. The difference between these two percentiles is smaller in the case of a 7 year sample than when a 1 year sample is used. This is similar to what has been found by Guo et al. (2019), where the catchment with the smallest number of data points had the largest uncertainty.

If samples are not within the limits of the Budyko framework, no ω value can be determined for this sample using the equation of Fu. In this case, the value of ω is set to 20, which is a very high value. The decision to do this does have an influence on the results, as the number of high values for ω increases. This will result in an ECDF that is shifted to higher values. The effect on $F(\omega_{after})$ is that this will be lower.

However, the number of times that a value is not within the bounds of the Budyko framework is limited. Therefore, this will not have a very large influence on the final results. Furthermore, as this will lead to a decrease in the value of $F(\omega_{after})$, the larger amount of high values can not be explained by this.

In this research, only one sample has been used after drought. This sample has been compared to 1000 samples before drought. An extension to this method could be to use more samples in the after drought situation. In this case, two ECDF curves will be generated, one with ω values before the drought and one with ω values after the drought. These curves can be compared against each other, to identify whether they are from the same distribution. This could give more certainty to the results.

6.2.4. Factors relating to change

In the comparison of different factors relating to a change in the rainfall-runoff relationship, a sample length of 5 years has been chosen. The choice for 5 years has been made on the basis of a trade off between having enough random samples and having a short time period after the drought. Furthermore, as discussed earlier, the uncertainty in ω increases with a shorter sample length.

Looking at the difference between catchments with an increase in runoff ratio and a decrease in runoff ratio, it can be seen that there are 2 factors that seem to have an influence on the changes that have been found. These are:

- Drought severity
- Seasonality and timing of precipitation

Catchments that show a reduction in the evaporative index have oftentimes gone through a more severe drought than catchments where the evaporative index has increased. This is contrary to what was found by Saft et al. (2015), who found that the drought climatic metrics had no influence on the change in the rainfall-runoff relationship during a drought period.

The effect of a drought also seems stronger in catchments that are in a regime with wet summers and relatively dry winters. A possible explanation for this can be that the vegetation in the catchments that normally have dry summers need to have a larger storage capacity compared to catchments with dry winters, when the amount of water that is evaporated is smaller.

This seems to be in contrast to the finding that the pre-drought root-zone storage capacity does not influence the response to drought. However, the root-zone storage capacities do not necessarily have to be larger in catchments with a dry summer. The root-zone storage capacity is not only linked to seasonality. It can be that a catchment is relatively wet and therefore the storage capacity determined with the mass curve technique is not large even though there is a high seasonality.

Factors related to the land use and land cover in the catchment do not seem to play as large of a role as factors related to climate. The land use and land cover factors that have been investigated are:

- Fraction of forest cover
- Fraction of eucalypt cover
- Change in NDVI
- Fraction of catchment burned during the drought

In all four cases, no significant relation has been found to changes in the rainfall-runoff relationship that were observed. Noticeable is that the spread is large in all four factors. This is especially the case for the forest cover and eucalypt cover. While most of the catchments where the relative evaporative factor increased were found to have a relatively large fraction of eucalypt cover, the variations are still large for all groups.

That the amount of forest cover does not have a large influence on the change that is presented does not eliminate the hypothesis that the change in rainfall-runoff relation is related to a change in the vegetative cover. This is because there is a value given for the amount of forest cover at a specific time, which does not indicate anything about forest die-off during the drought. It could for example be that there is a small part of the catchment that is forested. Tree die-off in this section can still have an effect on the rainfall-runoff relationship. On the other hand, if a catchment has a 100% forest cover, this does not mean that tree die-off takes place during drought.

Given this information, a better indicator could be the change in the NDVI that takes place during the drought. The idea is that this gives an indication of the tree die-off that has taken place. Research by Gazol et al. (2018) showed that in the year after an extreme drought the NDVI strongly reduced in the forest with the largest tree mortality rates. Data availability was however a problem, so a long-term difference in NDVI has not been investigated.

In this research, a pre- and post-drought NDVI mean of 3 years has been used, which is longer than the one year that is used by Gazol et al. (2018). No significant relation was found between the change in NDVI and the change in rainfall-runoff relationship. This could be an indication that the tree die-off in a catchment during drought has little effect on the long-term response to rainfall-runoff. Another explanation could be that during the three years, regrowth takes place. In boreal forests it has been shown that with increasing forest cover, the NDVI does not change or decline (Loranty et al., 2018), as the understory of the forest also plays a large role in the determination of NDVI. Boreal forests are different from the forests present in Australia, but the same mechanics could play a role.

Furthermore, the MODIS NDVI data that was used in this research was only available from 2000 onwards. This means that the data could not be used for all catchments. Another possibility could be to make use of AVHRR data, which has data from 1989 to the present (USGS, nd). This would make it possible to compare droughts for more catchment and look al longer term differences for catchment that had the longest drought during the Millennium drought.

In this research, only one factor has been compared with the value of $F(\omega_{after})$ at a time. Hydrological systems are complex and there is interaction between different variables. It may therefore be of value to look into analysis of multiple variables to see whether catchments can be grouped more systematically. This idea is strengthened by the large variation when looking at the relation between $F(\omega_{after})$ and the different factors, suggesting that more is going on than just direct relationships. Multiple regression may help in identifying combinations of factors that have an effect on the long-term response after drought.

6.3. Root-zone storage recovery

In this research, both pre-drought root-zone storage capacities and differences in root-zone storage capacities due to a drought period have been looked into.

The found root-zone storage capacities differ quite a lot between different regions of Australia. The highest values are found in Northern Australia, with root-zone storage capacities over 1000 mm. This division is similar to what is found in research by Wang-Erlandsson et al. (2016), where the largest root-zone storage capacities are also found in Northern Australia, followed by southern coastal areas. The method used is similar to the method used in this research. One difference is that in case of Wang-Erlandsson et al. (2016), transpiration and interception are combined. Furthermore, evaporation in Wang-Erlandsson et al. (2016) uses satellite-derived estimates of evaporation, compared to the estimation method based on precipitation and runoff used in this research.

Currently, a return period of 20 years has been used in the determination of S_R. Wang-Erlandsson et al. (2016) has shown that, based on model performance, the optimal value for the return period differed by land cover. Return periods in forested areas were higher than in grasslands. An extension could therefore be to calculate the root-zone storage capacity for different return periods, one return period for dense and high vegetation and one return period for grass- and shrubland. Subsequently, the found root-zone storage capacities can be multiplied by the fraction of cover of the land use type. This can give an aggregated value which takes into account different land uses. The value of $S_{R,1yr}$ is not influenced by the determined return period, as this always uses the yearly maximum deficit.

In this study the variable $\Delta S_{R,1yr}$ has been introduced to compare root-zone storage capacities before and after a drought. In this method, the median value for both periods has been used. As the root-zone storages have been found to form root systems capable of overcoming deficits with a return period of 10 to 20 years, this method may not be applicable to determine qualitative differences in the root-zone storage capacity of the catchment before and after drought.

The values determined for $\Delta S_{R,1yr}$ seem to be related to the value of $F(\omega_{after})$, based on the low p-value for the KS-test. Low values for $\Delta S_{R,1yr}$ are found in catchments that have a low value of $F(\omega_{after})$. Both of these variables are calculated using the precipitation, potential evaporation and discharge measurements. Given a similar precipitation, the catchments with an observed increase in runoff ratio logically have less water available for transpiration. This will result in smaller deficits and as a result a smaller value for $\Delta S_{R,1yr}$. However, this does not directly indicate that this change is due to change in vegetation. In Figure 6.1, the found value for $\Delta S_{R,1yr}$ is compared to the value of $\Delta_r NDVI$. This shows that there does not necessarily seem to be a relation between the value determined change in root-zone storage capacity and the vegetative cover.

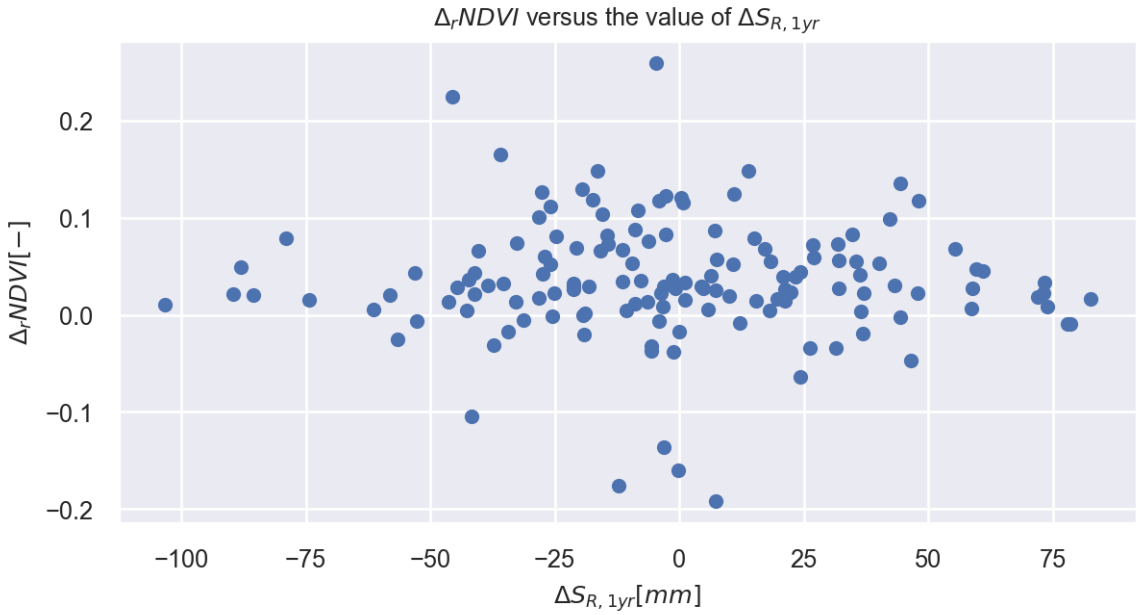

Figure 6.1: $\Delta S_{R,1yr}$ compared to a relative change of NDVI. A negative value of $\Delta S_{R,1yr}$ indicates a decrease in the root-zone storage capacity over the drought period, while a positive value indicates an increase.

In the determination of S_R it is important to have a good estimate of the evaporation fluxes. As it is hard to measure these fluxes directly, estimates have to be made based on assumptions.

The determination of the transpiration for $S_{R,1yr}$ has been performed using a water balance of 3 years. The first year of this 3 year water balance method has been used in the calculation of the deficit. The other two years are used in the determination of $\overline{E_t}$. This is done based on the idea that during recovery, the amount of vegetation is not constant and the evaporation increases over time.

Nijzink et al. (2016) used a water balance of 2 years instead of 3 years. In this research, 3 years has been chosen after a limited test in which the evaporation has been compared between different years. This test showed that with a water balance of 2 years, there were still significant differences between the evaporation determined for the same year. With a water balance of 3 years, there were still differences found between the transpiration that was determined for the same year. However, these differences were smaller than with a 2-year water balance. Therefore, the determined value

for E_t is still uncertain. As the transpiration has a large impact on the eventually determined deficit, it is important that more research is done to make a better assumption for the transpiration. One possibility could be to do additional examinations regarding the optimal duration of the timeseries for $S_{R,1yr}$.

Furthermore, under the assumption that after drought E_t values increase gradually, it might be better to use the middle of the three years for determining the deficit. Currently, the evaporation in the second and third year will be higher than in the first year. Therefore the determined $\overline{E_t}$ is high for the first year. If the second year is used, the lower evaporation during the first year counteracts the higher evaporation in the third year.

In this research, the value for I_{max} has been assumed constant at 2 mm. The maximum interception capacity has an influence on the amount of water that is available for interception evaporation. The amount of interception evaporation is subtracted from available potential evaporation. Furthermore, it is assumed that the effective precipitation is divided into runoff and transpiration. As the runoff is known, the transpiration is assumed based on the effective precipitation and runoff.

In case of catchment 225020A, the values for $S_{R,1yr}$ were frequently equal to 0 mm. This means that the effective precipitation is equal to or smaller than the generated runoff during the 3-year period. As the water balance has been tested in Chapter 3, there is sufficient precipitation to account for the runoff. That there is no water available for transpiration, must mean that the modeled interception evaporation was higher than it actually is. In Figure 6.2, the $S_{R,1yr}$ values after the drought are displayed for differing values of I_{max} for catchment 225020A. This Figure shows that with a lower value for I_{max}, the $S_{R,1yr}$ value indeed increases.

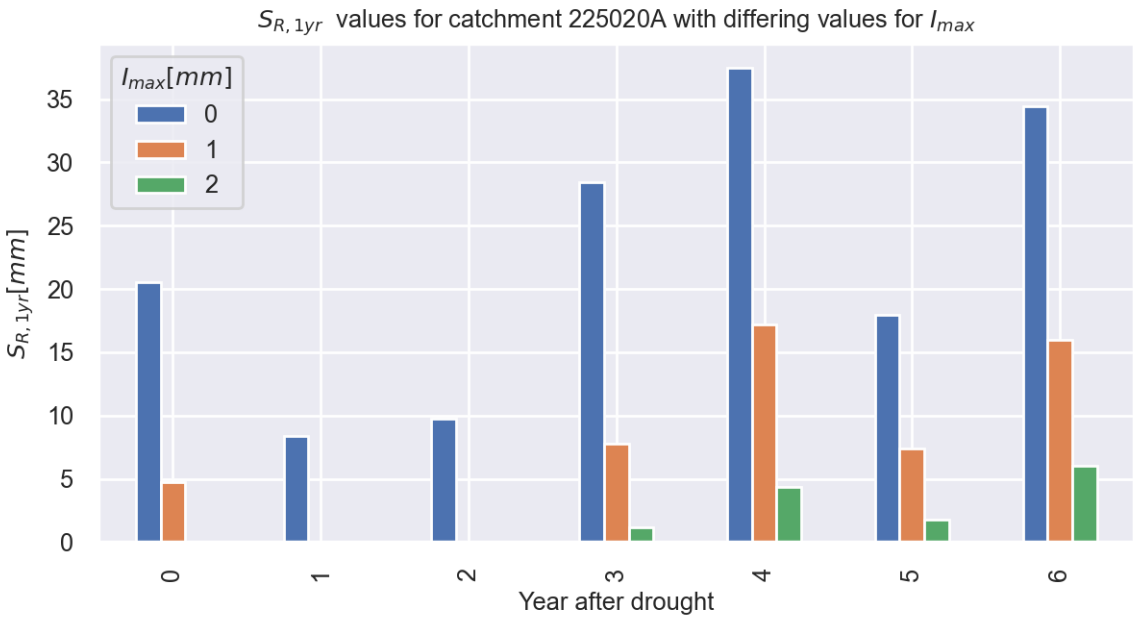

Figure 6.2: Comparison for $S_{R,1yr}$ for differing values of I_{max}

Given the information above, the assumption that I_{max} is constant in both space and time may not be valid for all catchments. This is something that can be improved in the future. A possibility could be to base the value of I_{max} based on land use classes and NDVI (Vegas Galdos et al., 2012). This could be used to make I_{max} dependent on both space and time, which could potentially improve the accuracy of the results.

7

Conclusions

The goal of this research was to determine if there is a difference in catchment response to rainfall after a drought, relative to the situation before drought. The main questions regarding this goal were:

1. Is there a change in runoff ratio in catchments after a long-term drought relative to the situation before the drought?
2. Is there a change in the root-zone storage capacity determined with the mass curve technique following a multiyear drought?

With regard to the question whether a change in the runoff ratio occurs, the hypothesis was that the runoff ratio would increase after a long-term drought.

What was found does not show that long-term droughts cause an increase in runoff ratio after a drought. Considering a 5-year period after the drought, a change was observed 71 of the 196 catchments. Out of these 71, only 27 catchments showed an increase in the runoff ratio. Shorter and longer periods after the drought showed similar results. The in- or decrease in runoff that was found was in most cases less than 10% of the total precipitation, with extreme cases of almost 30%.

Catchments that showed an increase in runoff ratio were found to have on average a higher drought severity and a distribution of the precipitation that is more concentrated in the summer months, compared to catchments with a decrease in runoff ratio that have more winter-based precipitation and had less severe droughts.

Besides climate factors, also land use and land cover factors were looked into. Land use factors that were considered, like fraction of forest present and a change in the NDVI after the drought relative to the situation before drought did not show a clear relationship with the differences found in the change of runoff ratio.

The expectation for the question regarding a change in root-zone storage capacity was that the root-zone storage capacity, determined using the mass curve technique, would decline following a multiyear drought.

What was found was that the changes determined in the root-zone storage capacity using the mass curve technique were overall comparable to the changes found in the runoff ratio. The majority of the catchments where the runoff ratio increased during drought did indeed show a decrease in the root-zone storage capacity.

However, the found change in root-zone storage capacity did not agree well with found changes in NDVI. This could also mean that other factors than vegetation change play a role in the found differences in the root-zone storage capacities.

Bibliography

Ajami, H., Sharma, A., Band, L. E., Evans, J. P., Tuteja, N. K., Amirthanathan, G. E., and Bari, M. A. (2017). On the non-stationarity of hydrological response in anthropogenically unaffected catchments: an Australian perspective. *Hydrol. Earth Syst. Sci.*, 21(1):281–294.

Allen, C. D., Macalady, A. K., Chenchouni, H., Bachelet, D., McDowell, N., Vennetier, M., Kitzberger, T., Rigling, A., Breshears, D. D., Hogg, E. H. T., Gonzalez, P., Fensham, R., Zhang, Z., Castro, J., Demidova, N., Lim, J.-H., Allard, G., Running, S. W., Semerci, A., and Cobb, N. (2010). A global overview of drought and heat-induced tree mortality reveals emerging climate change risks for forests. *Forest Ecology and Management*, 259(4):660–684.

Anderegg, W. R. L., Kane, J. M., and Anderegg, L. D. L. (2012). Consequences of widespread tree mortality triggered by drought and temperature stress. *Nature Climate Change*, 3:30.

Australia Government Department of Agriculture (2016). Land use. `https://www.agriculture.gov.au/abares/aclump/land-use`. Accessed: 19-November-2019.

Australian Government Department of the Environment and Energy (2018). National Vegetation Information Systems version 5.1. `https://www.environment.gov.au/land/native-vegetation/national-vegetation-information-system/data-products`.

Beck, H. E., Zimmermann, N. E., McVicar, T. R., Vergopolan, N., Berg, A., and Wood, E. F. (2018). Present and future Köppen-Geiger climate classification maps at 1-km resolution. *Scientific Data*, 5(1):180214.

Berghuijs, W. R., Sivapalan, M., Woods, R. A., and Savenije, H. H. G. (2014). Patterns of similarity of seasonal water balances: A window into streamflow variability over a range of time scales. *Water Resources Research*, 50(7):5638–5661.

Berghuijs, W. R. and Woods, R. A. (2016). A simple framework to quantitatively describe monthly precipitation and temperature climatology. *International Journal of Climatology*, 36(9):3161–3174.

Budyko, M. I. (1974). *Climate and Life*. Academic Press, New York.

Chiew, F. H. S., Potter, N. J., Vaze, J., Petheram, C., Zhang, L., Teng, J., and Post, D. A. (2014). Observed hydrologic non-stationarity in far south-eastern Australia: implications for modelling and prediction. *Stochastic Environmental Research and Risk Assessment*, 28(1):3–15.

Choat, B., Jansen, S., Brodribb, T. J., Cochard, H., Delzon, S., Bhaskar, R., Bucci, S. J., Feild, T. S., Gleason, S. M., Hacke, U. G., Jacobsen, A. L., Lens, F., Maherali, H., Martínez-Vilalta, J., Mayr, S., Mencuccini, M., Mitchell, P. J., Nardini, A., Pittermann, J., Pratt, R. B., Sperry, J. S., Westoby, M., Wright, I. J., and Zanne, A. E. (2012). Global convergence in the vulnerability of forests to drought. *Nature*, 491(7426):752–755.

Ciais, P., Reichstein, M., Viovy, N., Granier, A., Ogée, J., Allard, V., Aubinet, M., Buchmann, N., Bernhofer, C., Carrara, A., Chevallier, F., De Noblet, N., Friend, A. D., Friedlingstein, P., Grünwald, T., Heinesch, B., Keronen, P., Knohl, A., Krinner, G., Loustau, D., Manca, G., Matteucci, G., Miglietta, F., Ourcival, J. M., Papale, D., Pilegaard, K., Rambal, S., Seufert, G., Soussana, J. F., Sanz, M. J.,

Schulze, E. D., Vesala, T., and Valentini, R. (2005). Europe-wide reduction in primary productivity caused by the heat and drought in 2003. *Nature*, 437(7058):529–533.

Dai, A. (2011). Drought under global warming: A review. *Wiley Interdisciplinary Reviews: Climate Change*, 2(1):45–65.

de Boer-Euser, T., McMillan, H. K., Hrachowitz, M., Winsemius, H. C., and Savenije, H. H. G. (2016). Influence of soil and climate on root zone storage capacity. *Water Resources Research*, 52(3):2009–2024.

Didan, K. (2015). MOD13A2 MODIS/Terra Vegetation Indices 16-Day L3 Global 1km SIN Grid V006 [Data set]. NASA EOSDIS Land Processes DAAC. Accessed: 11-May-2020 from `https://doi.org/10.5067/MODIS/MOD13A2.006`.

Enku, T., Melesse, A. M., Ayana, E. K., Tilahun, S. A., Abate, M., and Steenhuis, T. S. (2020). Groundwater use of a small Eucalyptus patch during the dry monsoon phase. *Biologia*, 75(6):853–864.

Fu, B. P. (1981). On the calculation of the evaporation from land surface. *Sci. Atmos. Sin*, 5(1):23–31.

Gao, H., Hrachowitz, M., Schymanski, S. J., Fenicia, F., Sriwongsitanon, N., and Savenije, H. H. G. (2014). Climate controls how ecosystems size the root zone storage capacity at catchment scale. *Geophysical Research Letters*, 41(22):7916–7923.

Gazol, A., Camarero, J. J., Sangüesa-Barreda, G., and Vicente-Serrano, S. M. (2018). Post-drought Resilience After Forest Die-Off: Shifts in Regeneration, Composition, Growth and Productivity.

Giglio, L., Justice, C., Boschetti, L., and Roy, D. (2015). MCD64A1 MODIS/Terra+Aqua Burned Area Monthly L3 Global 500m SIN Grid V006 [Data set]. NASA EOSDIS Land Processes DAAC. Accessed: 19-November-2019 from `https://doi.org/10.5067/MODIS/MCD64A1.006`.

Goulden, M. L. and Bales, R. C. (2019). California forest die-off linked to multi-year deep soil drying in 2012–2015 drought. *Nature Geoscience*, 12(8):632–637.

Greve, P., Gudmundsson, L., Orlowsky, B., and Seneviratne, S. I. (2015). Introducing a probabilistic Budyko framework. *Geophysical Research Letters*, 42(7):2261–2269.

Guo, A., Chang, J., Wang, Y., Huang, Q., Guo, Z., and Li, Y. (2019). Uncertainty analysis of water availability assessment through the Budyko framework. *Journal of Hydrology*, 576:396–407.

Jaramillo, F., Cory, N., Arheimer, B., Laudon, H., van der Velde, Y., Hasper, T. B., Teutschbein, C., and Uddling, J. (2018). Dominant effect of increasing forest biomass on evapotranspiration: interpretations of movement in Budyko space. *Hydrol. Earth Syst. Sci.*, 22(1):567–580.

Jaramillo, F. and Destouni, G. (2014). Developing water change spectra and distinguishing change drivers worldwide. *Geophysical Research Letters*, 41(23):8377–8386.

Jeffrey, S. J., Carter, J. O., Moodie, K. B., and Beswick, A. R. (2001). Using spatial interpolation to construct a comprehensive archive of Australian climate data. *Environmental Modelling & Software*, 16(4):309–330.

Kinal, J. and Stoneman, G. L. (2012). Disconnection of groundwater from surface water causes a fundamental change in hydrology in a forested catchment in south-western Australia. *Journal of Hydrology*, 472-473:14–24.

Kundzewicz, Z. W. and Robson, A. J. (2004). Change detection in hydrological records—a review of the methodology / Revue méthodologique de la détection de changements dans les chroniques hydrologiques. *Hydrological Sciences Journal*, 49(1):7–19.

Lewis, S. L., Brando, P. M., Phillips, O. L., van der Heijden, G. M. F., and Nepstad, D. (2011). The 2010 Amazon Drought. *Science*, 331(6017):554 LP – 554.

Loranty, M. M., Davydov, S. P., Kropp, H., Alexander, H. D., Mack, M. C., Natali, S. M., and Zimov, N. S. (2018). Vegetation Indices Do Not Capture Forest Cover Variation in Upland Siberian Larch Forests.

McKee, T. B., Doesken, N. J., and Kleist, J. (1993). The relationship of drought frequency and duration to time scales. In *Proceedings of the 8th Conference on Applied Climatology*, volume 17, pages 179–183. Boston.

Mishra, A. K. and Singh, V. P. (2010). A review of drought concepts. *Journal of Hydrology*, 391(1):202–216.

Mueller, R. C., Scudder, C. M., Porter, M. E., Talbot Trotter Iii, R., Gehring, C. A., and Whitham, T. G. (2005). Differential tree mortality in response to severe drought: evidence for long-term vegetation shifts. *Journal of Ecology*, 93(6):1085–1093.

National Integrated Drought Information System (n.d.). Drought in california. `https://www.drought.gov/drought/states/california`. Accessed: 24-September-2019.

Nijzink, R., Hutton, C., Pechlivanidis, I., Capell, R., Arheimer, B., Freer, J., Han, D., Wagener, T., McGuire, K., Savenije, H., and Hrachowitz, M. (2016). The evolution of root-zone moisture capacities after deforestation: A step towards hydrological predictions under change? *Hydrology and Earth System Sciences*, 20(12):4775–4799.

Perrin, C., Michel, C., and Andréassian, V. (2003). Improvement of a parsimonious model for streamflow simulation. *Journal of Hydrology*, 279(1):275–289.

Petheram, C., Potter, N., Vaze, J., Chiew, F., and Zhang, L. (2011). Towards better understanding of changes in rainfall-runoff relationships during the recent drought in south-eastern Australia. In *19th International Congress on Modelling and Simulation, Perth, Australia*, pages 12–16.

Post, D. A., Timbal, B., Chiew, F. H. S., Hendon, H. H., Nguyen, H., and Moran, R. (2014). Decrease in southeastern Australian water availability linked to ongoing Hadley cell expansion. *Earth's Future*, 2(4):231–238.

Potter, N. J. and Chiew, F. H. S. (2011). An investigation into changes in climate characteristics causing the recent very low runoff in the southern Murray-Darling Basin using rainfall-runoff models. *Water Resources Research*, 47(12).

Rougé, C., Ge, Y., and Cai, X. (2013). Detecting gradual and abrupt changes in hydrological records. *Advances in Water Resources*, 53:33–44.

Saft, M., Peel, M. C., Western, A. W., Perraud, J.-M., and Zhang, L. (2016). Bias in streamflow projections due to climate-induced shifts in catchment response. *Geophysical Research Letters*, 43(4):1574–1581.

Saft, M., Western, A. W., Zhang, L., Peel, M. C., and Potter, N. J. (2015). The influence of multiyear drought on the annual rainfall-runoff relationship: An Australian perspective. *Water Resources Research*, 51(4):2444–2463.

Savenije, H. (2009). *CT4431 - Hydrological Modelling*. TU Delft.

Svoboda, M. D., Fuchs, B. A., and Integrated Drought Management Programme (2016). Handbook of drought indicators and indices. Technical report.

Tsakiris, G. and Vangelis, H. (2005). Establishing a drought index incorporating evapotranspiration. *European water*, 9(10):3–11.

USGS (n.d.). NDVI from AVHRR. `https://www.usgs.gov/land-resources/eros/phenology/science/ndvi-avhrr?qt-science_center_objects=0#qt-science_center_objects`. Accessed: 27-June-2020.

van der Velde, Y., Vercauteren, N., Jaramillo, F., Dekker, S. C., Destouni, G., and Lyon, S. W. (2014). Exploring hydroclimatic change disparity via the Budyko framework. *Hydrological Processes*, 28(13):4110–4118.

van Dijk, A. I. J. M., Beck, H. E., Crosbie, R. S., de Jeu, R. A. M., Liu, Y. Y., Podger, G. M., Timbal, B., and Viney, N. R. (2013). The Millennium Drought in southeast Australia (2001–2009): Natural and human causes and implications for water resources, ecosystems, economy, and society. *Water Resources Research*, 49(2):1040–1057.

Van Loon, A. F. and Laaha, G. (2015). Hydrological drought severity explained by climate and catchment characteristics. *Journal of Hydrology*, 526:3–14.

Vegas Galdos, F., Álvarez, C., García, A., and Revilla, J. A. (2012). Estimated distributed rainfall interception using a simple conceptual model and Moderate Resolution Imaging Spectroradiometer (MODIS). *Journal of Hydrology*, 468-469:213–228.

Vicente-Serrano, S. M., Beguería, S., and López-Moreno, J. I. (2009). A Multiscalar Drought Index Sensitive to Global Warming: The Standardized Precipitation Evapotranspiration Index. *Journal of Climate*, 23(7):1696–1718.

Vose, J. M., Miniat, C. F., Luce, C. H., Asbjornsen, H., Caldwell, P. V., Campbell, J. L., Grant, G. E., Isaak, D. J., Loheide, S. P., and Sun, G. (2016). Ecohydrological implications of drought for forests in the United States. *Forest Ecology and Management*, 380:335–345.

Wang-Erlandsson, L., Bastiaanssen, W. G. M., Gao, H., Jägermeyr, J., Senay, G. B., van Dijk, A. I. J. M., Guerschman, J. P., Keys, P. W., Gordon, L. J., and Savenije, H. H. G. (2016). Global root zone storage capacity from satellite-based evaporation. *Hydrol. Earth Syst. Sci.*, 20(4):1459–1481.

Yang, H., Yang, D., Lei, Z., and Sun, F. (2008). New analytical derivation of the mean annual water-energy balance equation. *Water Resources Research*, 44(3).

Yang, Y., McVicar, T. R., Donohue, R. J., Zhang, Y., Roderick, M. L., Chiew, F. H. S., Zhang, L., and Zhang, J. (2017). Lags in hydrologic recovery following an extreme drought: Assessing the roles of climate and catchment characteristics. *Water Resources Research*, 53(6):4821–4837.

Young, I. T. (1977). Proof without prejudice: use of the Kolmogorov-Smirnov test for the analysis of histograms from flow systems and other sources. *Journal of Histochemistry & Cytochemistry*, 25(7):935–941.

Zhang, D., Cong, Z., Ni, G., Yang, D., and Hu, S. (2015). Effects of snow ratio on annual runoff within the Budyko framework. *Hydrol. Earth Syst. Sci.*, 19(4):1977–1992.

Zhang, L., Dawes, W. R., and Walker, G. R. (2001). Response of mean annual evapotranspiration to vegetation changes at catchment scale. *Water Resources Research*, 37(3):701–708.

Zhang, L., Hickel, K., Dawes, W. R., Chiew, F. H. S., Western, A. W., and Briggs, P. R. (2004). A rational function approach for estimating mean annual evapotranspiration. *Water Resources Research*, 40(2).

Zhang, X. S., Amirthanathan, G. E., Bari, M. A., Laugesen, R. M., Shin, D., Kent, D. M., MacDonald, A. M., Turner, M. E., and Tuteja, N. K. (2016). How streamflow has changed across Australia since the 1950s: evidence from the network of hydrologic reference stations. *Hydrol. Earth Syst. Sci.*, 20(9):3947–3965.

Zhao, M. and Running, S. W. (2010). Drought-Induced Reduction in Global Terrestrial Net Primary Production from 2000 Through 2009. *Science*, 329(5994):940 LP – 943.

A

Additional climatic condition plots

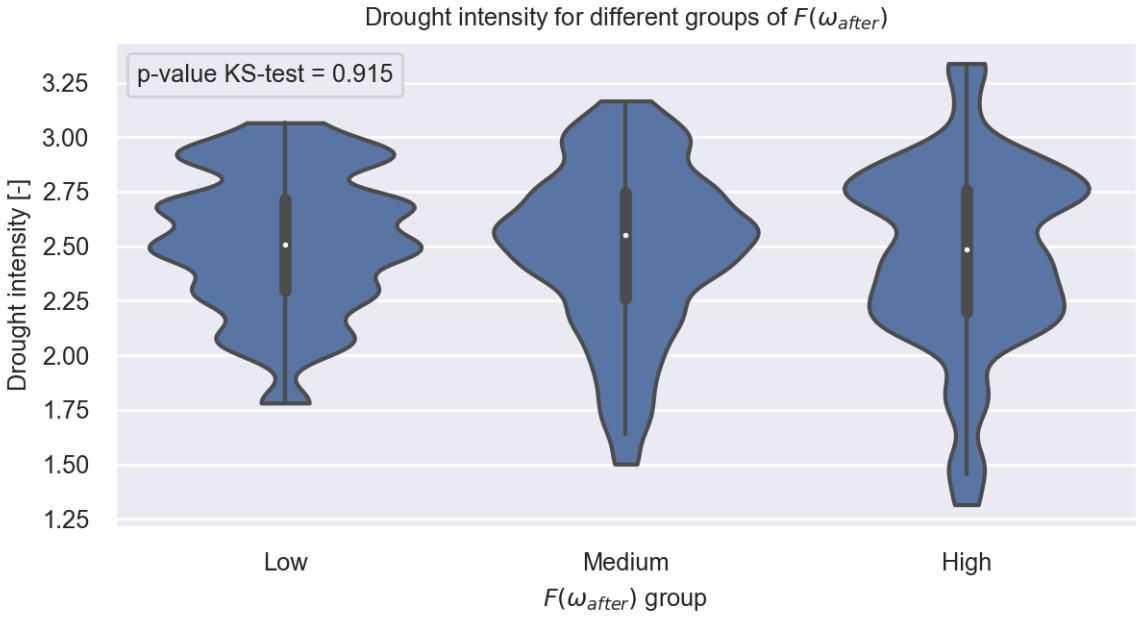

Figure A.1: Violinplot comparing the drought intensity for the three different groups

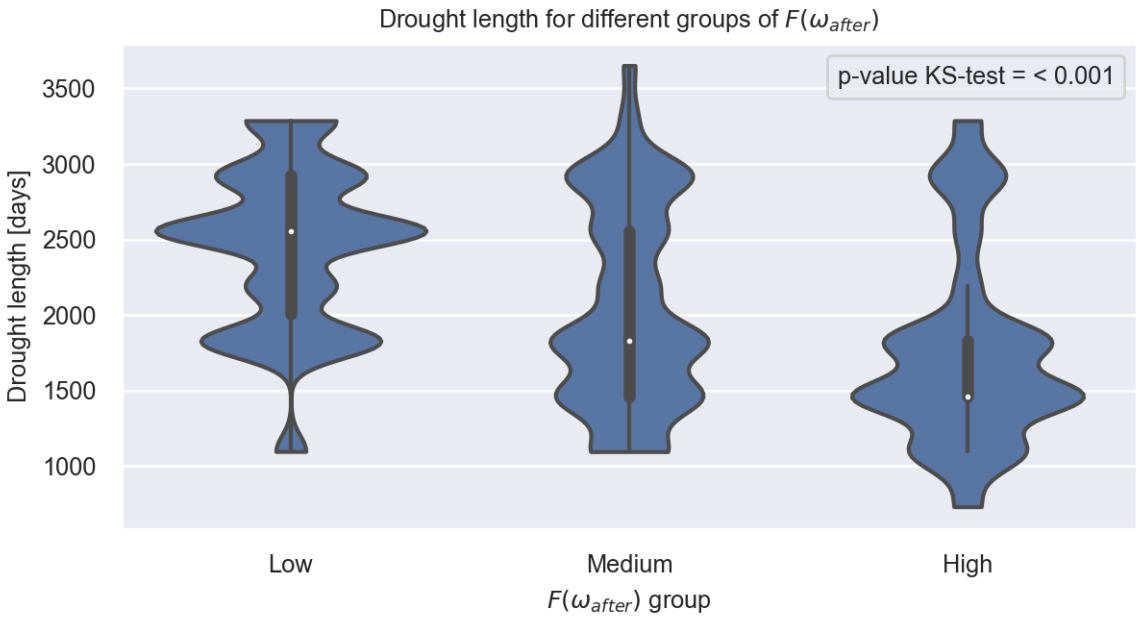

Figure A.2: Violinplot comparing the drought length for the three different groups

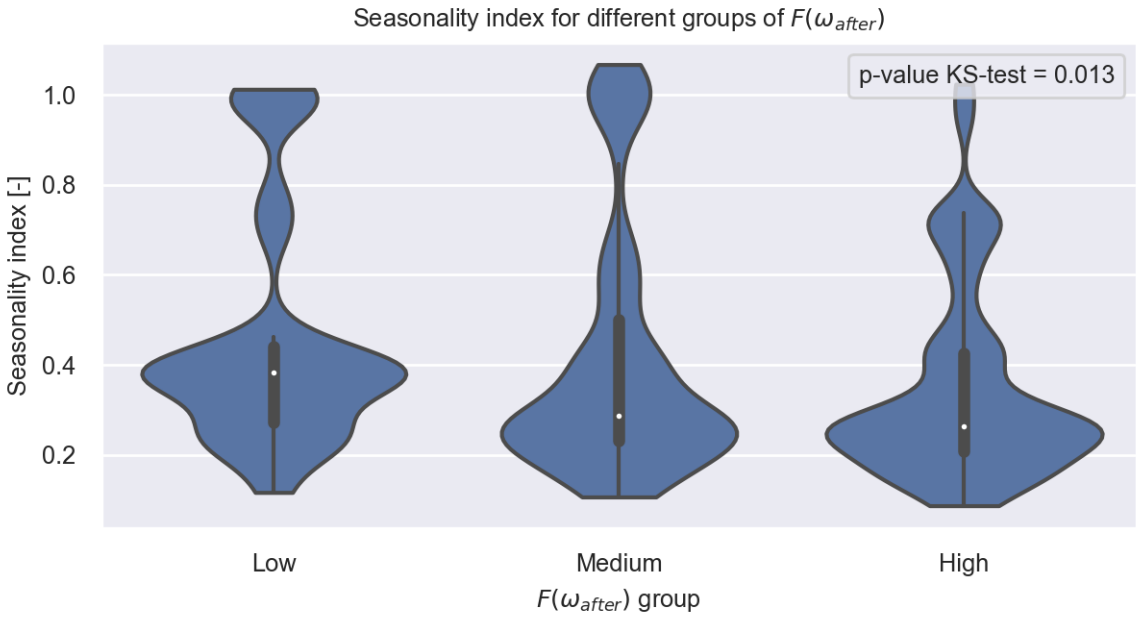

Figure A.3: Violinplot comparing the seasonality index for the three different groups

B

Additional Land Use / Land Cover plots

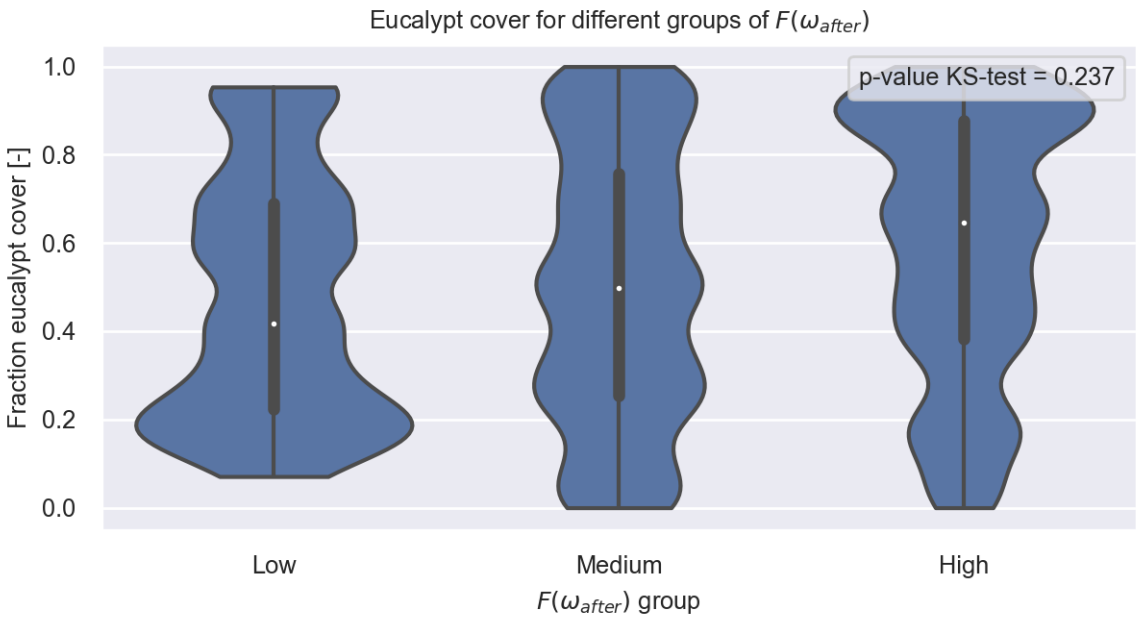

Figure B.1: Violinplot comparing the fraction of the catchment covered by Eucalypt trees for the three different groups

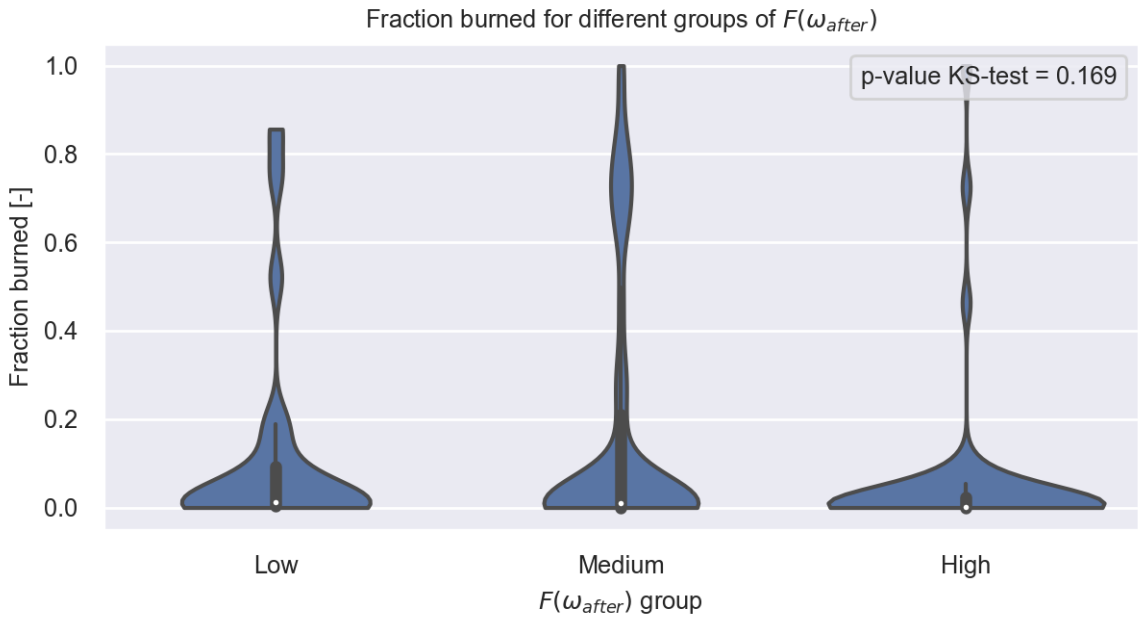

Figure B.2: Violinplot comparing the max fraction of burned area in a month for the three different catchments

C

Comparison with Jaramillo

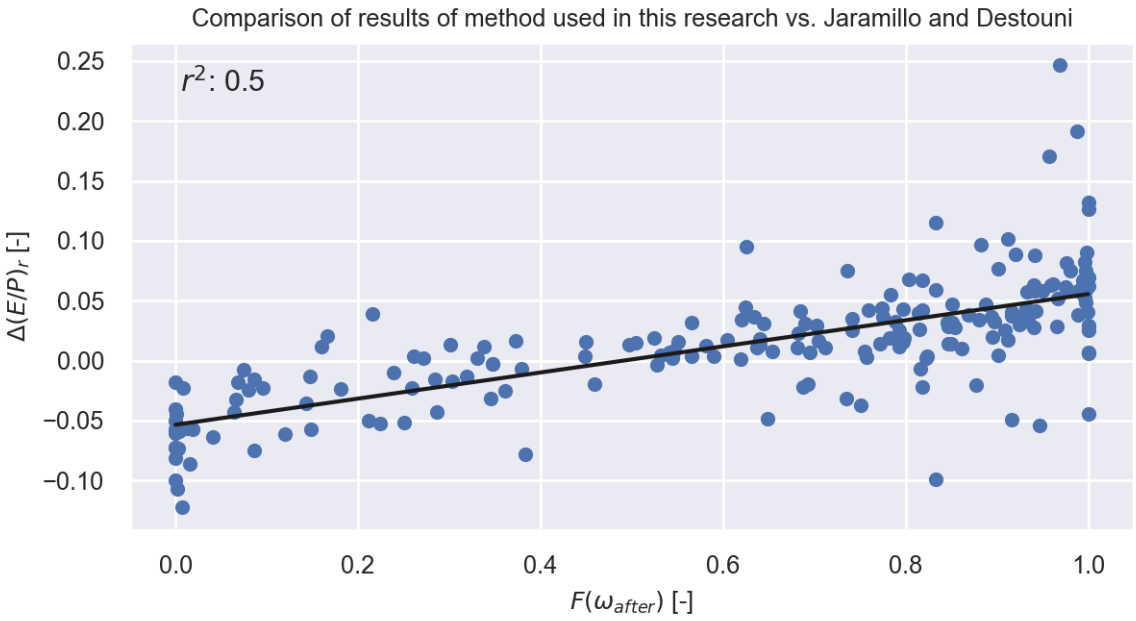

Figure C.1: Comparison between results of the method used in this research vs. method used by Jaramillo and Destouni

D

Uncertainty of ω

Table D.1: The values for ω at the 5 and 95 percentile and the difference between these two for a sample length of 1 year and 7 years.

	1 year			7 years		
Catchment	5%	95%	Difference	5%	95%	Difference
410730	1.81	3.61	1.81	2.19	2.92	0.73
410731	2.56	5.23	2.68	2.90	3.94	1.04
410734	2.17	5.11	2.93	2.37	3.42	1.05
410705	2.25	4.61	2.36	2.45	3.32	0.87
410761	2.61	7.62	5.01	2.88	3.77	0.89
204034	2.59	4.46	1.87	2.85	3.38	0.53
206014	2.27	4.42	2.14	2.32	3.15	0.82
206018	2.52	4.59	2.07	2.95	3.73	0.78
208007	1.67	2.89	1.22	1.93	2.42	0.49
208009	1.00	2.88	1.88	1.31	2.35	1.04
210006	2.20	4.31	2.11	2.70	3.64	0.94
210011	1.49	2.94	1.45	1.78	2.33	0.55
211008	1.27	3.55	2.28	1.80	2.59	0.79
212209	1.00	3.15	2.15	1.35	2.21	0.87
212260	1.69	3.42	1.74	1.99	2.62	0.63
215002	1.69	3.80	2.11	1.94	2.75	0.81
215004	1.11	2.25	1.14	1.34	1.70	0.36
215207	1.91	3.03	1.12	2.11	2.65	0.54
216002	1.00	2.69	1.69	1.06	1.64	0.58
216004	1.82	4.07	2.25	2.02	2.77	0.75
218001	1.47	3.65	2.18	1.63	2.20	0.57
219001	1.05	2.37	1.32	1.24	1.72	0.48
401009	2.56	4.31	1.75	2.80	3.62	0.82
401012	1.61	2.63	1.02	1.87	2.27	0.39
401015	2.09	6.63	4.53	2.40	3.13	0.73
410057	1.82	3.12	1.31	2.04	2.56	0.52
410061	1.93	4.58	2.65	2.24	2.96	0.72

Continued on next page

Table D.1: The values for ω at the 5 and 95 percentile and the difference between these two for a sample length of 1 year and 7 years.

	1 year			7 years		
Catchment	5%	95%	Difference	5%	95%	Difference
412028	2.03	3.90	1.88	2.42	3.24	0.82
412050	1.75	3.69	1.93	2.18	2.97	0.79
412066	2.02	3.89	1.87	2.36	3.22	0.86
416003	2.41	4.24	1.83	2.72	3.36	0.64
416008	2.09	3.26	1.17	2.25	2.85	0.60
418005	2.45	3.75	1.31	2.60	3.19	0.60
418014	2.34	3.67	1.34	2.60	3.08	0.48
419005	2.26	3.41	1.15	2.34	2.77	0.43
424002	2.13	3.00	0.87	2.20	2.54	0.34
G0010005	1.57	2.98	1.40	1.71	2.37	0.66
G0050115	1.47	4.20	2.73	1.62	2.40	0.79
G8110004	1.67	2.87	1.20	1.38	2.32	0.93
G8110016	1.56	2.42	0.86	1.71	2.01	0.30
G8140001	1.82	2.54	0.73	1.88	2.21	0.33
G8140040	1.87	2.67	0.79	2.01	2.26	0.25
G8140161	2.06	3.36	1.30	2.39	2.82	0.44
G8150018	1.24	2.83	1.59	1.42	1.83	0.41
G8170002	1.47	3.31	1.84	1.86	2.37	0.50
G8190001	1.37	2.99	1.62	1.68	2.15	0.48
G8200045	1.53	2.48	0.95	1.67	2.01	0.35
G8210010	1.36	2.04	0.68	1.53	1.77	0.24
G9030124	2.35	4.07	1.72	2.39	2.69	0.31
G9030250	1.98	3.13	1.15	2.19	2.52	0.34
G9070142	1.70	2.94	1.24	1.92	2.38	0.46
102101A	1.24	3.35	2.11	1.39	1.94	0.55
104001A	1.49	2.44	0.96	1.63	1.84	0.21
105101A	2.00	3.62	1.62	2.20	2.73	0.53
105102A	1.49	3.13	1.64	1.58	2.21	0.62
105105A	1.92	3.75	1.83	2.22	2.94	0.72
107001B	2.02	3.18	1.16	2.04	2.40	0.36
108002A	1.47	2.95	1.48	1.70	2.31	0.61
108003A	1.01	1.40	0.40	1.15	1.32	0.18
112002A	1.02	5.58	4.56	1.16	1.98	0.82
112102A	1.31	20.00	18.69	1.70	2.84	1.14
113004A	1.00	1.59	0.59	1.11	1.35	0.23
116006B	1.53	2.50	0.96	1.72	2.11	0.39
116010A	1.43	2.76	1.32	1.54	2.00	0.47
116011A	1.53	2.91	1.39	1.79	2.22	0.43
116012A	1.02	2.91	1.89	1.30	2.09	0.79
116013A	1.47	2.52	1.05	1.73	2.11	0.37
116014A	1.56	3.33	1.77	1.88	2.42	0.54
116015A	1.54	2.66	1.12	1.67	2.11	0.45
121001A	2.02	3.75	1.73	1.96	2.74	0.78

Continued on next page

Table D.1: The values for ω at the 5 and 95 percentile and the difference between these two for a sample length of 1 year and 7 years.

	1 year			7 years		
Catchment	5%	95%	Difference	5%	95%	Difference
122004A	1.26	2.83	1.57	1.37	2.03	0.66
126003A	1.35	3.98	2.63	1.58	2.19	0.61
136202D	2.38	4.80	2.42	2.62	3.52	0.90
136203A	2.31	5.31	2.99	2.70	3.54	0.84
136208A	2.39	4.35	1.96	2.59	3.48	0.88
137101A	1.92	4.29	2.37	2.10	3.22	1.12
137201A	1.90	4.33	2.43	2.08	2.95	0.87
138004B	1.91	3.90	1.99	2.20	3.10	0.90
138009A	2.14	4.92	2.78	2.25	3.09	0.84
138010A	2.41	5.66	3.25	2.68	3.84	1.15
138113A	1.68	5.02	3.34	2.03	3.04	1.02
143009A	2.17	4.18	2.02	2.51	3.29	0.78
143110A	1.84	4.00	2.16	2.08	2.66	0.58
143303A	1.39	2.91	1.52	1.62	2.20	0.57
145010A	1.94	3.24	1.30	2.09	2.54	0.45
145011A	1.82	4.50	2.68	2.31	3.15	0.84
145018A	1.74	3.98	2.24	2.15	2.91	0.76
145101D	1.71	2.97	1.26	1.90	2.48	0.58
145107A	1.91	2.98	1.07	2.09	2.60	0.51
146010A	1.95	3.09	1.13	2.03	2.67	0.64
146012A	1.55	3.28	1.73	1.76	2.17	0.41
146014A	1.11	2.95	1.84	1.35	1.92	0.57
146095A	1.67	3.79	2.12	1.94	2.67	0.74
422202B	2.31	4.58	2.27	2.50	3.45	0.94
422306A	2.27	4.89	2.63	2.43	3.45	1.02
422313B	2.39	5.02	2.63	2.67	3.74	1.07
422319B	2.31	5.71	3.40	2.54	3.43	0.88
422321B	1.73	3.31	1.58	1.99	2.52	0.53
422334A	2.61	4.33	1.72	2.72	3.38	0.66
422394A	2.37	3.95	1.58	2.48	3.11	0.63
424201A	1.83	2.74	0.92	1.90	2.20	0.30
912101A	1.81	2.39	0.58	1.80	2.02	0.22
912105A	1.60	2.34	0.74	1.69	1.92	0.23
915011A	1.89	3.57	1.68	2.13	2.66	0.53
917107A	1.95	3.38	1.43	2.00	2.58	0.59
919003A	1.47	2.41	0.94	1.61	1.97	0.36
919201A	1.48	3.07	1.59	1.71	2.38	0.66
919309A	1.60	2.56	0.95	1.76	2.11	0.35
922101B	1.15	2.05	0.89	1.34	1.61	0.27
925001A	1.78	3.43	1.65	1.96	2.36	0.41
926002A	1.42	2.62	1.20	1.61	1.97	0.37
A0020101	1.84	2.85	1.01	1.92	2.36	0.44
A0030501	2.21	3.49	1.28	2.32	3.13	0.81

Continued on next page

Table D.1: The values for ω at the 5 and 95 percentile and the difference between these two for a sample length of 1 year and 7 years.

	1 year			7 years		
Catchment	5%	95%	Difference	5%	95%	Difference
A2390519	2.95	5.61	2.65	3.25	3.90	0.65
A2390523	4.83	9.88	5.06	5.45	6.46	1.01
A2390531	2.81	20.00	17.19	3.22	4.43	1.21
A5030502	2.32	3.46	1.14	2.47	2.82	0.35
A5040517	2.15	2.92	0.77	2.24	2.47	0.23
A5040523	2.05	2.94	0.89	2.23	2.61	0.38
A5050517	2.13	3.99	1.86	2.30	2.78	0.48
A5130501	2.58	4.20	1.62	2.84	3.41	0.57
302214	1.87	2.96	1.09	2.08	2.39	0.31
304497	1.25	2.75	1.50	1.44	1.84	0.40
304499	1.55	2.10	0.55	1.70	1.92	0.22
305202	2.15	3.21	1.07	2.39	2.83	0.44
307473	1.10	1.81	0.71	1.28	1.55	0.27
308145	1.26	2.25	0.99	1.40	1.67	0.27
308799	1.26	20.00	18.74	1.55	1.96	0.41
312061	1.43	2.27	0.84	1.55	1.83	0.28
314207	1.51	20.00	18.49	1.80	2.38	0.58
314213	1.79	3.39	1.60	2.13	2.64	0.51
315450	1.30	20.00	18.70	1.62	2.30	0.68
318076	2.35	20.00	17.65	2.61	3.46	0.86
221207	1.75	3.31	1.56	1.98	2.46	0.48
221210	2.21	5.45	3.24	2.45	3.40	0.95
222206	2.39	3.98	1.59	2.52	3.16	0.65
222213	2.30	3.72	1.42	2.55	3.21	0.65
223202	2.72	4.63	1.92	2.86	3.72	0.87
224206	1.94	4.14	2.20	1.86	3.13	1.27
224213A	2.48	20.00	17.52	2.89	4.39	1.50
225020A	1.00	1.45	0.45	1.02	1.21	0.20
225110A	2.66	20.00	17.34	3.17	5.20	2.03
225219	1.69	3.26	1.58	2.06	2.57	0.50
226220	3.14	20.00	16.86	4.14	20.00	15.86
226222	2.12	20.00	17.88	2.98	20.00	17.02
226407	1.28	11.49	10.20	1.79	3.10	1.31
227225A	1.67	4.35	2.68	1.94	2.70	0.76
227226	2.37	5.38	3.01	2.74	3.46	0.72
227227	1.79	3.33	1.55	2.08	2.66	0.58
229650A	2.17	4.34	2.18	2.41	3.42	1.01
229661A	2.42	20.00	17.58	2.71	4.14	1.43
230210	2.60	7.56	4.96	2.88	4.02	1.14
231213	2.41	6.78	4.37	2.77	3.75	0.98
235205	1.57	20.00	18.43	2.06	3.67	1.62
236213	2.66	5.87	3.20	3.01	3.86	0.84
238208	2.08	3.45	1.37	2.21	2.77	0.56

Continued on next page

Table D.1: The values for ω at the 5 and 95 percentile and the difference between these two for a sample length of 1 year and 7 years.

	1 year			7 years		
Catchment	5%	95%	Difference	5%	95%	Difference
401203	2.25	4.68	2.43	2.60	3.60	1.01
401208	2.01	5.27	3.26	2.26	3.01	0.76
401210	1.60	3.04	1.44	1.89	2.39	0.50
401212	1.43	2.30	0.87	1.58	1.88	0.31
401216	1.59	2.86	1.27	1.88	2.36	0.48
401217	1.90	3.58	1.68	2.15	2.68	0.53
402204	2.18	4.38	2.20	2.39	3.00	0.61
402206	2.36	6.54	4.18	2.58	3.58	1.00
402213	2.27	4.58	2.31	2.47	3.18	0.72
402217	2.68	20.00	17.32	2.86	3.95	1.08
403213A	2.03	3.88	1.85	2.25	2.87	0.62
403214	2.73	13.05	10.31	2.93	4.02	1.09
403217	1.96	4.14	2.18	2.26	2.91	0.65
403221	1.80	2.92	1.12	2.10	2.54	0.45
403222	2.21	20.00	17.79	2.37	3.26	0.90
403226	1.87	3.28	1.41	2.13	2.62	0.49
403232	2.19	20.00	17.81	2.56	3.84	1.28
404207	2.07	3.89	1.82	2.31	3.02	0.70
405205	1.54	2.95	1.41	1.85	2.35	0.50
405209	1.62	4.04	2.41	1.99	2.53	0.53
405215	1.54	3.33	1.79	1.85	2.41	0.56
405217	1.83	3.59	1.76	2.20	2.82	0.63
405218	1.52	2.41	0.89	1.61	1.94	0.32
405219	1.99	3.35	1.37	2.15	2.59	0.43
405226	2.07	3.70	1.64	2.22	2.68	0.46
405227	2.04	4.32	2.28	2.29	2.96	0.66
405238	1.84	3.85	2.01	1.17	2.54	1.38
405245	2.33	4.55	2.23	2.65	3.30	0.65
405248	1.98	4.67	2.69	2.27	2.85	0.58
405251	2.39	4.07	1.69	2.60	3.26	0.65
405263	2.07	3.81	1.74	2.29	2.87	0.58
405264	1.90	4.82	2.92	2.27	3.15	0.88
405274	1.97	3.15	1.18	2.12	2.52	0.40
406208	2.09	6.50	4.41	2.61	3.53	0.92
406213	2.00	4.33	2.33	2.35	2.95	0.60
406214	2.11	4.61	2.50	2.25	2.76	0.51
406224	2.25	17.75	15.50	2.42	3.24	0.82
407214	2.26	4.29	2.03	2.55	3.23	0.68
407215	2.27	3.74	1.47	2.40	2.89	0.50
407220	2.01	3.59	1.58	2.30	2.90	0.61
407230	2.30	3.88	1.57	2.47	3.06	0.58
407253	1.98	2.91	0.92	2.15	2.54	0.40
408200	2.18	4.48	2.30	2.35	3.11	0.76

Continued on next page

Table D.1: The values for ω at the 5 and 95 percentile and the difference between these two for a sample length of 1 year and 7 years.

	1 year			7 years		
Catchment	5%	95%	Difference	5%	95%	Difference
408202	2.13	4.21	2.08	2.47	3.10	0.63
415207	2.33	4.58	2.25	2.61	3.28	0.67
415226	1.87	20.00	18.13	2.22	2.87	0.66
415237	2.04	4.24	2.20	2.32	3.06	0.74
224214A	2.68	5.80	3.12	3.11	4.20	1.08
604053	2.77	3.84	1.07	2.94	3.35	0.41
606001	2.77	4.20	1.43	3.18	3.61	0.43
606002	4.76	9.98	5.22	5.37	6.69	1.33
606185	2.31	3.31	1.00	2.49	2.81	0.33
607155	2.13	2.87	0.75	2.27	2.56	0.30
608002	2.96	6.55	3.59	3.40	4.21	0.81
610008	2.33	3.60	1.27	2.51	2.96	0.45
613002	2.04	2.29	0.25	2.03	2.18	0.14
613146	1.86	2.83	0.98	2.03	2.33	0.29
614044	3.57	5.22	1.65	3.76	4.33	0.57
616002	3.73	7.03	3.29	3.76	4.65	0.89
616013	3.34	4.50	1.16	3.54	4.06	0.52
616065	3.28	5.12	1.84	3.29	4.03	0.74
803003	1.20	2.43	1.22	1.39	1.67	0.29
804001	1.51	3.11	1.60	1.72	2.01	0.30
809310	1.57	3.69	2.11	1.73	2.11	0.38

E

Python code

The code used in this research has been published in an online repository. It can be found by following the link `https://gitlab.com/stijnvant/thesis_stijn_van_terwisga`.